699402, 2022, 8, Do



JGR Space Physics

REVIEW ARTICLE

10.1029/2021JA029928

Special Section:

Cluster 20th anniversary: results from the first 3D mission

Key Points:

- Space- and ground-based measurements strongly complement each other, and combining the two further enhances the insight they provide
- Studies exploiting ground-based observations have been a key aspect of the Cluster mission, yielding approximately 100 papers
- We review these studies, covering the full range of solar wind/ magnetosphere/ionosphere coupling and dynamics

Correspondence to:

R. C. Fear, R.C.Fear@soton.ac.uk

Citation:

Fear, R. C. (2022). Joint Cluster/ground-based studies in the first 20 years of the Cluster mission. *Journal of Geophysical Research: Space Physics*, 127, e2021JA029928. https://doi. org/10.1029/2021JA029928

Received 30 AUG 2021 Accepted 15 JUL 2022

© 2022. The Authors. This is an open access article under the terms of the Creative Commons Attribution License, which permits use, distribution and reproduction in any medium, provided the original work is properly cited.

Joint Cluster/Ground-Based Studies in the First 20 Years of the Cluster Mission

R. C. Fear¹

¹School of Physics & Astronomy, University of Southampton, Southampton, UK

Abstract Ground-based facilities make an important contribution to our understanding of the magnetospheric system. Coordination with ground-based facilities has been embedded within the Cluster mission since before launch, and this has given rise to a large number of studies which have exploited data from both Cluster and one or more of the diverse range of ground-based instrumentation that have been available during the mission timespan. In this paper, we review the advances that have been made to our understanding of the magnetosphere-ionosphere system, in which insight has been enhanced by combining ground-based observations with observations from Cluster. Topics covered span from the bow shock to the magnetotail and down to the aurora.

1. Introduction

The Cluster mission consists of four spacecraft which were launched in 2000 into a polar orbit with an apogee of $19~R_E$ and a perigee of $3~R_E$. Each spacecraft carries an identical payload of 11 instruments which measure the local plasma environment. This initial orbit allowed the regular sampling of several key regions of the magnetosphere and its environs—the magnetotail lobes, plasma sheet, auroral zones, cusps, magnetopause, magnetosheath, bow shock, foreshock, and the local solar wind. A major point of uniqueness of the Cluster mission is the fact that it consists of four identical spacecraft, typically arranged in a tetrahedron, which provides local three dimensional information about the plasma environment. This has allowed temporal and spatial effects to be distinguished, and enables measurements of inherently 3D quantities, such as the gradients, divergence and curls of plasma parameters, and the intrinsically 3D structure of plasma waves and boundaries (Escoubet et al., 2015). Over the lifetime of the mission, the scale size of the tetrahedron (i.e., separation of the spacecraft) has varied between ~ 1 and $\sim 60,000$ km, allowing plasma phenomena and structure on the corresponding scale sizes to be observed. Furthermore, the orbit has evolved (Escoubet et al., 2021) allowing other regions to be sampled, such as the auroral acceleration region, and new orbital configurations. For example, early cusp crossings allowed the latitudinal structure of the cusps to be examined in a narrow local time sector, whereas more recent crossings have allowed the longitudinal cusp structure to be probed.

The science returns of a mission such as Cluster can be greatly enhanced by combining its observations with complementary measurements that can be made on the ground. Therefore, coordination with ground-based facilities, and use of their data, has been a key aspect of the scientific exploitation of the Cluster mission. The importance of such coordination was recognized early, building on a heritage of earlier studies exploiting conjunctions between single-spacecraft and ground-based instruments (e.g., Lockwood et al., 1993; Pinnock et al., 1993; Potemra et al., 1992; Opgenoorth et al., 1989). This resulted in the formation of the Cluster Ground-based Working Group in 1991 (Opgenoorth, 1993), which led the preparation and coordination of joint Cluster/ground-based work in the pre-launch and early days of the Cluster mission. More recently, several ground-based data sets were incorporated into the Cluster Science Archive as a result of the EU-funded European Cluster Assimilation Technology programme (ECLAT) and Monitoring, Analyzing and Assessing Radiation Belt Loss and Energization (MAARBLE) projects (Escoubet et al., 2015), further facilitating studies exploiting ground-based facilities in support of Cluster research.

Lockwood and Opgenoorth (1995) outlined four main ways in which ground-based observations can complement in situ observations such as those provided by Cluster. First, ground-based observations can be used to resolve spatial and temporal variations that cannot be separated by satellite observations alone, for example, determining the longitudinal extent of a reconnection site that is observed in situ by a spacecraft. Second, ground-based observations are vital for placing in situ observations in a global context, for example, by determining the spatial

FEAR 1 of 46

location of the spacecraft relative to some magnetospheric boundary or structure. Third, they can be used to provide ionospheric boundary conditions, such as conductivity, for studies into magnetosphere-ionosphere coupling. Fourth, they can contribute to techniques which can yield measurements that would not be possible from either ground-based or space-based measurements alone, such as determining the mapping of particle populations, waves, etc., or changes in such particle populations, between the magnetosphere and ionosphere. Lockwood and Opgenoorth (1995) identified nearly 60 scientific objectives which could be realized through coordinated Cluster/ground-based studies, spread across three broad areas of (a) Magnetopause and boundary layer processes, (b) Tail phenomena and substorms, and (c) General magnetospheric topology, morphology and dynamics. Progress in these areas during the first 4 years of the Cluster mission was reviewed comprehensively by Amm et al. (2005); in this paper, we seek to update that review with more recent developments as the mission has developed.

Ground-based solar-terrestrial physics facilities are diverse; here, we provide a brief overview of the main facilities used in the studies discussed in this paper—for a more detailed summary of their capabilities, we refer to earlier reviews by Lockwood and Opgenoorth (1995), Opgenoorth and Lockwood (1997), and Amm et al. (2005). Incoherent scatter radars such as the European Incoherent Scatter facility (EISCAT: Folkestad et al., 1983), located in northern mainland Scandinavia, and the EISCAT Svalbard Radar (ESR: Wannberg et al., 1997), use powerful, high frequency transmitters to excite oscillations in ionospheric electrons which then radiate electromagnetic waves through collective processes. They are able to provide measurements of the electron density, electron temperature, ion temperature, ion drift speed and the collision frequency between ions and molecules, all of which are measured along the line of sight of the radar beam. The EISCAT mainland radars consist of a VHF and a UHF transmitter located in Tromsø, Norway, which are well placed to observe the auroral region when the radar is on the nightside. Two additional receiver sites located in Sodankylä, Finland, and Kiruna, Sweden, allow the local ionospheric electric field to be determined by tristatic measurements; in the early phase of the Cluster mission, this was a capability of the UHF radar, but more recently the remote receiver sites have operated on VHF. The higher-latitude ESR was constructed to provide observations of the cusp, during the daytime, and the boundary between the auroral oval and the polar cap on the nightside. Further west, the Søndrestrøm incoherent scatter radar (Kelly, 1983; Kelly et al., 1995) provided observations of the dayside auroral oval and nightside polar cap from Greenland until 2018. At lower latitudes, the Jicamarca Radio Observatory (Woodman & Hagfors, 1969), situated in Peru, provides incoherent scatter observations of the equatorial ionosphere, and has also been used to study the equatorial response to global processes observed at higher latitudes by Cluster and EISCAT.

Coherent scatter radars operate on a different principle, using lower power HF radio waves to measure backscatter from decameter-scale ionospheric irregularities. Doing so provides measurements of the line-of-sight velocity of the ionospheric plasma, the backscattered power and the width of the backscattered spectrum (indicating how "hard" the backscatter target is, which in turn gives information on ionospheric structure). The major coherent radar system is the Super Dual Auroral Radar Network (SuperDARN: Greenwald et al., 1995; Chisham et al., 2007), a global network of coherent scatter radars which was established in the 1990s. SuperDARN radar beams are steered electronically, meaning that the radar fields of view can be sampled rapidly (e.g., typically every minute, though specialist programs are available which can give higher frequency soundings on a subset of beams). Data from the global, interhemispheric network can be combined to provide global maps of the convection in the northern and southern hemispheres, though the extent of the convection sampled does depend on the backscatter conditions for a given event (as well as the spatial extent of the network, which has expanded over the course of the Cluster mission). A forerunner coherent radar system was the Scandinavian Twin Auroral Radar Experiment (STARE: Greenwald et al., 1978), which consisted of two VHF radars with overlapping fields of view, located in Midtsantan, Norway, and Hankasalmi, Finland, and which operated until 2005. Radar can also be used to stimulate the ionosphere through artificial heating experiments, for example, those performed by the Space Plasma Exploration by Active Radar (SPEAR) instrument (Robinson et al., 2006), which was located close to the ESR and which operated from 2004 to 2014. Ionospheric heaters such as SPEAR emit radio waves which are absorbed by the ionosphere, causing the electron temperature and density to increase, affecting the existing currents that flow in the ionosphere. This can be used, through spacecraft and/or other ground-based measurements, to study wave interactions in space plasmas. (Readers interested in the historical development of several of the radar facilities mentioned in this section are directed to the special issue on "The history of ionospheric radars" in Hist. Geo Space. Sci., https://hgss.copernicus.org/articles/special_issue6.html.)

FEAR 2 of 46

Globally, there are several chains of ground-based magnetometers which provide measurements of the perturbation of the magnetic field experienced on the ground due to ionospheric currents, and they can therefore be used to construct estimates of the two-dimensional ionospheric current systems, to identify the location and timing of substorm onsets (due to the diversion of the cross-tail current into the ionosphere through the substorm current wedge), and similarly they contribute to global indices used to identify storm and substorm activity (e.g., the Dst and AE indices, respectively). Examples include the magnetometers that formed part of the Canadian Auroral Network for the OPEN Program Unified Study (CANOPUS) program (Rostoker et al., 1995) in the Canadian sector, and the Sub-Auroral Magnetometer Network (SAMNET) and the International Monitor for Auroral Geomagnetic Effects (IMAGE) in the European sector (Viljanen & Hakkinen, 1997; Yeoman et al., 1990). Although these magnetometer chains are operated independently by different groups, their data has in recent years been collated through the SuperMAG collaboration (Gjerloev, 2012), which provides a coordinated means to access such data, as well as providing its own magnetic indices, and the International Real-time Magnetic Observatory Network (INTERMAGNET), which consists of a smaller subset of stations but which applies stricter data quality rules (Kerridge, 2001).

Riometers (relative ionospheric opacity meters) are passive instruments which measure the absorption of cosmic background noise and therefore provide a proxy for the level of high energy electron precipitation along the line of sight, while ionosondes (such as the Digisonde network: Reinisch et al., 2005) actively transmit HF radio waves vertically, in order to measure the heights and densities of various ionospheric layers. Ground-based optical instruments provide observations of the auroral emissions that are conjugate to processes occurring further out in the magnetosphere. All-sky imagers (ASIs) provide a local 2D field of view of the auroral emissions, either in a given narrow wavelength band or in "white light", by using fish-eye lenses or spherical mirrors to obtain an image of the entire sky as viewed from one point on the Earth's surface, whereas meridian scanning photometers (MSPs) observe emissions in specific wavelength bands along a 1D north-south slice. Like magnetometers, ground-based optical instruments are either deployed and operated independently, or can be part of a wider network of varied ground-based instruments. For example, the Magnetometer, Ionospheric Radar Auroral Cameras Large Experiment (MIRACLE: Viljanen & Hakkinen, 1997) was originally built to support the Cluster mission, and consists of the IMAGE magnetometer chain and a network of ASIs (and previously the STARE radar), while the CANOPUS network incorporated magnetometers, riometers, MSPs and ASIs (Rostoker et al., 1995). (NB The elements of the CANOPUS network are now operated separately; for example, the upgraded and expanded magnetometer network is now operated as the Canadian Array for Realtime Investigations of Magnetic Activity (CARISMA: Mann et al., 2008).)

Finally, space-based imaging also provides a 2D view of auroral dynamics, but often on a global scale; the main examples are the imagers onboard the NASA Polar and IMAGE satellites (Mende et al., 2000; Torr et al., 1995), which operated from 1996 to 2008 and 2000–2005, respectively, but the more recent Defense Meteorological Satellite Program (DMSP) satellites also include the Special Sensor Ultraviolet Spectrographic Imager (SSUSI) auroral imagers (Paxton et al., 2002) which have been used in support of some Cluster studies. Following Amm et al. (2005), we incorporate studies exploiting space-based auroral imagery in this review, as such images can be used in a very similar way (and provide similar benefits) to ground-based data.

Having outlined the range of ground-based instruments that are available to support Cluster observations, we briefly summarize the instrumentation onboard the Cluster spacecraft themselves. The full instrument suite is summarized by Escoubet et al. (2015), but here we outline specifically the instruments that are explicitly referred to in the following sections. The Cluster Ion Spectrometry (CIS: Rème et al., 2001) and Plasma Electron And Current Experiment (PEACE: Fazakerley et al., 2010) instruments make measurements of the ion and electron distributions at thermal energies (<40 keV for CIS and <30 keV for PEACE), with the Research with Adaptive Particle Imaging Detectors (RAPID: Wilken et al., 2001) instrument providing measurements of higher energy ions and electrons. The Fluxgate Magnetometer (FGM: Balogh et al., 2001), Electric Fields and Waves (EFW) experiment (Gustafsson et al., 2001) and Electron Drift Instrument (EDI: Paschmann et al., 2001) measure the DC magnetic and electric fields. The Spatio-Temporal Analysis of Field Fluctuation (STAFF: Cornilleau-Wehrlin et al., 2003) instrument measures waves in the magnetic field, while the Waves of High frequency and Sounder for Probing of Electron density by Relaxation (WHISPER: Décréau et al., 2001) experiment measures the spectrum of natural plasma oscillations, such as the plasma frequency, as well as providing a measurement of the plasma density that is independent of the particle instruments.

FEAR 3 of 46

Several of the studies cited below also exploited conjunctions between Cluster and other missions, particularly the Double Star and THEMIS missions, in addition to ground-based data sets. Double Star (Liu et al., 2005) consisted of two spacecraft in complementary orbits in the same local time sector as Cluster, which operated between 2003 and 2007. One spacecraft (Tan Ce 1, or TC-1) was in an equatorial orbit with an apogee of 12 R_E , while the other (TC-2) was in a polar orbit with an apogee of 6 R_F. The THEMIS mission (Sibeck & Angelopoulos, 2008), launched in 2007 and still operational, consists of five spacecraft which were initially launched into orbits in the same local time as each other with apogees of 10, 12, 20, and 30 R_F. These orbits were separated from the plane of the orbit of Cluster by several hours of local time, allowing simultaneous observations of different regions of the magnetospheric system (e.g., magnetopause and magnetotail, or dawn and dusk flanks), which are further enhanced by conjugate ground-based observations. At lower altitudes, the Fast Auroral SnapshoT (FAST) mission made in situ plasma observations within the low altitude auroral acceleration region, at altitudes below 4,175 km (Carlson et al., 1998). Lower still, the DMSP satellites provide in situ observations of the precipitating ion and electron population at an altitude of ~800 km (Redmon et al., 2017), and missions such as the Challenging Minisatellite Payload (CHAMP) and the three-satellite Swarm mission (Friis-Christensen et al., 2008; Reigher et al., 2002) make high resolution measurements of the Earth's magnetic field at low altitudes, and have been used for conjugate Cluster/ground-based studies. CHAMP consisted of a single spacecraft which had a 5 year lifetime, over which the orbit of the spacecraft slowly decayed from 460 km altitude to below 300 km. Swarm consists of two satellites which orbit side-by-side at 450 km altitude, with a third at slightly higher altitude (530 km). The potential for conjugate Cluster/Swarm/ground-based observations has been discussed by Chulliat et al. (2017), and we highlight that conjugate Cluster/Swarm studies are discussed in another review in this special issue (Dunlop et al., 2021).

In the following sections, we review the work that has been done combining Cluster and ground-based observations (including space-based auroral imagery). The majority of the studies discussed below are case studies exploiting either conjugate observations (i.e., where the footprint of the Cluster spacecraft can be traced down to within, or close to, the field of view of the ground-based instrument/s), or where the ground-based facilities provide coverage of a separate region from Cluster (e.g., providing observations of the dawn-side magnetosphere while Cluster is at dusk). Other studies, exploiting the longevity of both the Cluster mission and many of the ground-based instruments, have compared statistics of the two regions, for example, comparing magnetospheric and ionospheric convection, or ionospheric and magnetospheric current systems. We follow broadly the three areas outlined by Lockwood and Opgenoorth (1995), though we expand general magnetospheric topology/morphology/dynamics into several areas. In Section 2, we discuss studies which have examined dayside processes, including the bow shock, magnetosheath, magnetopause and cusp. In Section 3, we discuss nightside processes, including substorms and other nightside reconnection signatures. Section 4 summarizes research into ultralow frequency (ULF) waves. Sections 5 and 6 review studies into auroral structure and magnetospheric/ionospheric current systems (and their coupling), respectively. Section 7 reviews studies into global-scale dynamics (e.g., global convection and the response to storms and solar wind structures). Finally, in Section 8 we summarize the legacy of joint Cluster/ground-based studies with respect to subsequent and future missions.

2. Dayside Processes

In this section, we summarize conjugate Cluster/ground-based studies which have focused on dayside processes, from the bow shock and magnetosheath to the magnetopause and cusp, including northward IMF processes affecting the magnetopause tailward of the cusp. The bow shock/magnetosheath/magnetopause region represents the interface at which the solar wind directly interacts with the Earth's magnetosphere. The solar wind is variable, both in terms of its pressure and the orientation of the interplanetary magnetic field, and it may give rise to transient events when it interacts with both the bow shock and the magnetopause. As the solar wind passes through the bow shock to form the magnetosheath, the draped magnetosheath magnetic field can interact with the magnetospheric magnetic field through a process of magnetic reconnection which is the major driver of large-scale magnetospheric dynamics. Magnetopause reconnection can take place either quasi-steadily, or in bursts called "flux transfer events" (FTEs). Solar wind plasma enters the magnetosphere on newly opened magnetic field lines which form the cusp, and the convection of newly opened field lines gives rise to a spatial "dispersion" signature in the energy of solar wind particles observed in the cusp. The convection associated with bursty reconnection gives rise to pulsed flow signatures in the ionosphere, and poleward-propagating auroral structures (poleward

FEAR 4 of 46

moving auroral forms, or PMAFs). Ground-based observations (and global auroral imaging) can be used to estimate the location of the boundary between higher latitude magnetic field lines that have been "opened" by magnetic reconnection, and lower latitude field lines that are still "closed" (i.e., the open/closed field line boundary). Key questions that conjugate Cluster/ground-based studies have sought to address include: What is the relationship between magnetopause, cusp and ionospheric signatures of bursty reconnection? Where exactly on the magnetopause does reconnection occur? Does it occur strictly where the magnetic shear is close to 180° ("antiparallel" reconnection) or does it occur at lower shears ("component reconnection")? What is the longitudinal extent of individual reconnection events? When reconnection is bursty, is that due to time variation in the solar wind driving conditions, or inherent "burstiness" of the process? How do newly opened field lines evolve once magnetopause reconnection has taken place? What is the "size" of individual reconnection bursts, and is the global magnetospheric convection process typically driven by steady or bursty reconnection? Are "steps" in the cusp dispersion signature due to spatial variation in the reconnection rate, or temporal structure (i.e., time-varying reconnection)? What causes the "dim" region between sequential poleward moving auroral forms, given that field lines opened in sequential bursts of reconnection form a contiguous region? How and where does magnetopause reconnection occur when the IMF is northward?

2.1. Bow Shock, Magnetosheath and Magnetopause Motion

Several authors have used combined Cluster and ground-based observations to study the propagation of upstream changes through the magnetosheath, or the impact of magnetopause motion either in response to solar wind pressure variations or to bow shock/magnetosheath/magnetopause transients. (Examples of such transients are hot flow anomalies, which form at the bow shock when a current sheet embedded within the solar wind interacts with the shock, and which impact the magnetosheath and magnetopause, or FTEs which are bursts of reconnection that give rise to flux-rope-like structures at the magnetopause, which locally compress the magnetopause.) Some of these studies used radar or auroral observations to study the pulsing of the ionospheric flow, in order to distinguish between pressure and reconnection effects. Pitout et al. (2004) reported observations of pulsations in the ionospheric flow accompanied by ionospheric density structures, both observed by the ESR, which were associated with a series of magnetopause encounters observed by Cluster during a period of weakly northward (but B_{v} -dominated) IMF. The Cluster observations were inconsistent with signatures of reconnection, since the plasma observations failed the Walén test (which uses in situ plasma and magnetic field data to quantify whether an interface crossed by a spacecraft is a rotational discontinuity, and hence consistent with "open" field lines downstream of a reconnection site). Furthermore, the ionospheric flow pulsations consisted of alternating poleward and equatorward flows, rather than simply enhancements and decreases in the poleward convection as is the common signature of pulsed reconnection (see Section 2.2). The authors concluded that these combined observations were consistent with an ionospheric flow response to ULF waves driven by the periodic magnetopause motion. In a similar manner, Kauristie et al. (2001) linked oscillations in the dusk-sector magnetopause observed by Cluster with periodic variations in the average intensity of the aurora observed by an ASI, and weak but discernible Pc5 magnetic pulsations observed on the ground. Some of the auroral features were observed to propagate poleward, in a manner resembling the poleward propagation of reconnection-induced signatures (see Section 2.2), but in this case as a signature of the ULF wave activity excited by the magnetopause motion. Observing a slightly different scenario, Y. C. Zhang et al. (2011) compared the propagation of a series of solar wind dynamic pressure changes and a southward IMF rotation using three points of observation, with Cluster in the solar wind, just upstream of the bow shock, Double Star TC-1 at the near-noon magnetopause, and the Kerguelen SuperDARN radar near noon MLT. The dynamic pressure changes and IMF rotation observed by Cluster in the solar wind were compared with a series of magnetopause crossings made by TC-1, and the differences were used to infer the time taken for the pressure and magnetic field changes to propagate from Cluster to Double Star. The pressure variations arrived more promptly, leading the authors to suggest that the pressure change may have "outrun" the field rotation, with the pressure change being communicated by magnetosonic propagation. In a key difference from the Pitout et al. (2004) event, the Kerguelen radar exhibited an intensification of poleward flow, indicative of the initiation of dayside reconnection which started very shortly after the arrival of the IMF rotation at TC-1 (delayed only by the Alfvén travel time to the ionosphere), indicating that reconnection was initiated promptly after the arrival of the southward-directed field.

Other studies have used ionospheric radar and/or ground-based magnetometer observations to study "traveling convection vortices" (TCVs) and their magnetopause drivers. TCVs are vortical structures of ionospheric

FEAR 5 of 46

convection, which are observed to propagate longitudinally from dayside to nightside. They arise as a result of circular Hall currents which are produced by a pair of oppositely directed, moving field-aligned current systems. Several magnetopause drivers of the propagating field-aligned currents (and hence TCVs) have been proposed, including Kelvin-Helmholtz instability (KHI) (in which the shear in the flow between the magnetosheath and magnetospheric plasma drives waves at the magnetopause), FTEs, and the impact of either solar wind pressure pulses or ion foreshock instabilities on the magnetopause. Dougal et al. (2013) searched for the ionospheric signatures associated with seven intervals of KHI observed by Cluster, plus an additional interval observed by Geotail. They found that stationary or traveling convection vortices were observed by SuperDARN in four of their eight events (in at least one hemisphere), though the vortices were only within their estimated footprint region for two of the events. Pc5 magnetic oscillations (see Section 4) were observed by ground-based magnetometers in four events (there being some overlap with vortex signatures), consistent with a previous case study. Engebretson et al. (2013) presented observations of a TCV and its drivers from a wide array of space- and ground-based instrumentation, spread across a range of magnetic local times. An isolated burst of Pc1 waves, indicative of Electromagnetic Ion Cyclotron (EMIC) activity, was observed by ground-based search coil magnetometers located at ~1300 MLT. (EMIC waves are a category of ULF wave in Earth's magnetosphere which can transfer energy between different plasma populations and cause energetic ions and electrons to precipitate into the ionosphere and upper atmosphere.) Both the ground-based magnetometers and overlapping SuperDARN radars showed evidence of a vortical signature in the ionospheric convection, with the SuperDARN observations specifically showing azimuthal (antisunward) propagation of the vortex—that is, that it was a TCV rather than a stationary vortex. DMSP observations demonstrated that the EMIC activity and TCV signatures were on closed field lines, just equatorward of the open-closed boundary. Both ground-based optical and space-based particle instrumentation revealed evidence of enhanced proton precipitation associated with the EMIC activity, indicating that the Pc1 wave burst occurred on a flux tube in the outer dayside magnetosphere whose footprint was roughly 2° equatorward of the open-closed boundary. Several spacecraft which were situated far upstream of the bow shock observed a predominantly radial and steady IMF. However, the Geotail spacecraft showed several perturbations of the solar wind just upstream of the quasi-parallel bow shock, and Cluster observed a large outward bow shock excursion at ~1630 MLT. The observations confirmed that compression-related EMIC waves can be generated near the outer boundary of the dayside magnetosphere, and were interpreted as being caused by a bow shock instability, most likely a spontaneous HFA, which was observed by Geotail and gave rise to the significant bow shock excursion observed by Cluster (see also Section 4).

2.2. Magnetopause Reconnection

Study of magnetopause reconnection both directly (with Cluster at the magnetopause) and indirectly (with Cluster) ter in the cusp) has been fertile territory for conjugate Cluster/ground-based studies, and identifying magnetopause and cusp conjunctions was a high priority for the Cluster Ground-based Working Group. Several studies have examined the conjugate signatures of bursty magnetopause reconnection, known as FTEs. Key questions have included the relationship between magnetopause and ionospheric signatures of FTEs, and their longitudinal extent. Wild et al. (2001) examined conjugate signatures of FTEs at the magnetopause (observed by Cluster) and in the ionosphere. The SuperDARN Hankasalmi radar observed a continuous band of backscatter between 76° and 78° MLAT, which exhibited pulsations in the ionospheric flow (known as pulsed ionospheric flows, or PIFs—Figure 1), which had previously been identified as an ionospheric signature of FTEs. At higher latitudes (78° MLAT and above), poleward-moving regions of enhanced radar backscatter were observed which were separated by regions devoid of backscatter (also Figure 1). The authors referred to these signatures as poleward moving radar auroral forms (PMRAFs) in analogy to optical poleward moving auroral forms which are the auroral signature of FTEs. They drew a distinction between PMRAFs and PIFs, as the absence of backscatter adjacent to the PMRAF signature meant that it is not possible to identify whether a PMRAF is associated with a pulse in the flow. (The lack of backscatter adjacent to the PMRAF does not necessarily indicate a change in the flow, only that the ionospheric "targets" giving rise to the backscatter are limited spatially, though they are entrained in the poleward convection.) A compelling one-to-one correlation was found between FTEs observed by Cluster and PIF/PMRAF signatures observed by SuperDARN, despite the fact that the ionospheric signatures occurred ~2 hr of MLT to the west of the Cluster footprint, demonstrating that the reconnection events had a large spatial extent. The authors interpreted the PMRAF signatures as the "fossils" of the ionospheric structuring that takes place at the ionospheric footprint of the reconnection site, which are therefore observed some minutes after

FEAR 6 of 46

21699402, 2022, 8, Downloaded from https://agupubs.onlinelibrary.wiley.com/doi/10.10292021JA029928 by University Of Southampton, Wiley Online Library on [09/11/2022]. See the Terms and Conditions (https://agupubs.onlinelibrary.wiley.com/doi/10.1029/2021JA029928 by University Of Southampton, Wiley Online Library on [09/11/2022]. See the Terms and Conditions (https://agupubs.onlinelibrary.wiley.com/doi/10.1029/2021JA029928 by University Of Southampton, Wiley Online Library on [09/11/2022]. See the Terms and Conditions (https://agupubs.onlinelibrary.wiley.com/doi/10.1029/2021JA029928 by University Of Southampton, Wiley Online Library on [09/11/2022]. See the Terms and Conditions (https://agupubs.onlinelibrary.wiley.com/doi/10.1029/2021JA029928 by University Of Southampton, Wiley Online Library on [09/11/2022]. See the Terms and Conditions (https://agupubs.onlinelibrary.wiley.com/doi/10.1029/2021JA029928 by University Of Southampton, Wiley Online Library on [09/11/2022]. See the Terms and Conditions (https://agupubs.onlinelibrary.wiley.com/doi/10.1029/2021JA029928 by University Of Southampton, Wiley Online Library on [09/11/2022]. See the Terms and Conditions (https://agupubs.onlinelibrary.wiley.com/doi/10.1029/2021JA029928 by University Of Southampton, Wiley Online Library on [09/11/2022]. See the Terms and Conditions (https://agupubs.onlinelibrary.wiley.com/doi/10.1029/2021JA029928 by University Of Southampton, Wiley Online Library on [09/11/2022]. See the Terms and Conditions (https://agupubs.onlinelibrary.wiley.com/doi/10.1029/2021JA029928 by University Online Library on [09/11/2022]. See the Terms and Conditions (https://agupubs.onlinelibrary.wiley.com/doi/10.1029/2021JA029928 by University Online Library on [09/11/2022]. See the Terms and Conditions (https://agupubs.onlinelibrary.wiley.com/doi/10.1029/2021JA029928 by University Online Library on [09/11/2022]. See the Terms and Conditions (https://agupubs.onlinelibrary.wiley.com/doi/10.1029/2021JA02992 by University Online Library on [09/11/2029]. See the Univ

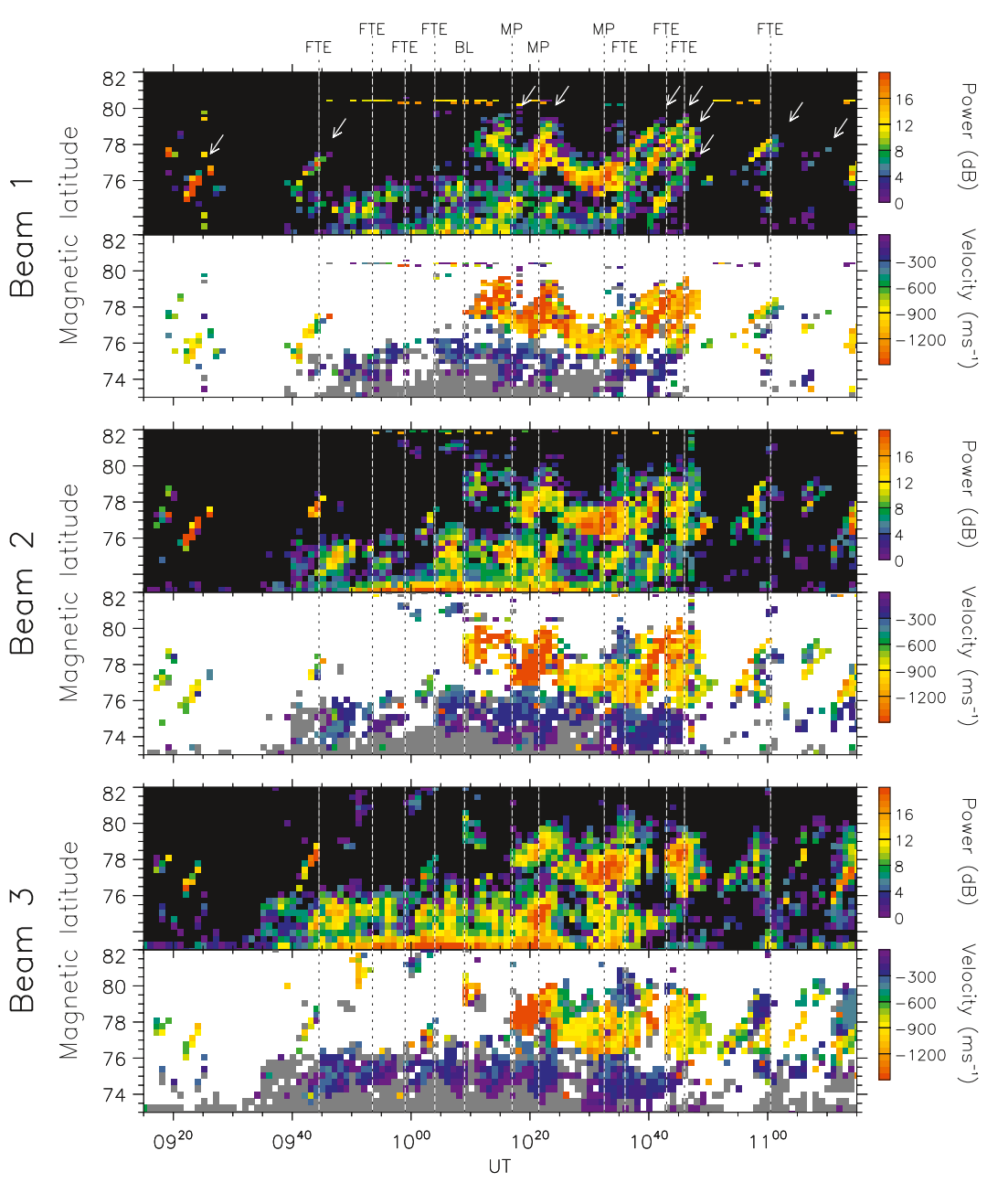


Figure 1. Ionospheric signatures of magnetopause reconnection, reproduced from Wild et al. (2001). Each pair of panels shows the backscatter power and velocity from a different beam of the Super Dual Auroral Radar Network Hankasalmi radar. Gray shading in the velocity panels indicates regions of ground scatter. Vertical dotted lines indicate the times at which Cluster observed flux transfer events (FTE), entry into the magnetopause boundary layer (BL) or a magnetopause crossing (MP). Pulsed ionospheric flows are observed between 1010 and 1050 UT between 76° and 78° MLAT in all three beams, corresponding to the region of continuous backscatter power and continuous antisunward flow (negative velocities) that is modulated in magnitude (orange/red). Regions of enhanced backscatter, preceded and followed by an absence of backscatter, are poleward moving radar auroral forms which are indicated by white arrows.

the associated burst of reconnection. This suggestion was supported by enhancements in the electron density observed by the ESR. The authors therefore suggested that PMRAFs act as useful tracers of the convection flow on newly reconnected field lines. The above analysis was based entirely on Cluster and northern-hemisphere ground-based observations, but by including southern hemisphere SuperDARN observations Wild et al. (2003) were able to infer that reconnection had to have occurred over an MLT extent of at least 4 hr (since a shorter

FEAR 7 of 46

reconnection line could not give rise to the same reconnected flux tubes observed in the northern and southern hemispheres simultaneously.)

Relatively early in the Cluster mission. Cluster and ground-based observations were combined with observations from additional spacecraft to obtain further insight beyond what can be deduced from Cluster and ground-based measurements alone. Some studies have used the additional in situ measurement point to infer the location of the reconnection site; Maynard et al. (2003) used ion signatures and Poynting flux associated with Alfvén waves measured by both the Polar spacecraft (skimming the subsolar magnetopause) and Cluster (at higher latitudes) to infer that a reconnection site lay between the two spacecraft, thus lying poleward of where they expected the location of a subsolar component reconnection line to be, and therefore more consistent with a high-latitude antiparallel reconnection line. The convection excited by the reconnection process was monitored by SuperD-ARN, which showed that variations in the reconnection rate continued for more than an hour. Conversely, Wild et al. (2005, 2007) used observations of FTEs at both the high and low latitude magnetopause (provided by Cluster and Double Star, respectively), together with near-conjugate (but not quite simultaneous) observations of pulsed ionospheric flows (provided by SuperDARN and the ESR) and a simple physics-based model of open field line motion (Cooling et al., 2001) to demonstrate that during a period of B_{ν} -dominated IMF, reconnection occurred at a low-latitude tilted reconnection line passing through (or near) the subsolar point, indicative of component reconnection. While a high-latitude reconnection site (as would result from more strictly antiparallel reconnection) could potentially have been present, it would be unlikely to be responsible for the FTE signatures observed by the spacecraft. Whether bursty reconnection arises because of time variation in upstream conditions, or because there is something in the reconnection process which can make it inherently bursty, is an interesting question; the authors noted that during this interval, the IMF was steady but ULF oscillations were present in the solar wind, magnetospheric magnetic field and in the ionospheric plasma flow. A range of periodicities were present, including some which matched the inter-FTE period observed in the pulsed ionospheric flows (~10–15 min), but not the much-shorter inter-FTE period observed by the spacecraft (~3–4 min). (The Cluster and ground-based observations of FTEs were not quite simultaneous, being separated by about an hour, and the SuperDARN and EISCAT data at the time of the Cluster FTE observations did not provide sufficient coverage or temporal resolution to investigate ionospheric signatures of the more rapidly recurring FTEs observed by Cluster.)

Another benefit to using an additional spacecraft (or constellation) is that it allows the chain of reconnection signatures from the magnetopause, through the cusp, to the ionosphere, to be observed simultaneously if the spacecraft are separated in altitude. Farrugia et al. (2004) analyzed a three-way conjunction between Cluster, which was situated immediately poleward of the cusp, the FAST satellite at the topside ionosphere, and ionospheric observations by SuperDARN and the Søndrestrøm incoherent scatter radar. Cluster observed a series of bursts of high speed flow in a boundary layer immediately poleward of the cusp, which were interpreted as reconnected flux tubes convecting past the spacecraft. These flux tubes/flow bursts were associated with fluctuations which were consistent with Alfvén waves carrying field-aligned current into the ionosphere, thereby mediating the transfer of stress between the magnetopause and ionosphere. At lower altitudes, the FAST satellite observed "cusp step" ion dispersion signatures (see Section 2.3), indicative of bursty reconnection, whilst the radars observed pulsed ionospheric flows and PMRAFs. Together, these formed an impressive collection of different signatures of magnetopause reconnection. The observations gave support to the idea that multiple "steps" in the cusp ion dispersion signature are due to temporal structuring in the cusp (i.e., time-varying reconnection) rather than spatial structure (see also Section 2.3), and also highlight the potential for stress transfer to take place at the high latitude boundary layer.

During periods of northward IMF, the reconnection site moves to high latitudes, tailward of the cusps, and can occur either independently in one or both hemispheres ("single lobe reconnection"), or as "dual lobe reconnection" in which the same interplanetary magnetic field lines reconnect in both hemispheres, thus forming additional closed magnetic field lines, populated by magnetosheath plasma, on the dayside. Retinò et al. (2006), Bavassano Cattaneo et al. (2006), and Marcucci et al. (2008) discussed an extended interval of northward IMF in which Cluster skimmed the high latitude dusk magnetopause. The complex boundary layer structure observed by Cluster indicated that reconnection was occurring simultaneously tailward of the southern hemisphere cusp and at a site in the northern hemisphere, speculated on the basis of the Cluster observations to be tailward of the northern hemisphere cusp. Northern hemisphere SuperDARN observations showed a convection pattern that confirmed that speculation. The open-closed field line boundary was determined from IMAGE observations of

FEAR 8 of 46

the aurora, cross-checked against DMSP observations of the electron precipitation and the SuperDARN spectral width boundary, and showed four poleward movements of the open-closed boundary, interpreted as evidence of sporadic closure of open magnetospheric flux by bursts of dual lobe reconnection.

Several studies (Daum et al., 2008; Q.-H. Zhang et al., 2008, 2010, 2011) have sought to compare the propagation of reconnected flux tubes as observed simultaneously at the magnetopause (in the form of FTE signatures observed by Cluster) and in the ionosphere (as PIFs/PMAFs observed by optical instrumentation or radars). Q.-H. Zhang et al. (2008) found qualitative agreement between the northward and dawnward motion of the FTEs observed by Cluster (consistent with the motion predicted by the Cooling et al. (2001) model) and the northward and westward flow observed by SuperDARN at the conjugate point in the northern hemisphere ionosphere. Daum et al. (2008), reinvestigating the conjunction (discussed above) analyzed by Wild et al. (2001, 2003), took the qualitative comparison of Q.-H. Zhang et al. (2008) further by projecting the FTEs observed by Cluster to subsequent locations along the magnetopause using the Cooling et al. (2001) model, and then tracing those projected locations down to the ionosphere (using the BATS-R-US MHD code) to infer a series of convection paths in the ionosphere. The authors also found good agreement with the northward and westward motion of the ionospheric flows as originally observed by Wild et al. (2001). The traced and observed paths were offset by about 10°, which the authors noted was likely due to a difference between the location of the magnetopause boundary in the Cooling and BATS-R-US models (i.e., the Cooling et al. (2001) magnetopause will not map to the BATS-R-US open/closed field line boundary at all locations, which will cause a stretching/compressing effect on the mapping process). In a subsequent study (based on a different event), Q.-H. Zhang et al. (2010) argued that the poleward and duskward motion of three FTEs observed at the magnetopause by Cluster was consistent with the poleward and eastward motion of optical PMAFs imaged from Svalbard. Furthermore, the authors identified "intensity gaps" in the keograms of ASIs (i.e., time series of 1D slices taken from the 2D images) just prior to the PMAFs, which they identified as evidence for equatorward erosion and subsequent poleward motion of the open-closed boundary associated with a variable reconnection rate. Similarly, Q.-H. Zhang et al. (2011) analyzed a further case where the motion of two FTEs observed by Cluster was shown to be broadly consistent with the ionospheric flow pattern observed by SuperDARN in both hemispheres, and with the presence of pulsed ionospheric flows observed by ESR. From the duration of the velocity enhancements, the authors inferred an FTE evolution time of about 20 min between their formation at a subsolar reconnection site to their addition to the magnetotail lobe. Furthermore, the observation of FTEs by the Double Star TC-1 spacecraft indicated the source was likely a low latitude reconnection site, and the fact that the northern hemisphere flow enhancements were slightly delayed with respect to those in the southern hemisphere led to the speculation that the reconnection site might have been offset toward the southern hemisphere.

Whereas the orbits of the Double Star mission were selected to provide observations, for example, of the magnetopause, at different latitudes in the same local time sector, the launch of subsequent multi-spacecraft missions has
allowed high quality measurements to be made of the magnetopause at widely separated local times (e.g., Dunlop
et al., 2011). In some of these studies, ground-based observations have also been used to provide a broader
longitudinal context. For example, Fear et al. (2009) examined a conjunction of 10 spacecraft, with the Cluster
tetrahedron situated near the dawn, high latitude magnetopause, the five THEMIS spacecraft spread in a string
along the dusk, low latitude magnetopause, and the Double Star TC-1 spacecraft near local noon. Cluster and
the THEMIS spacecraft observed multiple FTEs (on the dawn and dusk flanks, respectively) which could both
be traced back to a small region of a dayside reconnection line, whereas TC-1 (which was closer to noon but still \sim 7 R_E from the subsolar point) observed only a single FTE, but showed signatures of steady reconnection. The
SuperDARN observations indicated that the reconnection line covered several hours of local time in the pre-noon
sector, but the different rates of FTE occurrence at TC-1 and Cluster/THEMIS suggested that the variability of
the reconnection rate differed between the subsolar point and TC-1.

Ground-based observations have also provided valuable information when evaluating the "size" or global contribution of FTEs to global magnetospheric dynamics. As noted above, Wild et al. (2003) used interhemispheric SuperDARN observations to show that the reconnection site which gave rise to an FTE observed by Cluster must have extended over at least 4 hr of MLT. At its larger separations, the Cluster constellation also provides the capability to constrain a minimum spatial extent of reconnection, if signatures are observed by all four spacecraft. Fear et al. (2010) used observations from one of Cluster's early "large separation" (~10,000 km) seasons to show that during a period of strongly southward IMF, the spacecraft observed a mixture of spatially patchy and more

FEAR 9 of 46

longitudinally extended FTE signatures; interhemispheric SuperDARN observations showed that, despite the spatial patchiness of some events, they were part of a much broader region of reconnection extending over a large part of the dayside magnetopause (though there was neither a one-to-one correlation between the spacecraft and ionospheric FTE signatures, nor a direct spatial conjunction between the signatures, as the spacecraft footprint was in a longitude sector without radar coverage). More recently, Fear et al. (2017) have used conjugate Cluster and ground-based observations to address the question of the global contribution of FTEs to magnetospheric convection, as spacecraft-based studies have typically concluded their contribution to the global reconnection rate is small (i.e., dayside reconnection is predominantly steady, with small but highly visible bursty events) whereas some radar- or auroral-based studies have concluded that FTEs can be the major driver of magnetospheric convection. The authors argued that the mismatch between spacecraft and ionospheric estimates of flux transfer was due to implicit assumptions made about FTE structure, concentrating on the magnetic flux which gives rise to the highly visible magnetic field signature observed by spacecraft, rather than the total flux that is opened by the reconnection burst. By taking the latter into account, the authors were able to find a much better match between the flux estimates for individual bursts of reconnection observed by both Cluster and the Super-DARN radars, suggesting that bursts of dayside reconnection may indeed be the main driver of magnetospheric dynamics, at least in some cases.

2.3. Cusp Dynamics

Another aspect of dayside coupling which can be studied through Cluster/ground-based studies is the dynamics of the cusp, which responds to upstream conditions. This topic overlaps significantly with the previous section, as the magnetic reconnection signatures observed by ground-based facilities are mediated through the cusp, so the distinction only lies in whether the Cluster spacecraft are in the cusp or at the magnetopause during the conjunction in question.

Several of the Cluster "first results" studies exploited conjugate ground-based observations, from a single orbit (which provided Cluster's first observation of the cusp). Lockwood, Opgenoorth, et al. (2001) studied an interval when Cluster passed from the northern hemisphere lobe through the mantle region immediately poleward of the cusp, during a period of southward IMF. Cluster observed a series of enhancements in the flux of the electron and ion populations in the mantle, which were associated with a series of poleward-moving enhancements the F-region plasma density (i.e., polar cap patches) which were observed by ESR. One key question relating to cusp and ionospheric signatures of bursty reconnection concerns the minima in the luminosity of poleward moving auroral forms, or the density of polar cap patches, that are observed between events. (Polar cap patches are regions of enhanced ionospheric plasma density entrained within the polar cap flow.) Although pulsed reconnection gives discontinuities in the energy dispersion within the cusp ("cusp ion steps"), magnetosheath ions are found in a contiguous region of newly opened field lines, as each newly added region of open flux maps immediately equatorward of the previously added region, and hence a contiguous region of auroral emission/enhanced ionospheric density might be expected. The authors concluded that the combined observations of Cluster and a suite of ground-based and low-altitude instrumentation indicated that the variations in intensity of the polar cap patches was due to modulation of the precipitation of magnetosheath electrons into the ionosphere. They suggested this may be due to a potential barrier at the magnetopause preventing the lowest energy electrons from entering the magnetosphere, but with the barrier being reduced when the component of the magnetic field normal to the magnetopause was enhanced (during a reconnection burst). This made the polar cap patches and the plasma modulations observed in the mantle the "fossil remnants" of magnetopause reconnection pulses in a similar manner to the PMRAFs discussed by Wild et al. (2001) (see Section 2.2 above). The authors also noted the similarity of the pulses observed by Cluster and ESR, despite a 4 hr separation in MLT, indicating that the reconnection pulses must have extended at least this far across the magnetopause.

The IMF then suddenly turned northward, causing a contraction of the polar cap, and therefore Cluster moved into the dayside magnetosphere, from where it observed a series of transient entries by the four Cluster spacecraft onto closed field lines immediately sunward of the interior cusp. In other words, the spacecraft were approximately half way along the boundary field lines between the magnetopause and mid altitudes. The field lines were therefore connected to the low latitude boundary layer (LLBL), which is a boundary layer of magnetosheath-like plasma that forms immediately earthward of the magnetopause, either as a result of magnetopause reconnection (which results in an "open" LLBL) or diffusion of magnetosheath plasma onto closed field lines ("closed"

FEAR 10 of 46

LLBL). Lockwood, Fazakerley, et al. (2001) analyzed these closed LLBL incursions and noted that they exhibited all of the hallmarks of a magnetopause FTE, except for the fact there was no characteristic bipolar signature in the component of the magnetic field normal to the magnetopause. Equatorward motion of the cusp aurora, enhancement of the flow into the polar cap and poleward-moving events moving into the polar cap observed by ESR (albeit at a lower rate than the earlier poleward moving events during the period of southward IMF analyzed by Lockwood, Opgenoorth, et al., 2001), all supported the interpretation of the events being signatures of reconnection pulses. The authors ascribed the absence of a magnetic field signature in the boundary-normal component to a lack of pressure excess in the core, and interpreted their observations as the first observations of FTEs at middle altitudes.

Later still, on the same orbit, the Cluster spacecraft made their first encounter with the cusp. Opgenoorth et al. (2001) used data from several ground-based facilities to show that this unexpected cusp encounter arose from a large-scale reorganization of the high latitude convection, due to a further change in direction of the IMF toward a more B_Y -dominated (but still northward) configuration. Opgenoorth et al. (2001) used the time delays between the cusp encounter being observed at the four Cluster spacecraft to infer a velocity vector for the cusp motion, which was consistent with inferences from ground-based data. The same period was also analyzed by Moen et al. (2001), who compared the Cluster observations with ground-based auroral and low-altitude precipitation observations; they interpreted FTE signature discussed by Lockwood, Fazakerley, et al. (2001) as an entry onto the closed LLBL, and the signatures discussed by Opgenoorth et al. (2001) as cusp encounter. The key difference in their interpretation was that they inferred that the earlier LLBL entry was due to the passage of a boundary layer wave, rather than a mid-altitude signature of an FTE as concluded by Lockwood, Fazakerley, et al. (2001).

As seen above, ground-based observations have the benefit that they are able to provide global context during periods with changing interplanetary conditions. Pitout et al. (2001) analyzed a conjunction between the Cluster spacecraft, the ESR radar, several DMSP passes and the cusp during a period of changing upstream conditions. The IMF initially varied between northward and southward, before an extended period in which it was oriented northward. During the initial period of alternating IMF, the line-of-sight velocity observed by the ESR poleward-directed beam correlated well with the IMF B_z component, and poleward propagating transients were observed by ESR during the periods of southward IMF. Cluster encountered the cusp after the northward IMF turning; the spacecraft observed a "reverse" dispersion signature indicative that reconnection was occurring at lobe magnetopause, poleward of the spacecraft. The cusp at ionospheric altitudes, as observed by ESR at this time, was very different from the earlier period of southward IMF—the plasma density and temperature were both low, and the plasma flow was sunward (though the velocity was weak). The Cluster and DMSP observations revealed that the lobe reconnection process was sporadic or bursty in nature, as is also often the case for southward IMF, though evidence for similar transient behavior in the ionosphere was unclear. Interestingly, the lobe reconnection signatures were observed in the winter hemisphere, despite lobe reconnection being thought of as favored in the summer hemisphere. Cai et al. (2009) analyzed a separate interval during which the IMF B_z component also underwent multiple reversals; as in the Pitout et al. (2001) interval, the IMF remained in each orientation for about 30 min each time, but this time Cluster passed through the high-altitude cusp during the period of IMF B_z reversals, rather than afterward. As the IMF alternated between northward and southward, the cusp location was inferred to move back and forth in latitude, and so two of the Cluster spacecraft crossed the high-altitude cusp twice. (During the second cusp crossing, the cusp was situated sufficiently poleward to move across Clusters 1 and 3 again, but not Cluster 4 which was situated further poleward still.) The ionospheric responses were well-observed too: alternating periods of sunward and poleward plasma flow were observed by the ESR, corresponding to the periods of northward and southward IMF respectively; the motion of the open-closed field line boundary to and fro across the ESR field-aligned radar beam was observed in the form of changes in the electron temperature observed by ESR; and poleward-convecting density structures were also observed (Figure 2). The back-and-forth motion of the open-closed field line boundary in the vicinity of Svalbard was also observed via the equatorward and poleward motion of the boundary between low and high spectral width backscatter observed by one of the SuperDARN radars, and was consistent with the behavior expected for the alternating IMF polarities. The two Cluster cusp crossings both occurred during periods of northward IMF, but the cusp ion distributions were somewhat different. The first crossing exhibited a reverse ion dispersion, consistent with lobe reconnection, whereas the second consisted of ions with no evident dispersion; the authors suggested that the spacecraft were on newly closed field lines which were first opened at low latitudes, and then closed again poleward of the cusp.

FEAR 11 of 46

21699402, 2022, 8, Downloaded from https://agupubs.onlinelibrary.wiley.com/doi/10.1029/2021JA029928 by University Of Southampton, Wiley Online Library on [09/11/2022]. See the Terms and Conditions (https://agupubs.onlinelibrary.wiley.com/doi/10.1029/2021JA029928 by University Of Southampton, Wiley Online Library on [09/11/2022]. See the Terms and Conditions (https://agupubs.onlinelibrary.wiley.com/doi/10.1029/2021JA029928 by University Of Southampton, Wiley Online Library on [09/11/2022]. See the Terms and Conditions (https://agupubs.onlinelibrary.wiley.com/doi/10.1029/2021JA029928 by University Of Southampton, Wiley Online Library on [09/11/2022]. See the Terms and Conditions (https://agupubs.onlinelibrary.wiley.com/doi/10.1029/2021JA029928 by University Of Southampton, Wiley Online Library on [09/11/2022]. See the Terms and Conditions (https://agupubs.onlinelibrary.wiley.com/doi/10.1029/2021JA029928 by University Of Southampton, Wiley Online Library on [09/11/2022]. See the Terms and Conditions (https://agupubs.onlinelibrary.wiley.com/doi/10.1029/2021JA029928 by University Of Southampton, Wiley Online Library on [09/11/2022]. See the Terms and Conditions (https://agupubs.onlinelibrary.wiley.com/doi/10.1029/2021JA029928 by University Of Southampton, Wiley Online Library on [09/11/2022]. See the Terms and Conditions (https://agupubs.onlinelibrary.wiley.com/doi/10.1029/2021JA029928 by University Of Southampton, Wiley Online Library on [09/11/2022]. See the Terms and Conditions (https://agupubs.onlinelibrary.wiley.com/doi/10.1029/2021JA029928 by University Of Southampton, Wiley Online Library on [09/11/2022]. See the Terms and Conditions (https://agupubs.onlinelibrary.wiley.com/doi/10.1029/2021JA029928 by University Of Southampton, Wiley Online Library on [09/11/2022]. See the Terms and Conditions (https://agupubs.onlinelibrary.wiley.com/doi/10.1029/2021JA029928 by University Of Southampton [09/11/2022]. See the Terms and Conditions (https://agupubs.onlinelibrary.wiley.com/doi/10.1029/2021]. See the Terms and Con

tions) on Wiley Online Library for rules of use; OA artic

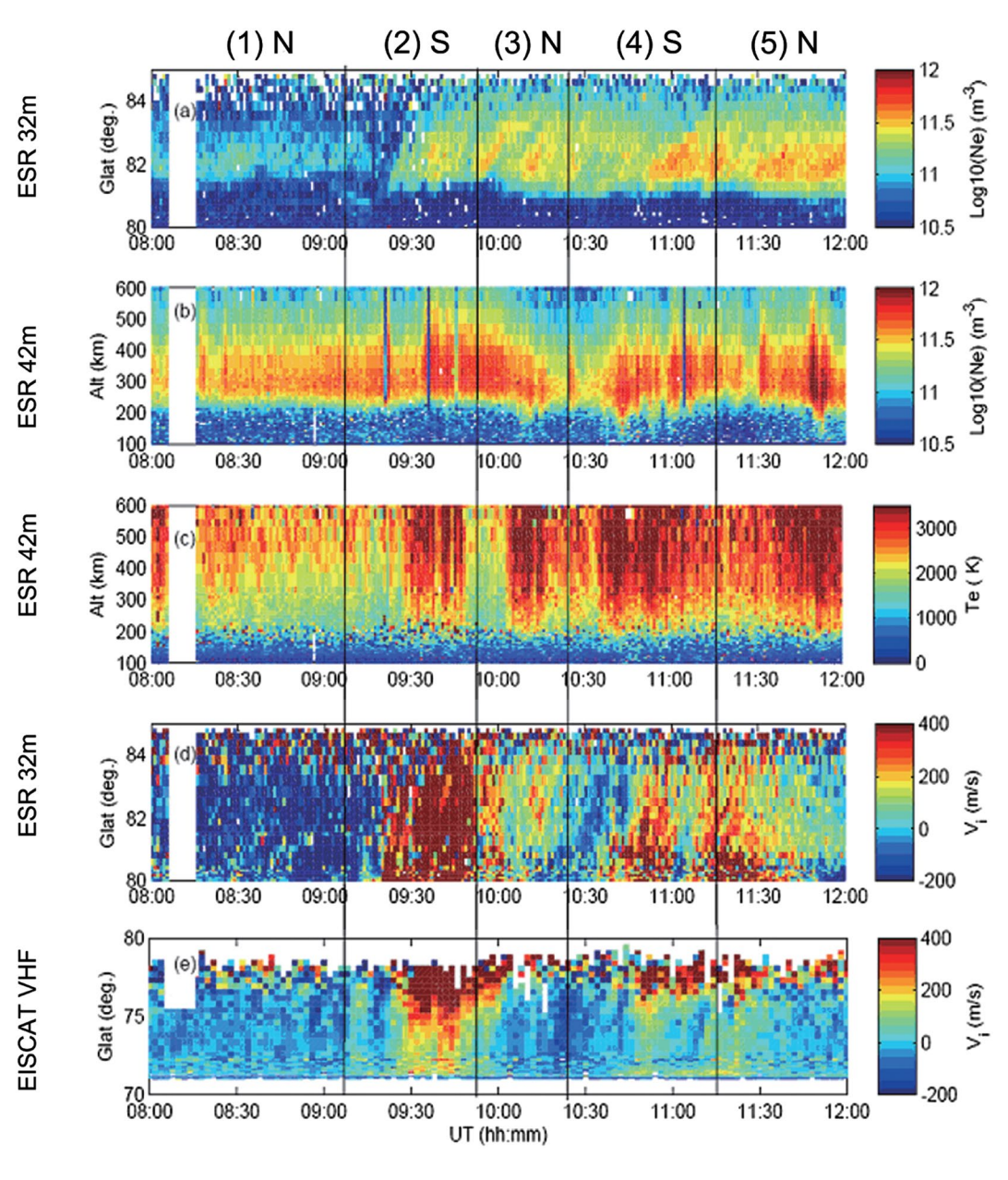


Figure 2. European Incoherent Scatter facility (EISCAT) observations of the cusp during a period of alternating northward and southward IMF, reproduced from Cai et al. (2009). Panels (a and d) represent the electron density and ion velocity, respectively, observed by the movable 32 m EISCAT Svalbard Radar (ESR) dish, which for this event was directed at low elevation toward the magnetic pole. Panels (b and c) show the electron density and electron temperature, respectively, from the fixed field-aligned ESR 42 m dish. The bottom panel shows the line-of-sight ion velocity observed by the lower latitude mainland VHF radar. Five periods of alternating northward (N) and southward (S) IMF are labeled at the top of the diagram—the alternating sunward and antisunward flows are evident in panels (d and e), though poleward-propagating electron density structures are observed in panel (a) from period (2) onwards, indicating (during the periods of northward IMF) fossil remnants of reconnection from earlier periods of southward IMF.

The structure of the cusp during periods of northward IMF was also studied by Bogdanova et al. (2005), who analyzed a crossing made by Cluster from the nightside to the dayside, across the high-altitude northern cusp, during a period of steady northward IMF. The particle distributions observed by Cluster indicated the existence of two reconnection lines: a reverse dispersion pattern in the cusp, coupled with dawnward and sunward plasma convection observed by Cluster and two conjugate northern hemisphere SuperDARN radars, indicated the occurrence of a reconnection site poleward of the northern hemisphere cusp on the dusk side, whilst subsequent

FEAR 12 of 46

observation of a bidirectional and at times isotropic plasma population, which was heated but corresponded to much slower convection (in a region termed the "stagnant exterior cusp"), indicated that the field lines were then re-closed by a second reconnection line poleward of the southern hemisphere cusp on the dawn side (i.e., dual lobe reconnection, as discussed above in Section 2.2). Further insight was provided by the SuperDARN observations, which showed alternately convection and stagnation near the Cluster footprint which were consistent with the interpretation of dual lobe reconnection, but also showed evidence of adjacent pulsed reconnection signatures more indicative of reconnection with closed dayside magnetic field lines. The authors therefore concluded that the SuperDARN observations indicated that the southern hemisphere reconnection line extended across the interface between closed dayside and open lobe magnetic field lines, hence providing both types of topology change (at different points along its length).

Conjunction studies have also been used to compare the convection observed in the cusp and in the ionosphere, in a similar manner to that done subsequently with magnetopause signatures of reconnection (discussed above in Section 2.2). Marchaudon et al. (2004) did so during a period in which Cluster was situated in the cusp whilst the IMF briefly rotated from northward and duskward to southward and dawnward, then back again. The changes in the convection direction observed by Cluster were well correlated with the IMF B_{γ} variations. Furthermore, a good correspondence was found between the changing convection velocity observed by Cluster and that observed by conjugate SuperDARN radars, if a delay of 2–3 min was assumed between the cusp effects at spacecraft and ionospheric altitudes. (The convection velocity observed by Cluster was systematically about 1.5 times larger than at SuperDARN, but the relative variations were consistent.) The authors observed a clear one-to-one correlation between three particle injection events observed by Cluster and corresponding bursts of enhanced convection observed by SuperDARN, where the ionospheric response was again delayed by 2–3 min relative to the spacecraft signatures. These signatures were interpreted as the signatures of bursty reconnection at the magnetopause, as seen in the cusp at high and ionospheric altitudes.

A key objective of the Cluster mission is to distinguish between temporal and spatial effects, and this objective is one that can be supported by ground-based measurements. The cusp ion steps discussed earlier occur as a result of temporal variations in the reconnection rate (resulting in sudden changes in the "age" of adjacent field lines, in terms of their time since being opened—e.g., Lockwood, Opgenoorth, et al., 2001; Farrugia et al., 2004), but they have also been argued to arise due to spatial structure, if a spacecraft maps to different reconnection lines at different times during a cusp pass (leading to "double," or multiple cusp events where distinct dispersion signatures are observed sequentially). Trattner et al. (2003, 2005) analyzed one such double cusp crossing and noted (a) a similarity in the multiple cusp step signatures when plotted spatially, rather than as a function of time, and (b) a correspondence between new steps and passage of the spacecraft onto a different convection cell, as inferred by SuperDARN observations, implicitly mapping the two cells to different reconnection lines. The authors argued that the differences in observations between the three spacecraft were due to spatial structure in the cusp consistent with separate pre-noon and post-noon reconnection sites as might be expected from strictly antiparallel reconnection straddling noon. Trattner et al. (2005) then used the low-velocity cut-offs of the downward-precipitating and mirrored populations in the sheath to calculate the distance from the Cluster spacecraft (in the cusp) to the reconnection line (at the magnetopause), and concluded that two of the distinct cusp signatures did indeed map to two different reconnection sites (one in the dusk sector of the southern hemisphere, and one close to noon in the northern hemisphere). However, a number of studies interpret cusp steps as temporal features—in particular, Bosqued et al. (2005) found that a series of cusp ion steps observed by Cluster during a crossing of the mid-altitude cusp in a period of steady southward and duskward IMF, but high and variable solar wind dynamic pressure, were well-correlated with brightenings in the Lyman- α auroral emissions observed by the IMAGE SI-12 instrument. These signatures were also well-correlated with observed solar wind pressure enhancements, leading the authors to conclude that in this instance, the magnetopause reconnection rate was modulated by the upstream pressure and/or variations in the IMF clock angle, rather than being inherently self-varying. In a further study into the same event, Cerisier et al. (2005) showed that following each reconnection burst as observed by Cluster and IMAGE, channels of fast ionospheric convection were observed by SuperDARN on the poleward side of the auroral intensifications. The ionospheric convection bursts started shortly after the auroral intensifications, and their duration was longer (~10 min, cf. 4–6 min for the auroral intensification), providing a coherent view of the spatial and temporal relationship between these signatures of magnetopause reconnection. (For further information on the debate on whether cusp ion steps are temporal or spatial features, we refer the reader to the parallel review of Cluster cusp studies by Pitout & Bogdanova, 2021.)

FEAR 13 of 46

Conjugate space- and ground-based observations can also be used to study energy deposition into the ionosphere, through the cusp. Yordanova et al. (2007) used Cluster, ESR and MIRACLE observations to compare the particle energy flux and Poynting flux at the altitude of Cluster with the F-region energy input inferred from the ESR observations and the Joule heating in the E-region, calculated using the electric field from the equivalent ionospheric current derived from MIRACLE magnetometer observations and Pedersen/Hall conductivities inferred from ESR data. The energy of the particles observed by Cluster was low, and so they were expected to deposit their energy at F-region altitudes. Indeed, the earthward energy flux of particles observed by Cluster closely matched the energy required to produce the observed F-region heating, suggesting that direct precipitation of the magnetosheath plasma was responsible for the heating of the F-region without the need for any further energization of the particles en route to the ionosphere. The Cluster estimation of the earthward Poynting flux was higher than that needed to produce the heating of the E-region inferred from MIRACLE observations, suggesting that part of the Poynting flux heated the E-region, with the remainder either contributing to Joule heating on smaller spatial scales than could be resolved, or being reflected or lost due to wave-particle interactions.

The launch of the Double Star mission provided an opportunity to study the mid- and high-altitude cusp simultaneously. Marchaudon et al. (2009) examined three injections of magnetosheath plasma into the cusp as observed by both Cluster and the Double Star TC-2 spacecraft, and the conjugate flows in the ionosphere observed by SuperDARN, during a period of southward and dawnward IMF. The velocity of the flux tubes containing the injected plasma was determined to be purely antisunward from the time delays between observations at the four Cluster spacecraft. This contrasted with the convection velocity of the plasma inside the flux tubes, which was both antisunward and dawnward, and in agreement with the corresponding ionospheric flows at the footprint of Cluster, as observed by SuperDARN. The minimum spatial extent of the flux tube containing injected plasma was determined transverse to the convection direction by the Cluster/TC-2 separation (which varied through the event) and found to be between 0.6 and 2 R_F, and the spatial extent along the convection direction was found (from the duration of the signature observed by Cluster) to be comparable. From minimum variance analysis on the magnetic field observations during each flux tube passage, the authors inferred that the flux tubes had a well-defined upstream edge, but a turbulent downstream edge. Finally, they compared quantitatively the field-aligned currents associated with the flux tubes at the altitudes of Cluster (using the curlometer technique, which exploits the tetrahedral configuration of Cluster to measure the curl of the magnetic field, and hence the current passing through the tetrahedron) and TC-2 (using a single-spacecraft method)—the two estimates compared well, and revealed that the flux tubes were associated with a pair of field-aligned currents, directed upward at the low-latitude edge of each structure and downward at the high-latitude edge.

3. Nightside Processes

In this section, we consider the contribution made by ground-based observations to Cluster studies of nightside processes. We focus in particular on the process of magnetic reconnection in the magnetotail, which occurs between the "open" field lines of the magnetotail lobes in each hemisphere (which are connected to the solar wind and, at the ionospheric end, to the polar cap), and which results in newly "closed" nightside magnetic field lines at lower latitudes (which form the plasma sheet, and which map to the auroral oval). The nightside reconnection process can occur quasi-steadily and on a small scale, but most nightside flux closure occurs during bursty events called substorms. Substorms consist of a "growth phase", in which the dayside reconnection rate exceeds the nightside rate resulting in a net addition of open flux to the lobes, followed by the substorm "onset", when a new reconnection site forms in the magnetotail, and "expansion phase" in which the nightside reconnection rate is much greater than the dayside rate. At onset, a pre-existing auroral arc brightens and fills the sky; this "auroral break-up" occurs initially in the midnight sector, but then expands rapidly poleward and westward (a "westward traveling surge"). Also at onset, the stretched magnetic field in the magnetotail plasma sheet suddenly becomes more dipolar; such a "dipolarization" is an indicator of a dramatic reconfiguration of the magnetotail and significant energy release in the magnetosphere. At the same time, the magnetospheric cross-tail current is diverted via field-aligned currents into, across, and back out of the ionosphere through a system called the "substorm current wedge" which enhances the auroral electrojet current in the ionosphere, and gives rise to magnetic perturbations that can be measured on the ground. The expansion phase is then followed by a recovery phase in which the magnetosphere returns to its pre-substorm state. A major topic of debate over the last quarter of a century has been whether the substorm process is initiated by the formation of a new magnetotail reconnection line, which

FEAR 14 of 46

causes the dipolarization of the (stretched) magnetotail magnetic field and hence diverts the cross-tail current to form the substorm current wedge (and enhance the auroral electrojet), or whether the cross-tail current is somehow disrupted, which causes the dipolarization and hence triggers the reconnection process. The signature of the magnetic field becoming more dipolar at an observation point in the magnetotail is often referred to as a "dipolarization front"; dipolarization fronts may arise as a consequence of a global dipolarization, but they may also occur in a more azimuthally narrow channel as a result of a more localized reconnection event, such as a "bursty bulk flow" (BBF), which is a substantial transport of magnetic flux in a localized flow burst. Both substorms and more localized reconnection events (e.g., BBFs) have an auroral and ionospheric response, and so ground-based observations allow the two to be distinguished. During both substorms and nightside reconnection under more "quiet" conditions, the nightside reconnection process may occur at multiple sites in the magnetotail which can give rise to flux ropes forming in the magnetotail which are then convected either Earthwards or downtail, which give rise to signatures that can be observed by spacecraft as they pass (e.g., "traveling compression regions", or TCRs). Furthermore, when the IMF is northward, the magnetotail typically becomes more twisted, and there is evidence that magnetotail reconnection may still occur. Northward IMF conditions also favor the formation of a relatively cold, dense plasma sheet (CDPS), which has been argued to form either due to dual lobe reconnection (see Section 2.2) "trapping" solar wind plasma in the dayside magnetosphere, followed by a period of reverse convection to bring it into the tail, or by transfer of magnetosheath plasma across the flank magnetopause via the KHI.

We divide this topic into two parts—in Section 3.1, we look at the study of substorms on a global scale, including the correspondence between substorm signatures in the magnetosphere and ionosphere, the global contribution made by substorms to magnetic flux closure, and the study of the substorm current wedge. In Section 3.2, we summarize work done on other signatures or modes of nightside reconnection, including BBFs and flux ropes (whether or not they occur within a substorm context) and non-substorm magnetotail reconnection during periods of northward IMF. Key questions that Cluster/ground-based studies have been able either to address, or to contribute to the debate on, include: Are substorms consistent with a current disruption model, or initiation by reconnection? How do dipolarizations of the magnetotail develop spatially? Precisely how are substorm magnetotail dynamics related to their auroral and ionospheric response? How do particular substorm signatures relate (quantitatively) to magnetic flux closure? What is the structure of the substorm current wedge? How are substorms and periods of lower magnetotail driving related? How are BBFs and flux ropes related to their auroral and ionospheric counterparts? What is the larger scale structure of BBFs? How do BBFs interact with the inner magnetosphere? What causes the nightside reconnection process to initiate? How does the magnetotail behave under northward IMF conditions? What causes the formation of the CDPS?

3.1. Substorms

Several Cluster substorm studies (e.g. Baker et al., 2002; Cao et al., 2008; Runov et al., 2008; Volwerk et al., 2008) have made use of either ground-based magnetometer observations or global-scale auroral imagery in order to identify substorm activity or time the onset. In order to limit the scope of this review, we focus on those substorm studies where the ground-based element forms a more intrinsic part of the study.

Ground-based observations lend themselves to substorm studies, since these observations can provide a more global picture than spacecraft measurements alone, and substorms are an inherently global process. Several early Cluster/ground-based studies examined the relationship between substorm signatures in the magnetotail, the inner magnetosphere and the ionosphere. Draper et al. (2004) examined two substorms within a 6 hr interval. In the first event, Cluster observed substorm signatures in the lobe (an increase in the magnetic field strength in the lobe during the growth phase, then a reduction in field strength following substorm onset), shortly after the occurrence of onset signatures in ground magnetometer data, with injection of plasma to geosynchronous orbit being observed by two LANL spacecraft later still (also a signature of substorm onset). The presence of substorm signatures at Cluster was despite the spacecraft being well away from the plasma sheet and at an earlier local time from the onset location (as inferred from ground-based magnetometer observations). The reduction in lobe flux at the onset of the expansion phase indicated that reconnection either began at, or had already begun by, onset. A little while later, Cluster observed an earthward-moving diamagnetic cavity embedded within the plasma sheet boundary layer (PSBL), the cause of which remains unclear (Draper et al., 2006). In the second event, the expansion phase onset was observed simultaneously by Cluster, ground magnetometer data and in the injec-

FEAR 15 of 46

tion signature observed by the Polar spacecraft. In both cases (and also in response to a pseudobreakup which occurred between the two substorms), the ionospheric response was an excitation of the nightside flow, which occurred shortly after the other signatures and was observed by SuperDARN. A key difference between the flows excited in response to the pseudobreakup and those in response to the substorm expansion onset was the location, with the expansion phase flows occurring equatorward of the pseudobreakup flows.

Borälv et al. (2005) also showed a good correspondence between space- and ground-based onset signatures (including three subsequent re-intensifications of a moderate substorm). At onset, a negative bay was observed in ground-based magnetometer data (indicative of the substorm current wedge enhancing the auroral electrojet), along with an enhancement in precipitation observed by EISCAT, an excitement of equatorward flows in the nightside of the polar cap observed by SuperDARN, and an auroral break-up signature which was observed by an all-sky camera. The three subsequent intensifications were identified by means of a further negative enhancement in the ground-based magnetometer data, and also corresponded to enhanced precipitation observed by EISCAT. The first intensification also corresponded to further enhanced nightside flows observed by SuperD-ARN. At each of these times, Cluster observed either the passage of a TCR, suggesting the presence of several reconnection lines being active at the NENL, or an entry to/exit ("drop-out") from the plasma sheet, interpreted as due to plasma sheet thickening and thinning during the substorm cycle. In several plasma sheet entries/exits, the component of the plasma sheet motion in the *Y* direction was found to be significant, from which the authors concluded that such events were due to an azimuthally localized, but expanding, region of plasma sheet thinning. The fact that substorm features were observed in the tail even during a relatively weak substorm indicated that even low-intensity substorms can have magnetospheric effects.

H. Wang et al. (2006) also studied the global manifestations of a substorm; an auroral breakup, which subsequently expanded azimuthally and polewards, was observed by the IMAGE satellite. A sharp drop was observed in the *X*-component of a conjugate ground-based magnetometer, indicative of the enhancement of the auroral electrojet, and hence the formation of a substorm current wedge. The low-altitude CHAMP spacecraft observed an intense upward field-aligned current close to the onset location, sandwiched between two downward currents; west-ward/eastward Hall currents were observed poleward and equatorward, respectively, of the upward field-aligned current, all of which was consistent with the signatures expected of a Harang discontinuity (which is a sharp reversal in the pre-midnight ionospheric convection pattern). Double Star TC-1 (southward of the neutral sheet) observed a dipolarization, which was followed ~1.5 min later by a dipolarization at Cluster (northward of the neutral sheet). Since Cluster and Double Star were also separated azimuthally, the delay between the two observations was indicative of a predominantly dawnward propagation of the dipolarization, the velocity of which was consistent with both that inferred from the difference in timings of the Cluster observations, and also the eastward expansion speed inferred from IMAGE Wideband Imaging Camera (WIC) observations.

Some of these early studies exploited data from nightside radial alignments with other spacecraft missions to provide a foretaste of the kind of studies that the THEMIS mission (which includes integrated ground-based observatories) would go on to enable, and in particular to comment on the initiation mechanism for substorms. Sergeev et al. (2005) observed the development of an isolated substorm that occurred during a fortunate radial configuration of the LANL-01A, LANL-02A, Polar, Geotail and Cluster spacecraft, and which was also observed in global auroral imagery and ground-based magnetometer data. During the substorm growth phase, the cross-tail current growth, magnetotail magnetic energy loading and expansion of the auroral oval were all observed to be very strong, but the following substorm expansion phase was characterized by a disproportionately weak dissipation of energy observed in the auroral current response, the energy deposited in the auroral oval, and the relatively low-energy injection signatures (as observed in ground-based magnetometer observations, global auroral images and at geostationary orbit, respectively). The authors suggested that this disparity between strong energization in the growth phase and relatively weak dissipation in the expansion phase could be understood by considering the relatively cool and dense nature of the plasma sheet at the time, due to a preceding extended period of northward IMF (see Section 3.2), which could impact the development of the substorm in a number of ways. The authors also concluded that the relative ordering of substorm onset signatures was consistent with initiation by midtail magnetic reconnection. On the other hand, Lui et al. (2007) used a near-identical set of ground- and space-based assets (except with the LANL-90 and GOES-12 spacecraft as monitors of the nightside geostationary orbit), which again happened to be aligned in a string downtail, to examine the temporal order of two substorm intensifications, as observed on the ground, in the aurora and at the various spacecraft. These were argued to be consistent

FEAR 16 of 46

with the current disruption model which places substorm initiation in the near-Earth region. Furthermore, the lack of significant plasma flow (and dawnward-directed electric field) observed by Cluster were consistent with this conclusion. More recently, Hwang et al. (2014) used conjugate Cluster and ground-based magnetometer observations to investigate the propagation of two dipolarization fronts observed at a substorm onset. Cluster was situated in the near-Earth plasma sheet and observed an enhancement in B_Z , which propagated tailward and was followed by a series of flux ropes (also moving tailward). About 5 minutes later, another B_Z enhancement was observed, this time propagating earthward and followed by a global magnetic dipolarization behind the front. The evolution of ground-based magnetometer signatures associated with the first dipolarisation front (from lower to higher latitudes) also indicated that it propagated tailward, while the more complex, but overall equatorward evolution of magnetic signatures associated with the second (more global) dipolarisation supported the conclusion of earthward propagation. The combined in situ and ground-based signatures were also interpreted as consistent with the current disruption model of substorms, with the first (tailward-moving) dipolarisation front being a consequence of current disruption in the near-Earth plasma sheet which propagates tailward, triggering magnetic reconnection tailward of the spacecraft which gave rise to the (earthward-moving) more global dipolarisation.

Another important contribution that ground-based measurements can make is that they allow the investigation of changes in the global open flux content of the magnetotail during substorms, in a similar manner to the determination of the "size" of dayside reconnection events discussed in Section 2.2 above, as this cannot be determined from spacecraft observations alone. Milan et al. (2006) analyzed a substorm which was observed in the magnetotail by both Cluster and Double Star TC-1, with supporting ground-based magnetometer, SuperD-ARN radar and space-based global auroral imagery observations. Collectively, these observations allowed the magnetotail dynamics, auroral evolution, convection response and development of the substorm current wedge to be monitored through this event. Several dipolarizations were observed by Cluster and Double Star, which each corresponded to a negative bay, or further negative enhancement, in ground-based magnetometer data, indicative of the development and evolution of the substorm current wedge. Several of the dipolarizations also corresponded to auroral brightenings, and the evolution of the auroral bulge was observed. Global SuperDARN observations allowed the cross polar cap potential to be monitored, which should approximate to the mean of the dayside and nightside reconnection rates. The first two dipolarizations were interpreted as signatures of a two-stage onset. The first dipolarization was due to the initiation of reconnection of closed field lines at the NENL (and was associated with a short-lived development of a small auroral bulge and a modest substorm current wedge magnetic bay, but no significant enhancement in the ionospheric convection). The second dipolarization represented the transition to reconnection of open field lines; this transition was associated with enhanced and prolonged auroral brightenings, the development of a westward-traveling surge, and an increase in the cross polar cap potential (indicating enhanced convection). IMAGE observations of the auroral oval in wavelengths sensitive to electron and ion precipitation, respectively, indicated that the westward-traveling surge was associated with a localized and intense region of electron precipitation, whilst the remainder of the auroral bulge was associated with a more distributed ion precipitation region; the authors identified these regions as the locations of the upward and downward field aligned currents associated with the substorm current wedge. Throughout the period, compressions of the lobe magnetic field observed by Cluster were interpreted as signatures of many small-scale, earthward-moving flux ropes (indicating that the NENL consisted of multiple reconnection lines). Following the onset of reconnection of open field lines, the subsequent dipolarizations were interpreted as step-wise movements of the NENL downtail, in response to flux pile-up in the near tail arising from field lines being closed but the subsequent return convection to the dayside being sluggish, as a result of enhanced ionospheric conductivity. The authors estimated that each dipolarization corresponded to the closure of about 0.1 GWb of open flux, and that the reconnection site moved tailward with an average speed of $\sim 20 \text{ km s}^{-1}$. After an initial increase during the growth phase, the total polar cap flux (estimated from the size of the polar cap in the IMAGE observations) remained constant until the last dipolarization, indicating that the nightside reconnection rate during most of this substorm was being balanced by the rate at which dayside reconnection added newly opened flux to the lobe.

An area of significant interest for conjugate Cluster/ground-based studies has been the structure of the substorm current wedge. Forsyth et al. (2014) used observations from two of the Cluster spacecraft during a perigee pass through the auroral acceleration region to examine the azimuthal structure of the substorm current wedge, finding it to be made up of a large number of north-south aligned current sheets (Figure 3). When integrated over sufficiently large spatial scales, these current sheets reproduced the traditional simple line current model of the substorm current wedge (flowing into the ionosphere from dawn and out to the ionosphere toward dusk).

FEAR 17 of 46

21699402, 2022, 8, Downloaded from https://agupubs.onlinelibrary.wiley.com/doi/10.1029/2021JA029928 by University Of Southampton, Wiley Online Library on [09/11/2022]. See the Terms and Conditions (https://agupubs.onlinelibrary.wiley.com/doi/10.1029/2021JA029928 by University Of Southampton, Wiley Online Library on [09/11/2022]. See the Terms and Conditions (https://agupubs.onlinelibrary.wiley.com/doi/10.1029/2021JA029928 by University Of Southampton, Wiley Online Library on [09/11/2022]. See the Terms and Conditions (https://agupubs.onlinelibrary.wiley.com/doi/10.1029/2021JA029928 by University Of Southampton, Wiley Online Library on [09/11/2022]. See the Terms and Conditions (https://agupubs.onlinelibrary.wiley.com/doi/10.1029/2021JA029928 by University Of Southampton, Wiley Online Library on [09/11/2022]. See the Terms and Conditions (https://agupubs.onlinelibrary.wiley.com/doi/10.1029/2021JA029928 by University Of Southampton, Wiley Online Library.

and-conditions) on Wiley Online Library for rules of use; OA articles are governed

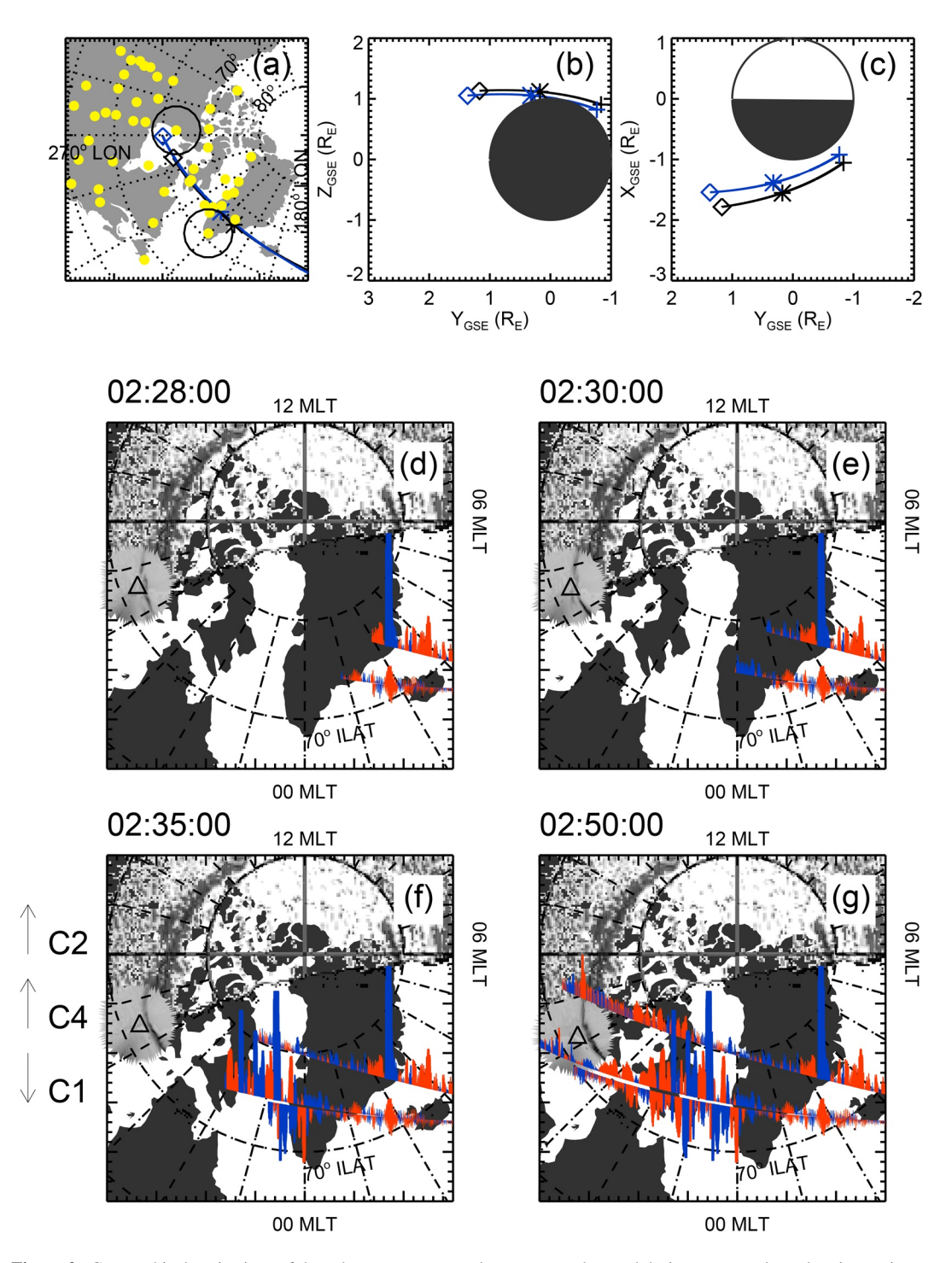


Figure 3. Geographical projections of the substorm current wedge structure observed during an auroral acceleration region pass, reproduced from Forsyth et al. (2014). Panel (a) shows the geographical footprints of Clusters 1 and 4 (black and blue traces) in relation to the ground magnetometer stations (yellow dots) and all sky imagers (ASIs) (black circles) used in the study. Panels (b and c) show the projections of the Cluster 1 and 4 orbits into the GSE YZ and XY planes, respectively. Panels (d–g) show the footprints of Clusters 1, 2, and 4, overlaid by the magnetic field gradients observed by the spacecraft (perpendicular to the footprint track—negative gradients in red, positive gradients in blue, corresponding to structure in the field aligned currents forming the substorm current wedge). The dayside aurora from a single image from a Defense Meteorological Satellite Program Special Sensor Ultraviolet Spectrographic Imager instrument is overlaid in grayscale in the top half of each panel. Also overplotted (surrounding the triangle in each panel) is auroral data from an ASI.

FEAR 18 of 46

Both spacecraft observed large-scale regions of net upward and net downward field-aligned current, consistent with the large-scale characteristics of the substorm current wedge, but sheets of oppositely directed current were embedded within both regions. Ground-based magnetometers allowed the large-scale current system to be reconstructed, but were unable to detect the small-scale currents observed by Cluster, consistent with the fact that the ground-based magnetometers detect the integrated effects of all ionospheric currents from a vantage point 100 km below. The fact that the current sheets observed by Cluster were north-south aligned was in contrast to previous statistical analyses that had shown that auroral currents tend to be aligned east-west, but was consistent with north-south aligned auroral forms in the substorm bulge (auroral streamers) that are associated with BBFs (see Section 3.2). It had previously been proposed that the substorm current wedge may be made up of a number of "wedgelets" each associated with a separate BBF, but by comparing their observations with previous observations of BBF current systems, the authors concluded that their observations did not support the scenario in which BBFs created the small-scale structure comprising the substorm current wedge. The lack of auroral data or magnetotail observations of plasma flows meant that Forsyth et al. (2014) could not conclusively rule out BBFs as the source of the observed structure, but they noted that their observations presented a significant challenge to the idea. However, this latter explanation was favored by Palin et al. (2016), who used global-scale IMAGE observations of the aurora, and ground-based magnetometer observations to study further a previously examined substorm observed by Cluster, Polar and Geotail. In particular, they showed that during the substorm expansion phase, the substorm current wedge (as observed indirectly by ground-based magnetometer observations) was modulated by the arrival of multiple BBFs (referred to in this, and some other studies, as "nightside FTEs"), with the arrival of multiple BBFs leading to the formation of multiple small substorm current wedges. The authors concluded that together, these multiple intensifications added to form the envelope of the magnetic disturbance pattern associated with a substorm. In particular, the first bursty bulk flow (observed at substorm onset), which was responsible for the first significant global dipolarization of the magnetosphere, was associated with a major tail current reduction or disruption, and was also responsible for the initial substorm current wedge formation.

3.2. Other Nightside Reconnection Events

Several studies have investigated the dynamics of BBFs, including their relationship with their auroral counterparts. Two main types of auroral signature have been observed to be linked with BBFs—pseudobreakups, which are a localized brightening of the aurora which then fades, and auroral streamers, which are approximately north-south aligned, longitudinally narrow auroral forms which first appear at the poleward boundary of the auroral oval, and then expand equatorward. Grocott et al. (2004) studied an interval during a substorm growth phase (and relatively quiet background geomagnetic conditions) in which the Cluster spacecraft observed the passage of a BBF in the near-Earth inner central plasma sheet. Conjugate SuperDARN observations revealed a transient enhancement to the flow seen in the midnight sector, consistent with idea of a BBF being a burst of convective transport in the tail. This transient flow enhancement was located just poleward of a localized auroral brightening (a pseudobreakup) observed by the IMAGE satellite, indicative of electron precipitation, Ground-based magnetometers observed Pi2 pulsations, which are known to be driven by BBFs, but only small-amplitude perturbations, implying (given the significant ionospheric flow) very low levels of ionospheric Hall conductivity. The field-aligned currents implied by the flow data were consistent with a substorm current wedge-type system, but on a much smaller scale (carrying up to ~0.1 MA, an order of magnitude less than is thought to be carried in the substorm electrojet). The transpolar voltage deduced from the global flow pattern increased during the BBF; careful analysis indicated that although this was in part due to an enhancement in the dayside driving, it was also partly due to an enhancement in the nightside reconnection rate which the authors inferred gave rise to the BBF. This in turn was consistent with the observation of the open-closed field line boundary contracting poleward before then expanding equatorward, as a burst of nightside reconnection was embedded within a substorm growth phase in which there was a net addition of open flux to the magnetotail. Therefore, although the event exhibited similarities to a substorm, it was a significantly smaller-scale event, indicating that the simplistic distinction between substorm cycle versus quiet times was not sufficient to explain the variety of ways in which the tail responds to varying levels of dayside driving.

Volwerk et al. (2004) examined the events surrounding a nightside bulk convection event observed by Cluster, which they referred to as a rapid flux transport event. This event bore some similarities to a BBF except that Cluster was situated in the lobe and found itself in a region locally evacuated of magnetic field. Ground-based

FEAR 19 of 46

magnetometer data demonstrated that the reconnection event was spatially patchy. The local reduction in magnetic flux arose as a result of the earthward flow of plasma and magnetic flux observed by Cluster, and resulted in a reconfiguration of the pressure balance between the different regions of the tail and the solar wind. The changes in equilibrium resulted in the magnetotail magnetic field oscillating with a period of \sim 20 min, demonstrating how an oscillation of the magnetotail can be instigated by fast flows.

Several more recent studies have examined the relationship between BBFs and auroral streamers. Streamers start with a poleward boundary intensification, which is an auroral emission which initiates at the poleward boundary of the auroral oval (i.e., at the open-closed field line boundary), but an auroral streamer then extends equatorward, onto field lines that cross the equator closer to the planet (consistent with the Earthward motion of the BBF). Some studies have investigated this relationship by exploiting ground-based magnetometer data (e.g., from the IMAGE/MIRACLE magnetometer network) to calculate the ionospheric equivalent currents associated with BBFs. Nakamura et al. (2005) studied the disturbance in the magnetosphere and ionosphere caused by an isolated BBF observed by Cluster; the footprint of Cluster was located in a region of upward field-aligned current, consistent with the magnetospheric observations, and the wider ionospheric equivalent current system (and inferred field-aligned currents) were shown to be similar to the pattern observed in previous observations of auroral streamers. In a statistical study of the ionospheric equivalent currents associated with BBFs observed by Cluster, Juusola et al. (2009) showed that in the majority of cases, the BBFs were associated with a relatively narrow channel of northwestward equivalent current density with upward field-aligned current at its southwestern flank (which would be expected to correspond to an auroral streamer) and downward field-aligned current at its northeastern flank. The mean duration of BBFs observed when the footprint of the Cluster spacecraft was close to the poleward boundary of the oval was longer than that when the footprint was close to the equatorward boundary, consistent with the suggestion that braking of high-speed flows takes place between 20 and 10 $R_{\rm r}$ downtail.

Pitkänen et al. (2011) studied a series of BBFs observed by Cluster during a period of quiet geomagnetic activity, and the corresponding streamer signatures which were observed both as an auroral signature by an all-sky camera, and in the form of latitudinally restricted enhancements in the F-region electron temperature by EISCAT (Figure 4). Both the spacecraft and auroral observations implied that the streamer/BBF had a significant tilt in the magnetosphere, meaning that Cluster sampled the plasma flows dawnward and duskward of the BBF, as well as within it. Cluster observed typical signatures of an earthward-moving BBF, including deflection and compression of the plasma sheet plasma ahead of the BBF, magnetic signatures of shear flow, and flow within the BBF. These observations were consistent with the "bubble" model of BBFs, in which the bubble represents depleted flux tubes which are propelled earthward by the interchange instability, arising due to the decreased cross-tail current across the flux tubes. Furthermore, Cluster showed clear evidence of tailward return flows adjacent to the bubble. The duskside return flows were associated with a decrease of plasma density, supportive of a previous suggestion of a wake being formed by the depleted flux tubes which slips tailward around the edge of the bubble, though the dawnside return flows were associated with an increase in plasma density. The conjugate flow patterns observed by the EISCAT VHF radar were consistent with the Cluster observations, including the return flows, thus providing the first simultaneous observations of BBF return flows in both the plasma sheet and ionosphere. An enhancement in the nightside reconnection rate was inferred from the EISCAT measurements. Overall, these combined observations provided support for the "bubble" model of BBFs.

BBFs, and streamers, are also observed during substorm activity. Forsyth et al. (2008) used the curlometer technique to calculate the field-aligned currents within a BBF that was observed a few minutes after substorm onset; when the current density was projected into the ionosphere, it compared favorably with previous (ground-based) estimates of the field-aligned currents associated with auroral streamers. Furthermore, the combined plasma and magnetic field observations from the Cluster PEACE, CIS and FGM instruments were consistent with the BBF being created by the reconnection of open field lines Earthward of a substorm-associated near-Earth neutral line. The theoretical interpretation put forward by the authors was also consistent with the idea that pseudobreakup signatures (as observed, e.g., in the BBF study by Grocott et al. (2004), discussed above) are the auroral signatures of BBFs observed outside of substorm times.

Juusola et al. (2013) presented Cluster observations of earthward and tailward flow signatures during a substorm onset, and their ionospheric signatures. Similar to the quiet-time observations of Pitkänen et al. (2011), the earthward flow signatures corresponded to equatorward-propagating auroral streamers and a channel of enhanced poleward equivalent ionospheric current (observed by or inferred from observations from the MIRACLE

FEAR 20 of 46

21699402, 2022, 8, Downloaded from https://agupubs.onlinelibrary.wiley.com/doi/10.1029/2021JA029928 by University Of Southampton, Wiley Online Library on [09/11/2022]. See the Terms and Conditions (https://agupubs.onlinelibrary.wiley.com/doi/10.1029/2021JA029928 by University Of Southampton, Wiley Online Library on [09/11/2022]. See the Terms and Conditions (https://agupubs.onlinelibrary.wiley.com/doi/10.1029/2021JA029928 by University Of Southampton, Wiley Online Library on [09/11/2022]. See the Terms and Conditions (https://agupubs.onlinelibrary.wiley.com/doi/10.1029/2021JA029928 by University Of Southampton, Wiley Online Library on [09/11/2022]. See the Terms and Conditions (https://agupubs.onlinelibrary.wiley.com/doi/10.1029/2021JA029928 by University Of Southampton, Wiley Online Library on [09/11/2022]. See the Terms and Conditions (https://agupubs.onlinelibrary.wiley.com/doi/10.1029/2021JA029928 by University Of Southampton, Wiley Online Library.wiley.com/doi/10.1029/2021JA029928 by University Of Southampton, Wiley Online Library.wiley.com/doi/10.1029/2021JA02929 by University Online Library.wiley.com/doi/10.102

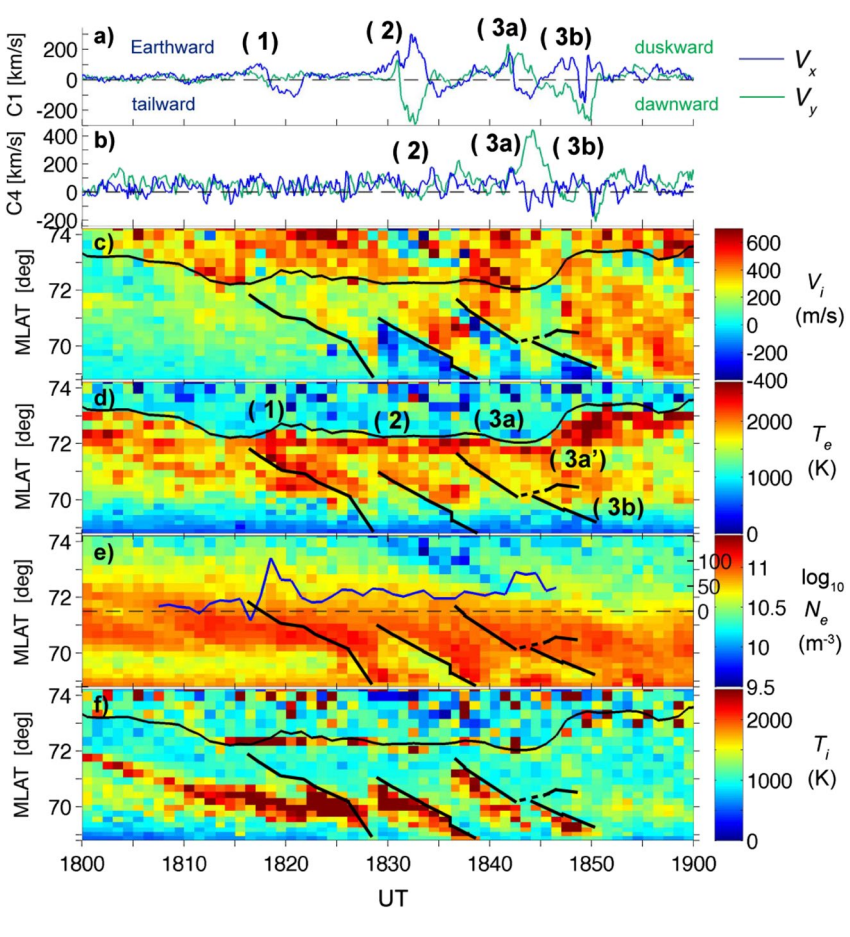


Figure 4. Cluster and European Incoherent Scatter facility VHF data, reproduced from Pitkänen et al. (2011). Panels (a and b) show the Cluster Ion Spectrometry HIA V_X and V_Y velocity components in GSM, for Clusters 1 and 4, respectively. Panels (c-f) show the line of sight ion velocity (positive toward the radar), electron temperature, electron density and ion temperature, respectively. Bursty bulk flows are evident as positive enhancements in the V_X component, observed primarily at Cluster 1. The black continuous line in panels (c, d, and f) is the estimate of the polar cap boundary, and the thicker, discontinuous black lines indicate the equatorward propagation of features which are the radar analog of auroral streamers, and associated with the earthward-propagating bursty bulk flows.

ground-based auroral cameras and magnetometers, respectively). In contrast to the Pitkänen et al. (2011) observations, a large-scale magnetotail dipolarization was observed by both Cluster and Double Star, even though the satellites were separated by 3 hr in MLT, which resulted in an additional poleward expansion of the ionospheric signatures. The tailward-propagating flows observed by Cluster were associated with a region of equatorward equivalent ionospheric current on the flank of the poleward current channel corresponding to the earthward plasma sheet flow. Given that the tailward flow observed by Cluster was immediately preceded by earthward flow with an embedded dipolarization front, and followed immediately by a large-scale dipolarization, the tailward flow (and corresponding ionospheric signatures) were interpreted as the rebound of earthward flow from the intense dipolar magnetic field of the inner magnetosphere, rather than deflection of the plasma sheet plasma ahead of the earthward flow channel (as in Pitkänen et al., 2011). Amm et al. (2011) reported Cluster observations of a BBF and conjugate auroral streamer during a substorm recovery phase, in a period in which the nightside auroral oval exhibited a distinct "double oval" configuration (which is a typical configuration during substorm expansion and recovery phases). The combined analysis of EISCAT mainland radar, IMAGE satellite and MIRACLE ground-based magnetometer observations revealed some significant differences between the auroral streamer during this double oval event and previously studied streamers without such a double oval configuration. In particular, the equivalent current system calculated from MIRACLE observations differed from the more typical streamer current system, in that the current system was almost completely poleward (linking the two elements of the auroral oval), without a clear vortical structure at its flank. The total meridional equivalent current transported

FEAR 21 of 46



Journal of Geophysical Research: Space Physics

10.1029/2021JA029928

by this recovery phase streamer was weaker than typically observed in expansion phase streamers, just as magnetospheric/ionospheric currents are weaker more generally in the recovery phase. The authors attributed these differences to a poleward-pointing polarization electric field being generated at the boundaries between the two oval portions and the dim, less conductive region between them.

Pitkänen et al. (2013) presented observations of two BBFs observed by Cluster during the growth and expansion phases of a substorm; one of the BBFs was preceded by a channel of enhanced flow in the polar cap, observed by EISCAT, which impinged on the open-closed boundary (as determined from EISCAT temperature observations). SuperDARN observations, covering a larger area, indicated that this flow was part of a larger-scale, but twisted, two-cell convection pattern. As the flow channel reached the open/closed boundary, an elevation in the F-region electron temperature was observed by EISCAT, which was interpreted as a signature of a poleward boundary intensification. This was followed by enhanced equatorward flows which were observed in the auroral oval by EISCAT, and which corresponded to the second BBF observed by Cluster. It had previously been suggested that enhanced flows on open field lines could trigger plasma sheet flow bursts on arrival at the open/closed boundary, and the observations were interpreted as consistent with that idea. In particular, they provided the first observations of all stages in this process—a polar cap flow channel impinging on the open/closed boundary, an equatorward ionospheric flow burst within the auroral oval and the corresponding plasma sheet flow burst.

Recently, Wei et al. (2021) have used observations from Cluster, Swarm, and ground-based magnetometer data collated from SuperMAG (plus supporting observations from several other satellites) to investigate the ionospheric/ground response to magnetospheric BBFs. The authors concluded that localized substorm currents detected by the ground-based magnetometers were caused by BBFs observed in the inner magnetosphere by Cluster. A similar field-aligned current structure was observed by both Cluster (calculated using the curlometer technique) and Swarm, which connected the intense ground perturbations to the BBFs in the inner magnetosphere directly. The authors concluded that intense variations in the surface magnetic field (which drive geomagnetically induced currents in ground-based technological infrastructure) can be driven by BBFs in the inner magnetosphere.

Flux ropes are another signature of magnetotail reconnection, which can occur either during substorms or non-substorm intervals. Zong et al. (2007) analyzed the auroral and ionospheric signatures associated with an earthward-moving magnetotail flux rope observed by Cluster. The IMAGE satellite observed a localized auroral brightening just poleward of the Cluster footprint, at the same time as the flux rope was observed by Cluster. The brightening then moved equatorward past the Cluster footprint. Both IMAGE and the Polar UVI imager (observing the northern and southern hemisphere auroral regions, respectively) observed auroral forms moving to lower latitudes over the next few minutes, consistent with the expected mapping of earthward-convecting field lines. The equivalent ionospheric currents deduced from the ground-based IMAGE magnetometer network showed a westward equivalent current, which became enhanced at the time of the flux rope observation, and subsequently moved equatorward. The flux rope was not associated with a substorm, but authors argued that the westward currents observed by the IMAGE magnetometer network demonstrated that the flux rope inhibited the cross-tail current, which was then diverted down to the ionosphere in a manner similar to the substorm current wedge. Amm et al. (2006) and Juusola et al. (2008) also examined the auroral and ionospheric signatures associated with a pair of earthward-moving flux ropes observed by Cluster, this time during the expansion and recovery phase of a substorm, respectively. For the first event, Amm et al. (2006) found the ionospheric footprints of Cluster coincided with a region of reduced auroral emission, reduced conductances and downward field-aligned current, which together with a trailing region of upward current they suggested corresponded to the ends of the flux rope, whereas for the second event Juusola et al. (2008) found no clear signatures in the conjugate ionosphere that could be related to the flux rope. The authors concluded that the absence of clear ionospheric signatures might arise due to the orientation and/or length of the second flux rope, as although a flux rope is embedded in an environment that maps to the ionosphere, the flux rope itself is only connected to the ionosphere at its dawnward and duskward ends. (Indeed, the authors note that a flux rope that maps across the entire tail may not connect to the ionosphere at all.)

Moving to lower latitudes, Parkinson et al. (2007) used Cluster WHISPER observations, and EUV observations from the IMAGE satellite, to map the location of the plasmapause relative to a Subauroral Polarization Stream (SAPS) that was observed by one of the SuperDARN radars. SAPS are large westward flows which occur at, or equatorward of, the lower edge of the auroral oval (though in this study, the authors used the term "auroral westward flow channel"). Usually, SAPS are associated with substorms, but in this case it was observed during

FEAR 22 of 46

a period of persistent, moderate geomagnetic activity. The peak flows were located just poleward of the plasmapause, though the equatorward edge of the flow channel overlapped the plasmapause. The peak of the flow channel was also situated close to the peak of the Region 2 field-aligned current, which maps to the ring current. DMSP observations confirmed the flow channel was located equatorward of the nightside plasma sheet.

Magnetotail reconnection can also occur during periods of northward IMF, giving rise to azimuthal flow bursts called Tail reconnection during IMF Northward, Non-substorm Intervals (TRINNIs) that can be observed in the ionosphere and magnetosphere, and which are asymmetric about midnight MLT. Grocott et al. (2007) provided conjugate observations of two such flow bursts using data from Cluster (in the central plasma sheet) and Super-DARN. In both cases, Cluster observed isolated bursts of earthward plasma convection, but there was also an azimuthal component of the velocity vector perpendicular to the magnetic field (V_{1V}) . In the first case, V_{1V} was duskward, consistent with the westward azimuthal flows observed in the midnight sector by the northern hemisphere SuperDARN radars. In the second event, Cluster 4 observed a significant dawnward flow, which was again consistent with the eastward midnight sector flows observed by the northern hemisphere radars, but Cluster 3 observed a duskward flow which was consistent with the duskward sense of convection observed by the southern hemisphere SuperDARN radars. This implied that the two spacecraft were on different field lines which straddled the sector dividing the field lines which convect back to the day side via the dawn flank from those which do so via dusk. The observations were consistent with previous SuperDARN observations of northward IMF nightside reconnection-induced flows, but constituted the first in situ evidence for magnetotail reconnection in a twisted tail under northward IMF conditions. Similar observations were reported by Pitkänen et al. (2015)—in their event, the neutral sheet flapped over the Cluster spacecraft, and as Cluster crossed the neutral sheet a reversal of the $V_{1,1}$ component was observed. Interhemispheric SuperDARN observations revealed the presence of TRINNI signatures. The reversal in $V_{\perp Y}$ as the spacecraft crossed the neutral sheet was consistent with the TRINNI mechanism, given the inclination of magnetotail field lines in a twisted tail and the location of the spacecraft in the midnight sector (i.e., near to the plane separating dawnward from duskward return convection). Consequently, as the spacecraft moved southward relative to the plasma sheet, it moved from field lines which return dawnward to those which return duskward. The authors noted a small offset between the $V_{\perp Y}$ reversal and the neutral sheet—although in this specific case, the offset was statistically insignificant, they noted that in general such an offset may arise if the spacecraft is located slightly further away from midnight MLT, as the axis separating dawnward from duskward flows is inclined in the Grocott et al. (2007) scenario, and hence the expected reversal in $V_{\perp V}$ occurs further away from the neutral sheet at earlier and later local times.

Another magnetotail phenomenon associated with periods of northward IMF is the formation of the CDPS. Two main mechanisms have been put forward to explain the formation of the CDPS: "trapping" of magnetosheath plasma on the day side by dual lobe reconnection (see Section 2.2) which then undergoes reverse convection into the tail, and transfer of magnetosheath plasma across the flank magnetopause by the KHI. Taylor et al. (2008) used a wide array of space- and ground-based data sets, including observations from Cluster, the two Double Star spacecraft and Polar, to investigate a case study of the formation of the CDPS during a period of sustained northward IMF. Polar, situated in the southern hemisphere post-noon sector, observed a persistent LLBL with no evidence of magnetopause waves, and which was consistent with a solar wind origin. Global SuperDARN observations showed clear evidence of sunward convection in the northern hemisphere, indicating the occurrence of high latitude (lobe) reconnection (see Section 2.2). The IMAGE satellite observed a cusp spot signature poleward of the main auroral oval, also indicative of lobe reconnection but this time in the southern hemisphere; therefore, the two data sets combined were indicative of high latitude reconnection occurring in both hemispheres simultaneously. Similar plasma populations were observed further downtail by Double Star TC-1, in a boundary layer further down the dusk flank, and by TC-2 in the near-Earth magnetotail. The TC-1 boundary layer entries were periodic, indicative of boundary wave activity, but the Cluster spacecraft (situated in the post-noon magnetosheath) did not observe any such activity, indicating that the waves observed by TC-1 were locally driven. Comparisons of the electron phase space density showed that the boundary layer observed by Polar was not sufficient to source the flank boundary layer observed by TC-1, and so the authors concluded that the boundary layers and CDPS were formed as a result of a combination of dual lobe reconnection and flank KHI in this interval.

FEAR 23 of 46

21699402, 2022, 8, Downloa

4. ULF Waves

Conjugate ground-based observations have made important contributions to the study of ULF waves with Cluster. ULF waves are oscillations of magnetospheric magnetic field lines, which can be excited by the solar wind. They are categorized into several classes based on their frequency and whether the pulsations are continuous (Pc1-Pc5, with Pc1 waves corresponding to periods of 0.2-5 s and Pc5 waves with periods of 150-160 s) or irregular (Pi1 and Pi2, corresponding to periods of 1-40 and 40-150 s, respectively). Several mechanisms have been proposed to excite ULF waves from solar wind dynamic pressure changes, including: direct transmission of ULF oscillations in the solar wind into the magnetosphere; abrupt step-like changes in the solar wind dynamic pressure compressing the magnetosphere and exciting broadband fast mode waves, which then couple to local standing Alfvén waves through field line resonance; quasiperiodic oscillations in the solar wind dynamic pressure buffeting the magnetopause such that compressional-mode waves are excited; and KHI at the flank magnetopause driving ULF magnetopause oscillations, which in turn couple to standing Alfvén waves. Key questions that Cluster/ground-based studies have addressed include: Which mechanisms are responsible for ULF waves observed in different frequency bands? Under what conditions are the wave packets local or global phenomena? Can fluctuations on the ground be directly linked to driving processes, for example, at the magnetopause or bow shock, or in the solar wind? Can the path of energy transfer be observed all the way from source to ground? What is the role of field line resonances in electron acceleration and the generation of discrete auroral arcs? Are theories of the linkage between magnetospheric and ground-based ULF pulsations correct? Are theories that connect ULF activity with the growth of chorus waves correct? Are there preferred frequencies for field line resonances? How do waves at different frequencies couple with field lines at different latitudes? Can artificial heating experiments be used to "tag" field lines to test conjugacy?

Mann et al. (2002) presented Cluster and ground-based magnetometer, radar and auroral observations of Pc5 ULF waves being excited at the magnetopause, and observed on the ground. Cluster, situated on the dusk flank, observed a quasi-periodic motion of the magnetopause boundary layer back and forth across the spacecraft, which was interpreted as due to the KHI. The frequency of these Cluster boundary layer entries matched closely the discrete frequencies of ULF waves (field line resonances) observed on the ground in magnetometer, radar, and auroral data, giving strong support to the idea that fluctuations on the ground were directly related to the magnetopause observations, with the oscillating wave mode at the magnetopause being converted into a field line resonance deeper within the magnetosphere. Although there were no in situ observations available on the dawn flank, similar ULF waves were observed in dawn-side ground-based data, suggesting that KHI was simultaneously causing these wave modes and field line resonances on both the dawn and dusk flank. This study was the first time that field line resonance signatures had been seen simultaneously, and at the same location, with radar, magnetometer and optical instrumentation. The presence of wave activity in the auroral observations provided evidence of a close relationship between field line resonances and the generation of discrete auroral arcs.

Subsequent studies were able to provide observations directly within the region of mode conversion. Rae et al. (2005) did so with observations of Pc5 wave activity during a favorable radial alignment of Cluster, Polar and geosynchronous satellites during another period of fast solar wind. Cluster again observed magnetic field and ion variations that were interpreted as oscillatory motion of the magnetopause boundary layer across the spacecraft, again presumed to be due to the KHI. These compressional waves coupled to resonant field line oscillations in a region close to Polar and the geostationary satellites; Polar observed Poynting vectors that were consistent with a standing Alfvén wave oscillation. These standing waves were then observed in both SuperDARN radar and ground-based magnetometer data. In all regions, there was a peak in the wave power in the same frequency range (1.4-1.6 mHz), allowing the authors to argue a well-defined path of energy transfer from magnetopause oscillations driven by the solar wind, down to the inner magnetosphere and ionosphere (Figure 5). There was no corresponding peak in the same frequency range in the solar wind dynamic pressure, allowing the authors to conclude that the magnetospheric waves observed were not due to direct driving by solar wind pressure oscillations. In a separate study, Sung et al. (2006) also provided Polar observations from the mode-coupling region, this time from an interval when Cluster was situated near the bow shock. Cluster observed a series of bow shock crossings in response to observed upstream variations in the solar wind dynamic pressure; a ~30 min interval of compressional oscillations in the Pc5 band was observed by Polar. These oscillations were interpreted as being driven by the motion of the bow shock and magnetopause in response to the solar wind pressure variations. High coherence between the electric and magnetic field oscillations observed by Polar suggested a coupling

FEAR 24 of 46

21699402, 2022, 8, Downloaded from https://agupubs

onlinelibrary.wiley.com/doi/10.1029/2021JA029928 by University Of Southampton, Wiley Online Library on [09/11/2022]. See the Terms

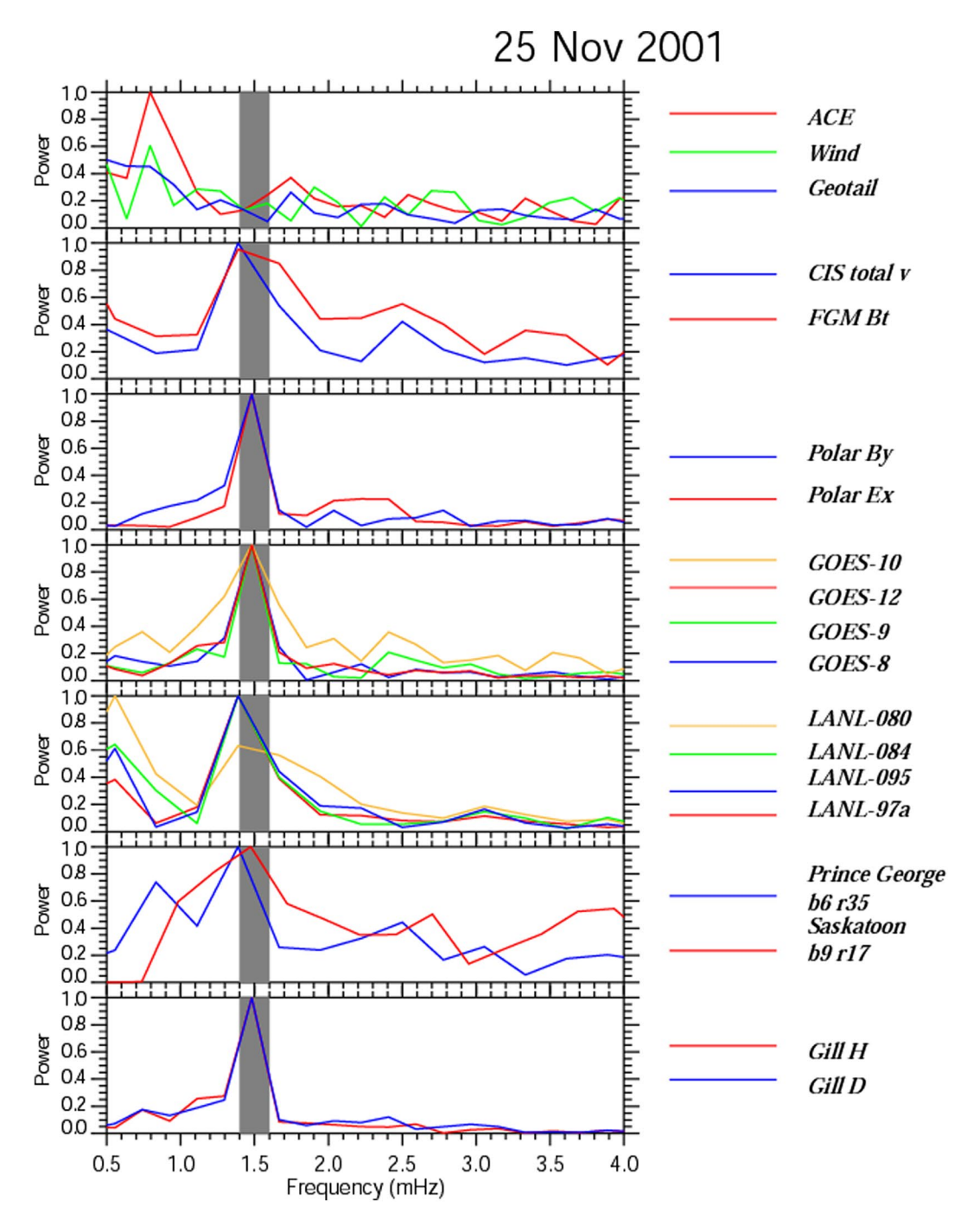


Figure 5. Normalized power spectra of the wave activity observed in the (a) solar wind dynamic pressure, (b) Cluster 3 total magnetic field strength and ion speed, (c) Polar satellite electric and magnetic field, (d) geostationary orbit azimuthal magnetic fields, (e) geostationary orbit electron energy flux, (f) Super Dual Auroral Radar Network line of sight velocity data, and (g) ground magnetometer observations, reproduced from Rae et al. (2005). The peak in all data sets, except the solar wind, at 1.4–1.6 mHz indicates a well-defined path of energy transfer from the magnetopause down to the ionosphere.

between these oscillations at or near the location of Polar. Geostationary satellites (separated by up to 7 hr of local time from Polar) observed near identical perturbations in energetic particle fluxes and the magnetic field, indicating that the particle flux enhancements were due to adiabatic acceleration from magnetic field compressions associated with the waves. A corresponding period of Pc5 oscillations at the same frequency was observed by ground-based magnetometers in the SAMNET and IMAGE chains. Ground-based magnetometer data were

FEAR 25 of 46

used to construct the ionospheric equivalent current, which revealed vortices indicating the presence of a pair of field-aligned currents, flowing upward in the west and downward in the east, during the compression of the magnetosphere. This current system was similar to that which occurs during sudden impulse/sudden storm commencement events, except that the magnetospheric compression in this case was localized.

Spacecraft studies of field line resonances usually exploit observations on the dayside or flanks, but ground-based magnetometer and radar observations of ULF pulsations are common in the nightside sector. Zheng et al. (2006) studied an interval of standing Alfvén waves which were observed by Cluster in the mid-tail, during which pulsations at the same (very low) frequency were observed at the footprint of Cluster. Simultaneously, oscillations (at different frequencies) were observed by the GOES, Polar and Geotail satellites in the post-midnight/pre-dawn sector. The waves were again postulated to be driven by Kelvin-Helmholtz interaction at the dawn flank (and the solar wind was fast, providing favorable conditions for KHI), though in this study the authors were not able to exclude other possible drivers. The pulsation frequency observed at the Gillam magnetometer (in the CANOPUS chain) was particularly low (1.1 mHz); similarly low frequencies had been observed at this station before, which had been puzzling given the low latitude of the station (66.4° MLAT) and the fact that such low frequencies could not be understood in terms of a dipolar magnetic field configuration. However, the observation of a similar pulsation frequency at the conjugate Cluster spacecraft, coupled with application of the Tsyganenko magnetic field line model, demonstrated that such low frequencies could arise because Gillam could be located at the footprint of very stretched nightside field lines.

Another use of conjugate observations has been to test theoretical predictions of the linkages between space- and ground-based observations of ULF pulsations. C. Wang et al. (2010) used Cluster electric field and ground-based magnetometer observations of a ULF wave triggered by an interplanetary shock to test a modeled relationship between the electric field within the equatorial plane of the magnetosphere for a ULF wave, and the associated ground magnetic pulsation. The predicted and observed ground pulsations compared well, for a specific magnetometer station which was close to the footprint of the spacecraft.

The impact of Pc5 waves was studied by Tan et al. (2011), who presented observations of magnetospheric ULF waves excited by quasi-periodic solar wind dynamic pressure variations following a sudden storm commencement event. The direct driving by solar wind pressure variations was demonstrated by a phase correlation between the solar wind pressure fluctuations and the magnetospheric ULF waves. Comparison of the ground-based observation of the ULF waves by magnetometers in different local time sectors allowed the authors to determine the buffeting region (i.e., source of the magnetospheric ULF waves) to be in the post-noon sector. Cluster, passing through perigee near noon MLT, observed a modulation in the poloidal mode electric field (measured by EFW) and similarly modulated energetic electron fluxes in the energy range measured by RAPID (30-100 keV). A magnetically conjugate LANL spacecraft showed that at even higher energies (500-750 keV), the electron flux peaks were not simply modulated by the electric field, but instead experienced energization by the ULF waves, thus indicating that compressional mode wave activity is an important mechanism for accelerating electrons after the initial compression (and related particle energization) arising from the sudden storm commencement. Motoba et al. (2013) also investigated the impact of Pc5 pulsations on the modulation of energetic electron precipitation. Cluster and ground-based magnetometers observed 4 mHz Pc5 oscillations in the dawn sector, with the ground-based observations confirming that the center of resonance occurred close to Cluster. Riometers, co-located with some of the ground-based magnetometers, revealed a modulation of the cosmic noise absorption at the same frequency, indicative of a modulation of the precipitating energetic electrons, and the Cluster STAFF experiment observed a banded, intense, emission of chorus waves (between a few hundred Hertz and 3 kHz) in both the electric and magnetic fields, which was also modulated at ~4 mHz. Collectively, the observations were consistent with theory which describes how a compressional magnetic pulsation in the magnetosphere modulates the growth rate of chorus waves and hence modulates the precipitation of energetic electrons. However, some aspects of the observations were not in accordance with this theory, and suggested that an additional contribution to the modulation of electron precipitation was made by the resonant Pc5 oscillation directly.

Moving to higher frequencies, Pc4 waves have periods of 45–150 s and are thought to be generated either by KHI at the magnetopause, or by wave-particle interactions upstream of the bow shock. Clausen et al. (2008) analyzed the most prominent of a series of five wave packets in the Pc4 range, which were observed by two of the Cluster spacecraft and several ground-based magnetometer chains spanning most MLT sectors, indicating that the wave packets were a global magnetospheric phenomenon. The simultaneous appearance of the wave at different

FEAR 26 of 46

magnetometer stations strongly indicated the wave packets were a temporal, rather than spatial, phenomenon, A comparison of the onset times of the pulsation, as observed on the ground, and the Poynting flux calculated from Cluster magnetic and electric field observations indicated that the wave propagated from dayside to nightside, suggestive of an upstream source. In the absence of an identifiable trigger in the solar wind, the authors postulated that the wave was generated by backstreaming ions in the foreshock which may occur when the IMF cone angle is low, giving rise to a wave whose compressional element propagated through the bow shock and magnetosheath, into the magnetosphere where it was partially converted into the Alfvénic standing waves, with Cluster observing both wave modes and the ground-based magnetometers observing the Alfvénic modes. An estimate of the frequency of such foreshock waves given the observed IMF magnitude and cone angle during this period matched the observed frequency of the magnetospheric waves. Since the solar wind is supersonic, the waves generated in the foreshock are convected downstream contributing to the tailward progression of the wavepackets observed in the magnetosphere and on the ground. Comparison of the phase shifts observed between the two Cluster spacecraft suggested that wave observed at the Cluster location had a node structure related to the fundamental. The fundamental frequencies of field lines threading the various magnetometer stations were calculated, and it was found that at latitudes comparable to Cluster, the pulsation was oscillating at a frequency between the local fundamental and the second harmonic (consistent with the phase shift observations at Cluster). Thus the authors concluded that the driving wave resonantly interacted with geomagnetic field lines where the driving frequency was harmonically related to the local fundamental frequency, driving field line resonances. In a follow-up study, Clausen et al. (2009) reported observations of the foreshock waves postulated in their previous study, this time observed by Geotail. The foreshock waves were followed shortly afterward by an increase in the magnetospheric wave power at the same frequency, observed by Cluster in the dayside magnetosphere and by magnetically conjugate magnetometers on the ground, thus providing the first simultaneous observations of waves created by back-streaming ions at the bow shock, in the dayside magnetosphere and on the ground. Clausen and Yeoman (2009) used ground-based SuperDARN and magnetometer observations to demonstrate the validity of a statistical study of Pc4 and Pc5 oscillations observed by Cluster, which they used to investigate the suggestion of certain preferred frequencies for field line resonances—so-called "CMS frequencies." Statistical analysis of the Cluster data revealed no clear, consistent preference for CMS frequencies, although there were indications for preferred frequencies above 5 mHz. The authors hypothesized that the mechanism selecting these frequencies is the same waveguide/cavity model as put forward to explain CMS frequencies, but that in the inner magnetosphere (at the perigee of Cluster), higher harmonics than the CMS frequencies were observed. They suggested that the absence of a clear preference for CMS frequencies in their study may arise because the perigee of Cluster was located significantly earthward of the expected position of the turning point in the cavity/waveguide model.

At higher frequencies still, Pc3 waves have periods of order 10-45 s. Two distinct populations of Pc3 waves occur—one exhibits a frequency dependence on the strength of the upstream IMF, and is thought to be caused by foreshock waves which in turn are caused by backstreaming particles just upstream of the bow shock (similar to the observations of Clausen et al., 2009, above). Since the solar wind flow is supersonic, the waves are convected into the magnetosheath and to the magnetopause, where they can convert to Alfvénic fluctuations in the magnetosphere. The other population peaks between 20 and 30 mHz and has no dependence on the IMF strength. The cause of this second population is not well understood, but has been linked to various transient phenomena at the magnetopause, or to internal magnetospheric processes. Eastwood et al. (2011) presented observations of an HFA (see Section 2.1) by Cluster, which was situated upstream of the bow shock and close to the Sun-Earth line. Cluster observed the upstream signatures of an HFA, while the Rosetta spacecraft, near closest approach of an Earth fly-by, and ground-based magnetometer stations observed an interval of Pc3 activity. Cluster observed no upstream waves that could have been the source of the Pc3 waves in this interval, and it was concluded that the Pc3 activity was due to the disruption at the magnetopause that was caused by the HFA. The delay between the onset of Pc3 signatures at different ground stations demonstrated that the disturbance moved antisunward, consistent with the above explanation. The authors therefore concluded that magnetopause disturbances resulting from HFAs could explain, at least in part, the population of Pc3 waves which does not depend on IMF strength. In a separate study, Balasis et al. (2015) found evidence of excitation of both Pc3 and Pc5 waves in the dayside magnetosphere, in observations from Cluster (in the dayside pre-noon sector), CHAMP (at the topside ionosphere) and on the ground. Geotail, upstream of the bow shock, observed oscillations in both the Pc3 and Pc5 band. The frequency of the Pc3 waves observed in the magnetosphere was consistent with the dependence on IMF strength for the first (foreshock-wave-driven) population, and were therefore interpreted as

FEAR 27 of 46

such. As Cluster crossed the plasmapause, it observed a shift in the Pc3 wave power to higher frequency (from ~20 to ~50 mHz) and the disappearance of the Pc5 waves, whilst simultaneously the intensity of Pc3 activity measured both upstream of the bow shock (by Geotail) and on the ground also intensified. The observations were consistent with theoretical expectations that the driving fast mode waves in the Pc4–Pc5 range would be absorbed at higher L-shells and unable to penetrate to lower L-shells, whereas the higher frequency Pc3 fast mode waves would be able to resonate with local Alfvén waves at lower L-shells. Furthermore, magnetometer stations in the post-noon sector did not observe clear evidence of Pc3 waves, indicating that these were most easily seen close to local noon.

Pi2 pulsations are transient waves which are observed in space and on the ground at the time of substorm onsets or pseudobreakups (see also Section 3.2). Kawano et al. (2011) combined multi-point space-based observations from Cluster, and multi-point ground-based magnetometer observations to determine the profile, with L-shell, of a Pi2 pulsation which took place at the start of a substorm. At this time, the Cluster spacecraft straddled the plasmapause. They found a systematic phase pattern, with constant phase through the plasmasphere (and at the footprints of plasmaspheric field lines), but the phase was shifted earlier through the plasmapause and plasmatrough (a low density region just outside the plasmapause). This phase pattern, derived from combined Cluster and ground-based observations, supported the idea that the source for the Pi2 oscillation was tailward of the spacecraft, and the oscillation propagated toward the plasmasphere. Furthermore, the relatively small amplitude of oscillation observed at Cluster 2 and at a corresponding ground station (at $L \sim 5$) led the authors to suggest that mode conversion was occurring in that region, causing the wave energy of the Pi2 to be lost to some other wave type.

Finally, ULF waves can also be stimulated artificially by ionospheric heating. Badman et al. (2009) reported the results of an experiment where the SPEAR ionospheric heater transmitted a 1 Hz modulation signal with a 10 min (1.67 mHz) on-off cycle during a conjunction with the Cluster spacecraft. The 10 min period was intended to enhance an existing field-line eigenmode at that frequency. Ground-based magnetometers near the SPEAR site showed enhanced power in ULF wave activity at 1.67 mHz during the SPEAR heating interval, with power maximized during a half hour window when ionosonde data showed that ionospheric conditions were most favorable for such heating experiments, indicating that SPEAR modulated currents in the local ionosphere and enhanced a field line resonance at 1.67 mHz. Fourier analysis of the Cluster FGM data during the pass indicated that the spectral power at 1.67 mHz was enhanced at Cluster 2, which passed closest of the four spacecraft to the heating experiment, by a factor of 4-5 during the SPEAR heating experiment. Therefore, a SPEAR-enhanced ULF wave was detectable both on the ground and in space (at Cluster). A much weaker signature was observed in the electric field measurements made by EFW, which the authors attributed to the harmonic mode of a standing wave on a field line, which might explain the amplitude of the wave magnetic field being close to a maximum whilst the wave electric field amplitude is small. No significant power enhancement was observed by the other three spacecraft, indicating that the enhancement was spatially localized to the field lines conjugate with SPEAR. Their observations constituted the first joint space- and ground-based detections of artificial enhancement of a field line resonance at high latitudes, demonstrating the feasibility of "tagging" a field line to aid the study of field line configurations.

5. Auroral Structure

As described in Section 3, the Earth's auroral oval maps out to magnetically "closed" regions of the magnetosphere. Within the auroral oval, arcs form which are elongated in the east-west direction but narrow in their north-south extent, as a result of the instigation of field-aligned current systems and the acceleration of downward-propagating electrons. Acceleration is caused either by electric field structures or wave processes (discussed in Section 4). The acceleration mechanisms give rise to an "inverted-V" signature in spectrograms as a spacecraft passes through accelerated precipitation (below the acceleration region). As also described in Section 3, at substorm onset an arc suddenly brightens and expands to fill the whole sky, as seen from a point on the ground. This "auroral break-up" occurs first in the midnight sector but then expands rapidly poleward and westward, which is termed a "westward traveling surge". In some substorms, undulations can form in the poleward edge of the diffuse aurora, giving rise to "omega bands", so-called after the inverted Ω shape produced in the auroral boundary (though as discussed below, their relation to particular phases of the substorm cycle is unclear). On the other hand, when the interplanetary magnetic field is northward, a more complex global configuration of the aurora occurs, with

FEAR 28 of 46

sun-aligned auroral arcs formed within the polar cap some of which cause the night and day sides of the global auroral oval to be joined by a bar of auroral emission forming a greek Θ; such auroral features and configurations are called "polar cap arcs" and "transpolar arcs" or "theta auroras". Some studies have used conjugate Cluster and ground-based observations to probe the current systems and acceleration processes associated with individual auroral arcs, and large-scale auroral structure. These studies have sought to address questions such as: How do the current systems associated with individual auroral arcs evolve? Can reconnection in the magnetotail provide sufficient acceleration of particles for auroral arcs to form? If not, then where does the acceleration of particles take place? What is the relationship between auroral arcs and broadband electric fields? How does arc motion relate to magnetospheric motions? How are the ionospheric dynamics of omega bands related to magnetospheric dynamics? What is the source mechanism (and source region) for omega bands? What are the source mechanisms (and source regions) for polar cap arcs and transpolar arcs?

Aikio et al. (2004) studied the evolution of two auroral arcs that were observed by Cluster, two all-sky cameras, EISCAT and STARE. Three of the Cluster spacecraft crossed a pre-existing auroral arc and measured the associated upward and downward field-aligned current system. During the crossing of the pre-existing arc, a pseudobreakup occurred (confirmed by Pi2 oscillations observed on the ground). A few minutes later, a new arc formed poleward of the original arc, and was crossed by the two trailing Cluster spacecraft. As the spacecraft sequentially crossed the original (equatorward) arc, the widths of the upward and downward field aligned currents broadened, but the integrated upward and downward currents matched for each spacecraft. As a result of the widening, the total amount of current flowing in the arc current system doubled during the course of the Cluster crossings; this increase was attributed to the pseudobreakup which occurred, but the Cluster measurements demonstrated that the current enhancement did not immediately follow the pseudobreakup, instead occurring 1-2 min later. All three spacecraft measured a southward electric field in the region of the field-aligned currents, and showed an indication of the electric field turning northward at the poleward part of the downward field-aligned current, thus forming a divergent electric field structure. The southward electric field was consistent with the field-aligned currents, with the current circuit consisting of a downward current sheet at the poleward edge of the arc, a southward Pedersen current in the ionosphere, and an upward current sheet at the equatorward edge. A similar current structure was observed across the poleward arc by the two trailing spacecraft, with the maximum upward field-aligned current being observed as the spacecraft passed through a fold in the auroral arc (as observed by the all-sky camera). At the time of the formation of this poleward arc, conjugate EISCAT observations showed the formation of a deep density cavity just poleward of the poleward arc, associated with the downward current (i.e., upward flow of electrons) adjacent to the arc. The electron densities decreased at all altitudes between 100 and 600 km, but particularly in the lower F and E region. The ion temperature in this altitude range increased by a factor of three, indicating frictional heating by a very intense electric field. The appearance of the density cavity on the field lines observed by EISCAT coincided with the appearance of the poleward arc at the zenith, and persisted while the arc remained at the longitude of EISCAT; the physical reason given for the cavity was that the downward field-aligned current is carried by upward moving electrons, whereas the connecting horizontal Pedersen current in the ionosphere is carried by ions in the E- and lower F-region. In order to maintain plasma neutrality, there is therefore a net outflow of charge carriers in the current closure region. Cluster PEACE data were available for the poleward arc crossing; observations from Cluster 2 (the first to cross the poleward arc) revealed intense fluxes of downgoing and upgoing electrons (<100 – 300 eV) as current carriers in the upward and downward field-aligned current regions, respectively. In the upward field-aligned current region, a depletion of upward moving electrons at this energy range indicated that the downward-moving electron population was being locally accelerated, most likely by dispersive Alfvén waves. However, the energy of the electrons observed by Cluster was not sufficient to produce the visible aurora observed, hence further acceleration must have taken place below the spacecraft. Cluster 4 PEACE observed even more energetic upward electrons in the downward field-aligned current region, this time extending to energies of 1 keV and starting to resemble an "inverted-V" structure. Cluster EFW observations also revealed the presence of a (separate) density cavity at higher altitudes, in which the poleward arc was situated, and which was bounded at its equatorward edge by the equatorward arc. From the Cluster observations, the high-altitude density cavity was more long-lived than the arcs. Two types of electric field fluctuations were observed associated with the arcs: an intense low-frequency fluctuation in the upward field-aligned current region, and an even more intense broadband fluctuation observed in the downward current region. These waves were highly localized in space and time, and could appear and disappear between

FEAR 29 of 46

two spacecraft passages of the same arc, demonstrating that visual auroral arcs are not always associated with broadband electric fields, even though the latter are commonly observed by spacecraft.

Figueiredo et al. (2005) studied the evolution of the electrostatic structures observed by Cluster that were associated with two auroral arcs; for one of these events, they also made use of ground-based data. In that latter event, associated with the expansion phase of a moderate substorm, DMSP images showed that the Cluster spacecraft crossed the auroral "horn" which lies ahead of the westward traveling surge. Conjugate ground-based all-sky images observed the motion and evolution of an east-west aligned auroral arc, which was 30-50 km wide. Cluster observed intense electric field variations as it crossed above the arc, which were co-located with the poleward edge of the plasma sheet boundary, and were coupled with intense upward-flowing field-aligned currents. The evolution of the electric field structures observed by the four spacecraft, which crossed the arc sequentially, demonstrated that the surge horn initially consisted of multiple arc (and electric field) structures, and the ASIs also showed small-scale structure embedded in the arc. The evolution of the Cluster observations showed that these multiple structures then merged and the associated field-aligned current density intensified. The width of the structure also increased. Equatorward of this structure, there was a region without auroral emissions which was associated with predominantly downward field-aligned currents, followed by a broader region of auroral emissions associated with mainly upward field-aligned currents, but a weaker potential drop. The motion of the arc was closely linked to the motion of the poleward edge of the plasma sheet—both moved poleward with a velocity of ~0.5 km s⁻¹, consistent with the fact that this event occurred during a substorm expansion phase. More recently, some studies of Cluster passes through the auroral acceleration region exploited space-based auroral imagery in order to contextualize the particle and electric field observations made by the spacecraft—we refer the reader to the parallel review by Marklund and Lindqvist (2021) for further information on these studies.

Two inter-related studies have considered the question of whether the reconnection process in the tail is able to accelerate electrons sufficiently to generate the aurora, or whether additional acceleration mechanisms are required. Borg et al. (2007) presented simultaneous observations of a magnetic reconnection site observed in the magnetotail by Cluster, and a bright auroral spot that appeared in both UV and X-ray global auroral observations (measured by the Polar spacecraft) at the ionospheric footprint of the Cluster constellation. They found that the electrons measured by Cluster in the ion diffusion region were not sufficiently accelerated by the reconnection process to produce the auroral X-ray fluxes observed. Furthermore, a DMSP spacecraft passed over the auroral spot, and found that the auroral emissions were produced by a precipitating population which has passed through a ~30 kV potential drop, pointing to an acceleration process somewhere between Cluster and DMSP, in addition to the acceleration provided by reconnection. Østgaard et al. (2009) examined several further magnetotail reconnection events observed by Cluster, several of which had conjugate imaging observations in either UV or X-ray, and two of which also had approximately conjugate DMSP passes. They found that the electron distributions in the reconnection region were typically insufficient to produce the auroral intensities observed. Where available, particle data from DMSP showed evidence of the precipitating electrons being accelerated either by a potential drop, or by Alfvén waves.

Conjugate Cluster and ground-based observations have also been used to study so-called auroral omega bands, which is where the aurora takes an undulating shape with a series of inverted Ω shapes which propagate eastward (Figure 6). The successive bright and dark regions that are observed above a given point as time progresses are thought to correspond to successive pairs of localized upward and downward field-aligned current. Wild et al. (2011) presented a case study where Cluster was in the magnetotail plasma sheet, conjugate to a ground-based ASI. The imager observed a series of five clear omega bands, which started within 5 minutes of a substorm expansion phase intensification. The substorm onset and intensification occurred in the immediate pre-midnight sector (2300-2400 MLT), and the omega bands were observed immediately post-midnight (0000–0030 MLT), and were observed propagating eastward (i.e., dawnward), away from the onset region. The omega bands were accompanied by a series of Ps6 magnetic pulsations (10–20 min quasi-periodic signatures in the east-west magnetic field), measured on the ground, which are usually associated with omega bands and which are consistent with the passage of vortical Hall currents associated with upward and downward field-aligned currents. There was no clear evidence of any ionospheric shear flows at the poleward boundary of the auroral oval in the co-located SuperDARN observations, though this could not be confirmed conclusively due to limited radar coverage. The Cluster spacecraft observed a series of bursts of 0.1-3 keV electrons streaming parallel to the magnetic field into the northern hemisphere ionosphere throughout the interval, which showed signs of

FEAR 30 of 46

onlinelibrary.wiley.com/doi/10.1029/2021JA029928 by University Of Southampton, Wiley Online Library on [09/11/2022]. See the Terms

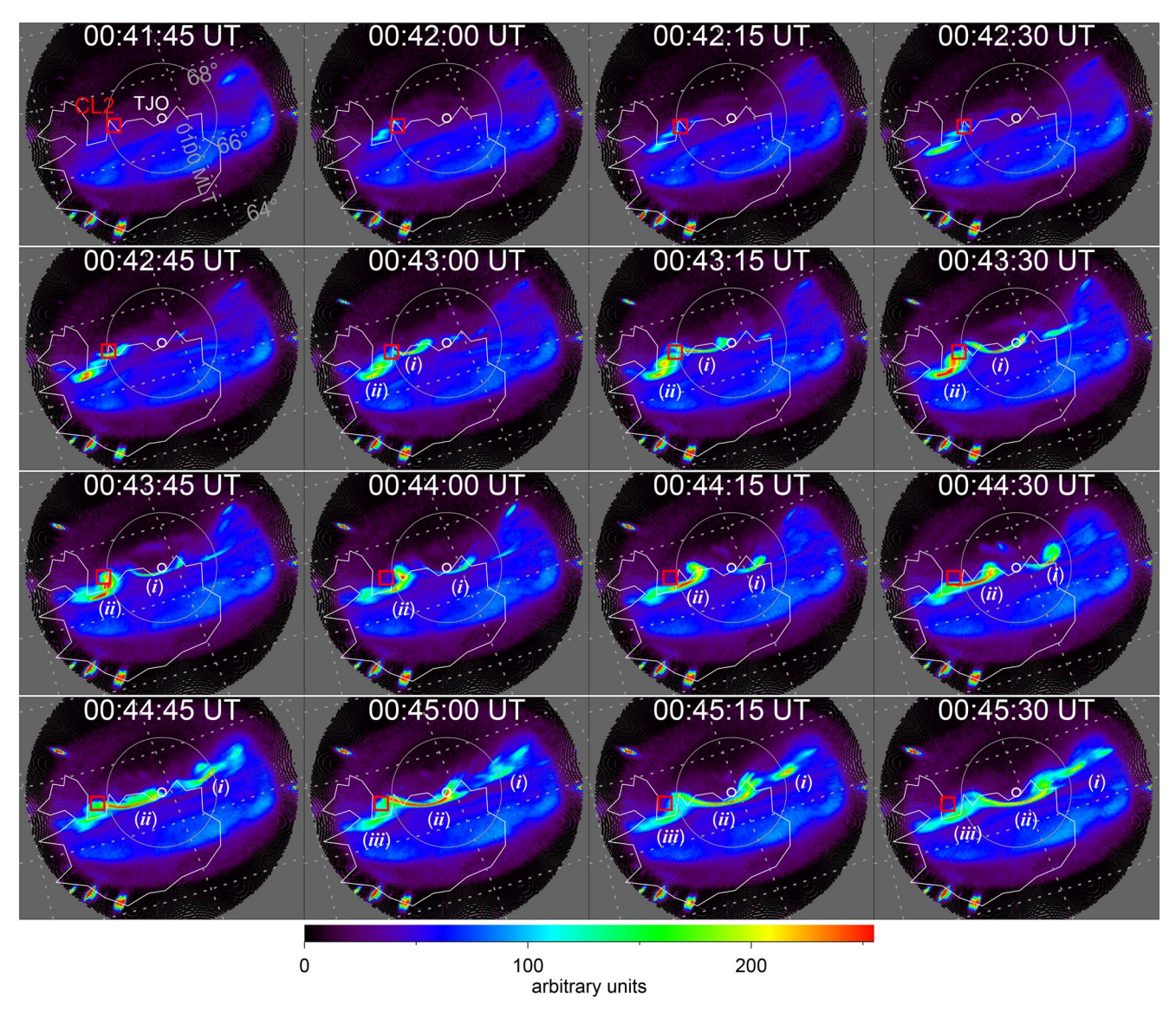


Figure 6. All sky camera images, mapped onto geographic coordinates, showing a period of auroral omega bands, reproduced from Motoba et al. (2012). The red square shows the footprint of Cluster 2, and the dotted lines are geomagnetic longitudes and latitudes.

having been accelerated in the field-aligned direction. There was generally enhanced Alfvénic Poynting flux, the field-aligned component of which was almost continuously directed toward the northern hemisphere. There was not a one-to-one correspondence between the Cluster electron signatures and the omega bands, which the authors attributed to limitations in the magnetic field line model used to trace the footprints, but the observations were consistent with Alfvén waves in the plasma sheet (around $8~R_E$ downtail) accelerating the electrons and being responsible for the field-aligned currents that cause the Ps6 pulsations and auroral brightenings. The authors' findings were consistent with previous work that suggested that omega bands have a source mechanism in the midtail plasma sheet; furthermore, their observation in the immediate post-midnight sector, during a substorm expansion, indicated that omega bands may not be restricted to the morning sector and substorm recovery phase as often stated.

Subsequently, Motoba et al. (2012) presented observations of a series of auroral undulations which were smaller in wavelength than typical omega bands (100–300 km, compared with typical lengths of 400–1,000 km), but in many other respects were similar (Figure 6). The footprint of Cluster 2 was particularly close to the auroral forms, which drifted along the poleward boundary of the aurora; the field-aligned currents inferred from the Cluster 2

FEAR 31 of 46

FGM observations matched the corresponding auroral emissions at the footprint, with bright and dark regions of the drifting aurora corresponding to upward and downward field-aligned currents, respectively. Similar magnetic field variations were observed by Cluster 1, situated 2 R_E dawnward of Cluster 2, but delayed in a manner consistent with the longitudinal propagation of field-aligned currents from Cluster 2 to Cluster 1, and in agreement with the eastward (i.e., dawnward) propagation of the auroral signatures. Contrary to the observations reported by Wild et al. (2011), co-located SuperDARN observations did show the presence of shear flows around the first three undulations. The later arcs were starting to develop into spiral-like or vortex-like forms, and any sheared flows were unclear for these events. Magnetic field pulsations were observed on the ground, similar to the Ps6 pulsations often reported with omega bands, but with a shorter period (consistent with the shorter length scale of the auroral undulations). Collectively, the simultaneous Cluster and ground-based measurements provided a direct linkage between the magnetospheric and ionospheric evolution of these mesoscale undulations at the poleward edge of the auroral oval, which were most likely due to field-aligned currents propagating eastward in and near the PSBL. However, they were unable to provide a definitive answer on the generation of the currents in the near-Earth tail.

Finally, several studies have combined global-scale auroral imagery from the IMAGE and/or low-altitude satellites with Cluster observations in order to better understand the dynamics of Earth's magnetotail during northward IMF conditions. Maggiolo et al. (2012) used a global scale image of the auroral emissions in the polar region to infer conjugacy between accelerated ion beams observed by Cluster above the polar cap (polar cap ion beams) with a thin but elongated polar cap arc. The polar cap ion beam consisted of an upflowing ion beam with an inverted V structure, indicative of acceleration by a quasi-static electric field below the spacecraft. (Such an observation is consistent with being the higher-altitude counterpart of a downward-accelerated electron beam below the acceleration region, which gives rise directly to the polar cap arc, and therefore the authors argued that a polar cap ion beam is a high altitude signature of a polar cap arc.) One key topic that has been debated over the last couple of decades has been the topology of field lines that thread polar cap arcs—whether they are closed (and hence connect to the ionosphere in the opposite hemisphere) or open (connected to the solar wind). The polar cap ion beam observations reported by Maggiolo et al. (2012) demonstrated the complexity of this question, as a mixture of plasma distributions consistent with open and closed field line topologies were observed within different beams. The question of topology is somewhat clearer for larger-scale "transpolar arcs," which are typically the predominant form of polar cap are observed by high altitude satellite imagers. A few studies have combined global-scale images of transpolar arcs from the IMAGE satellite with Cluster observations to investigate the magnetotail lobe structure associated with such auroral features; transpolar arcs are associated with a hotter population than polar cap ion beams, which has been interpreted either as due to a localized growth of the plasma sheet into the lobe due to "trapping" of field lines that are newly closed by magnetotail reconnection (Fear et al., 2014; Fryer et al., 2021), or as due to entry of solar wind plasma resulting from lobe reconnection (Mailyan et al., 2015). For further details on these studies and the role that Cluster and ground-based instrumentation have separately played in developing our understanding of northward IMF dynamics, we refer to the recent review by Fear (2021).

6. Current Systems

Another area of research that has combined Cluster and ground-based observations has been determining the relationship between the interconnected magnetospheric and ionospheric current systems that can be observed by Cluster and ground-based facilities, respectively. The arc-related field-aligned currents discussed above form just one part of the large-scale magnetosphere-ionosphere current system. Some magnetospheric currents, such as the magnetopause and cross-tail currents, form at the interface between different magnetic field configurations as a consequence of Ampère's law, while the ring current forms as a result of differential motion imparted on electrons and positive ions by gradient and curvature drift. In the ionosphere, the auroral electrojet forms within the auroral oval due to the enhanced conductivity caused by particle precipitation, and is constituted by Hall and Pedersen currents. The two are linked by field-aligned current systems, for example, the Region 1 and 2 current systems for southward IMF. (The substorm current wedge referred to in Section 3 consists of a deflection of the cross-tail current, via field-aligned currents, which enhances the auroral electrojet during substorm periods.) The magnetopause, cross-tail and ring currents are sampled by Cluster and can be measured either by single space-craft techniques (making simplifying assumptions) or by the curlometer technique which exploits the tetrahedral

FEAR 32 of 46

configuration of Cluster to measure the curl of the magnetic field, and hence the current passing through the tetrahedron. The auroral electrojet creates a magnetic field which can be measured by ground-based magnetometers in the auroral regions, and used to estimate the strength and direction of the electrojet current. The upper and lower portions of field-aligned current systems can be measured by Cluster and analysis of ground-based data, respectively. Two studies have combined both of these techniques in order to answer the questions: What is the relationship between field-aligned and horizontal electrojet currents at the convection reversal boundary? How does the convection reversal boundary deduced from electrojet currents compare with that deduced from radar observations? How do field-aligned current calculations deduced from ground-based observations compare with those estimated from Cluster data? What proportion of the current is carried by ions and electrons, respectively? And how do asymmetries in the ring current compare with measurements of the magnetopause current?

Amm et al. (2003) used conjugate Cluster, ground-based magnetometer and HF coherent scatter radar data (from SuperDARN and the Scandinavian STARE radar) to investigate the relationship between field-aligned and horizontal electrojet currents at the convection reversal boundary (at the edge of the polar cap) at ionospheric and magnetospheric altitudes. The ground-based magnetometer data were used to infer the horizontal electrojet currents and hence the convection reversal boundary in the dawn sector (at the boundary between the westward electrojet and a higher latitude region of eastward currents). This "magnetic convection reversal boundary" lay $\sim 0.5^{\circ}-1^{\circ}$ poleward of the convection reversal boundary deduced from electric field measurements from both the STARE coherent scatter HF radar and Cluster EFW; the authors attributed the discrepancy between these two estimates as being due to the magnetic effect, on the ground, of field-aligned currents—the positive displacement of the magnetic convection boundary could be explained by a longitudinal gradient in the field-aligned currents, though the observations could not be used to check for such gradients. Poleward of the magnetic convection reversal boundary, CIS observed a high energy ion population, and the authors placed the open-closed field line boundary at the poleward edge of this region, that is, 3°-4° poleward of the convection reversal boundary inferred from the radar and EFW observations. (Though not commented on explicitly by the authors, this discrepancy between the two boundaries may arise if there is a viscous contribution to the global convection, in addition to the dominant reconnection-driven convection, e.g., Cowley, 1982; Chen et al., 2016.) The ground-based magnetometer data were then combined with measurements of the ionospheric electric field to derive the Hall conductance (assuming a fixed Hall-to-Pedersen conductance ratio) and the field-aligned currents flowing into/out of the region. The field-aligned currents compared favorably with those deduced from EFW, with both methods revealing a three-sheet structure, with an upward and downward field-aligned current sheet at the equatorward and poleward edge of the westward electrojet, respectively, and another downward current sheet in the region of the convection reversal boundary. The upward field-aligned current region was associated with a band of diffuse aurora, as imaged by a ground-based all sky camera. Cluster particle data were available as the spacecraft crossed through the downward field-aligned current regions; there were no clear particle boundaries associated with the field-aligned current regions, but calculations showed that the downgoing ions carried at most 0.5 nA m⁻², whereas the total field-aligned current (from the ground-based calculations) reached 9 nA m⁻², indicating that a substantial part of the downward field-aligned current must have been carried by upward accelerated electrons (though these could not be clearly identified in the PEACE observations).

More recently, Haaland and Gjerloev (2013) investigated the statistical connection between asymmetries in the ring current (measured by the global SuperMAG network of ground-based magnetometers) and magnetopause currents measured by Cluster (using single spacecraft techniques and, for a subset of events, the four-spacecraft curlometer method). The authors found a persistent dawn-dusk asymmetry in the ring current, with a more intense ring current in the dusk sector (consistent with previous studies), but they also found that the magnetopause current densities were stronger on the dusk side than the dawn side during disturbed conditions. The magnetopause was, on average, thicker at dawn than dusk (for both quiet and disturbed conditions), but the total magnetopause current was greater on the dusk side during disturbed geomagnetic conditions, suggesting a coupling between the two current systems. Given the influence that each current system can exert on each other (magnetic perturbations from enhancements in the ring current can increase the magnetospheric magnetic field inside the magnetopause, and hence the magnetic shear, whereas enhancements in the magnetopause currents do make an albeit minor contribution to the magnetic deflections measured on the ground), the authors were not able to identify unambiguously a direct connection in the form of a current loop between the ring current and magnetopause current, but the consistency in behavior of the two current systems did not exclude such a possibility.

FEAR 33 of 46

10.1029/2021JA029928



7. Global Dynamics and Convection

Two further areas in which ground-based facilities can support spacecraft observations are the study of global magnetospheric dynamics (including the global response to abrupt changes in the interplanetary magnetic field direction and to major solar wind transients, such as coronal mass ejections, interplanetary shocks and magnetic clouds), and the study of the global response to solar wind driving (combining the dayside and nightside aspects discussed in Sections 2 and 3). In this section, we summarize Cluster/ground-based studies into the global response to a series of different types of transient (coronal mass ejections, interplanetary shocks, magnetic clouds and IMF rotations) before summarizing studies of the open-closed field line boundary (which, as already encountered above, is an important parameter for quantifying the global state of the magnetosphere). Important questions which conjugate studies have addressed include: What is the global magnetospheric response to extreme driving conditions? What is the energy transfer under such extreme conditions and how do they compare with predictions of empirical relations? What is the global magnetospheric and ionospheric response to interplanetary shocks, solar wind pressure changes, and abrupt changes in the different components of the interplanetary magnetic field? Over what timescales do different parts of the magnetosphere-ionosphere system respond? How do different methods of estimating the open-closed field line boundary location compare at different local times? How do changes in the open-closed field line boundary in the ionosphere compare with changes in the magnetotail? How do in situ and ionospheric estimates of the nightside reconnection rate compare?

7.1. Coronal Mass Ejections

Rosenqvist et al. (2005, 2006) studied the global response to two large geomagnetic storms which occurred on 29 and 30 October 2003 (the "Halloween storms"). As part of a broader investigation of these storms, using observations from a range of space- and ground-based instrumentation, Rosenqvist et al. (2005) examined a particular interval in which the Cluster spacecraft, situated at the dusk flank, abruptly crossed the magnetopause four times (out/in/out/in) at the same time as several substorm-like signatures were observed at geostationary orbit (particle injections observed by several of the LANL spacecraft) and on the ground (magnetic bays corresponding to some of the strongest ever recorded in northern Scandinavia). The combined observations of Cluster and two geostationary satellites indicated that the entire magnetosphere was compressed at this time; due to the extremely high density and velocity of the solar wind, the ACE SWEPAM particle instrument was saturated and reliable plasma moments were unavailable, but significant pressure pulses were inferred from the SYM-H index. Examination of the local electrojet, derived from data from the IMAGE magnetometer chain in Scandinavia, demonstrated that the substorm-like intensifications did not exhibit the usual recovery phase associated with typical substorms; each compression was associated with a large and suddenly enhanced electrojet which ended as abruptly as it started. Furthermore, these substorm-like signatures occurred after the IMF B_7 component had been negative for 2 hr and when the magnetotail was very stretched, indicating that there was sufficient stored energy available in the tail for a substorm, but for some reason the magnetosphere had remained stable and not initiated a substorm. However, the two major compressions and decompressions of the magnetosphere (observed by Cluster) managed to enforce two substorm-like energy releases from the magnetotail. The authors described these events as "substorm-like" because they appeared to be isolated expansion phases, lacking a growth or recovery phase, initiating substorm onset with a major compression, but then abruptly stopping the process with a subsequent relaxation of the magnetosphere. Rosenqvist et al. (2006) estimated the local energy flow from the magnetosheath into the magnetotail during one of the magnetopause crossings, using Cluster measurements of j ×B (from the curlometer technique), the tangential magnetosheath velocity (observed by CIS) and the velocity of the magnetopause motion (from the four spacecraft timing technique), which was then extrapolated over the magnetopause surface to provide a global estimate of energy transfer into the tail. The authors then used the Assimilative Mapping of Ionospheric Electrodynamics (AMIE) technique, informed by data from a global network of ground-based magnetometers, SuperDARN radars plus DMSP and NOAA satellites, to estimate the global Joule heating rate. This was cross-checked against a local Joule heating rate determined from EISCAT observations (exploiting the capability of the mainland EISCAT radar to measure the ionospheric electric field using observations from the Kiruna and Sodankylä receiving stations), coupled with supporting assumptions, which also gave a local estimate of the energy deposition from precipitating electrons. The global power input to the magnetosphere (from the extrapolated Cluster observations) was found to be between 17 and 40 TW (depending on the location assumed for the Near Earth Neutral Line, which was needed for the global extrapolation),

FEAR 34 of 46

which was about 4%–10% of the solar wind bulk flow energy calculated to be incident on the magnetopause at this time. The amount of power dissipation through Joule heating in the ionosphere was about 30% of the global power input estimated from Cluster. Estimates of these quantities based on empirical relationships were low compared with the calculated and extrapolated values, suggesting that empirical relations are insufficient for energy budget calculations during storms and substorms of such an extreme nature.

The interval studied by Rosenqvist et al. (2005, 2006) occurred during a wider period in October/November 2003 in which several extreme CMEs were ejected by the Sun. One such CME impacted the Earth's magnetosphere on 24 October 2003; Balan et al. (2007) showed that the resulting compression caused Cluster to pass from the southern hemisphere lobe, into the magnetosheath, before crossing the magnetopause again and entering the exterior cusp and then the dayside magnetosphere. The IMF reversed from southward to northward during this event, and was northward as Cluster entered the cusp; Cluster briefly observed sunward convection in the cusp, consistent with lobe reconnection, before moving into a region of stagnant flow. The EISCAT mainland VHF radar observed signatures of strong coupling, with antisunward flow, strong ion heating and enhanced electron density at low altitudes (indicating precipitation of high energy particles). The cusp was observed by EISCAT at extremely late local time (~17 MLT) and relatively low latitude (66°N), indicative of an extreme response to the severe solar wind conditions. Balan et al. (2008) studied the impact of a pair of long-lasting CMEs which impacted the magnetosphere on 7 and 9 November 2004 and triggered two conjoined geomagnetic storms. The compression of the magnetosphere arising from the first CME was observed by Cluster, which moved from the southern lobe into the magnetosheath and then observed an increase in magnetosheath ion fluxes in response to the arrival of the second CME. The authors used high latitude and equatorial radar data, from the EISCAT and Jicamarca, to investigate coupling down to lower latitudes.

7.2. Interplanetary Shocks and Magnetic Clouds

Interplanetary shocks are MHD discontinuities caused by regions of faster solar wind colliding with slower-moving solar wind ahead of it, which give rise to sudden increases in the solar wind dynamic pressure that is experienced by the magnetosphere. Zong et al. (2008) briefly examined the magnetospheric and ionospheric response to the impact of an interplanetary shock. Cluster was near perigee, near 09 MLT, and observed a strong compression to the geomagnetic field, followed by substantial fluctuations in all magnetic field components. The ionospheric response was examined in the form of altitude profiles from a global network of digital ionosondes (digisondes). Nightside stations did not exhibit a strong, immediate response to the shock, but the maximum density and thickness of the F layer did start to decrease, and the F layer peak height started to increase. On the dayside, the response was more prompt; the density in the F layer increased abruptly and the height of the F layer decreased slightly, whilst the thickness remained unchanged. The dayside response was most clear at mid latitudes.

Juusola et al. (2010) used data from several spacecraft and ground-based assets to study the response of the magnetosphere to step-like increase in the solar wind dynamic pressure arising as a result of the passage of a magnetic cloud (a region of enhanced interplanetary magnetic field strength, with a smooth rotation of the field direction). Timing analysis on data from three solar wind monitors (ACE, SoHo, and Wind) revealed that the pressure front was highly inclined to the GSE Y-axis, and thus made first contact with the magnetosphere on the dawn side. The study concentrated on the effects of the leading edge of the cloud, during which the IMF was northward. Several spacecraft were fortuitously situated in the dawnside magnetosphere (Cluster, Double Star TC-1, and Geotail); all four Cluster spacecraft and Geotail initially observed the magnetopause move earthward in response to the arrival of the pressure increase, but the magnetopause then rebounded and ended up straddled by the Cluster constellation. Double Star TC-1 remained within the magnetosphere, but observed a corresponding increase in the magnetic pressure. Coinciding with the inward, then outward, motion of the magnetopause, the equatorial magnetic field was observed to strengthen, and then weaken, by low latitude ground-based magnetometers (at solar magnetic latitudes lower than 45°). At high latitudes, the electrojet exhibited a two-stage response, in both the AE index and the ionospheric equivalent current constructed from ground-based magnetometers in the Fennoscandinavian sector. The first stage was shorter and less intense; shortly after the arrival of the pressure increase, an increase in the AE index was driven by a decrease in AL, and a faint increase in the eastward equivalent current in the dawn sector, and was also associated with a decrease in the PC (polar cap) index. A longer and more intense stage followed, in which there was an increase in the AU and PC indices, and a second, latitudinally more extensive, increase in the eastward equivalent current. Both of these stages were associated

FEAR 35 of 46

with the initial compression of the magnetosphere; as the magnetopause moved outwards and settled within the Cluster tetrahedron, the electrojet signatures faded. The authors also constructed a global convection pattern from global ground magnetometer data, by rotating the horizontal magnetic field vectors 90° anticlockwise in order to obtain a proxy for the ionospheric $\mathbf{E} \times \mathbf{B}$ drift. The initial signature, following the arrival of the pressure increase, was a pair of reverse convection cells, consistent with the fact that the IMF was northward, and corresponding in time to the initial stage of the electrojet response. This then evolved toward mainly westward convection (i.e., a single convection cell) at all local time sectors at the time of the second stage. As the impact of the pressure increase faded, the convection returned to its pre-existing state (but slightly enhanced relative to beforehand). SuperDARN data in this sector were limited, but observations from a poleward-pointing radar showed that the polar cap was contracting at this time, and showed a significant southward component to the flow consistent with the convection pattern deduced from the magnetometer data. The authors compared their convection response to two other studies of the response to magnetic clouds, and attributed the differences to the different IMF \mathbf{B}_Z components in each case.

7.3. IMF Rotations

Magnetospheric dynamics are highly dependent upon IMF orientation, in particular the north-south (B_{τ}) component. Volwerk et al. (2011) used an excellent conjunction of spacecraft (including both the Cluster and THEMIS multi-spacecraft constellations) and ground-based instrumentation to study a series of rotations in the IMF B_z component, and their interaction with the Earth's magnetosphere, from the L1 Lagrangian point to the ground. These rotations were observed in the solar wind by ACE and Wind (separated by 70 R_F in the Y_{GSF} direction); comparing the normals of the rotation fronts and the time delays between observations of the fronts at these two spacecraft, the authors found a mixture of planar, concave and convex fronts. Observations from THEMIS and Cluster (in the post-noon and dawn sector magnetosheath, respectively) were used to verify the shock relation for a quasi-perpendicular bow shock, and the assumption that clock angle was preserved as the solar wind passes through the bow shock. A discrepancy between the ratio of the solar wind/magnetosheath plasma velocities and the ratio of the duration of the rotations as observed in the solar wind and magnetosheath (which should match, assuming plasma continuity and frozen-in flow) indicated a "squeezing out" of plasma just earthward of the quasi-perpendicular shock, reducing the plasma pressure (akin to the plasma depletion layer at the nose of the magnetopause) and hence changing the size of the rotation structure. The propagation velocities of the rotation structures in the magnetosheath matched the magnetosheath velocity well at Cluster, confirming that the structures were frozen in to the flow, but the comparison was less good at THEMIS. The Geotail and Double Star TC-1 spacecraft were located near the magnetopause, at dusk and local noon respectively, and Geotail made multiple crossings of the magnetopause. Ground-based auroral observations showed two intervals of poleward-moving aurora, both associated with periods when Geotail and TC-1 observed northward magnetosheath magnetic field. The northward turnings of the magnetosheath field were associated with enhancements in the ionospheric currents (evidenced by signatures in ground-based magnetometer data) and enhancements in convection. The latter were observed in both global SuperDARN flow data, and global ionospheric equivalent currents, which broadly correspond to the Hall current system in the assumption of uniform conductivity. Given that the Hall currents flow antiparallel to the sense of plasma convection, there was a very good correspondence between the global convection measured by SuperDARN and the equivalent current maps.

Nowada et al. (2012) used the Cluster and THEMIS constellations, plus ACE and Geotail (in the solar wind), GOES (at geostationary orbit) and ground-based facilities to study the global response of the magnetosphere to a B_X reversal in the IMF, indicative of a current sheet passage, which was observed by both ACE and Geotail. The B_Y and B_Z components exhibited no significant change across the current sheet; the solar wind speed and density (and hence dynamic pressure) dropped as the current sheet passed. At this time, the THEMIS constellation was in the dawn magnetosphere, whilst Cluster was at dusk, such that the THEMIS/Cluster/GOES superconstellation extended in a line along the Y_{GSM} axis, at $X_{GSM} \approx -5$ R_E . After each IMF B_X reversal, THEMIS-A briefly entered the magnetosheath, indicating a brief pulse-like "in-out" motion of the magnetopause. The THEMIS-D and E spacecraft, also in the dawnside magnetosphere but further from the magnetosphere, and thereafter the magnetic field signatures indicating a localized compression of the magnetosphere, and thereafter the magnetic field strength increased. Cluster, situated on the dusk side at a similar X_{GSM} location, observed no such signature. Ground-based magnetometers in the local time sector of the THEMIS spacecraft observed negative bay signatures and periodic fluctuations at frequencies corresponding to the Pi2 band, and there was an enhancement

FEAR 36 of 46

in the AE index. Global auroral images from the Polar spacecraft revealed low levels of auroral activity, including two weak and localized auroral spots (i.e., pseudobreakups), one of which was in the post-midnight sector as THEMIS was. The magnetic field observed by two of the GOES spacecraft showed signs of dipolarization. The authors concluded that significant changes to the magnetosphere could occur as a result of a change of a single solar wind parameter, even in the absence of a major signature such as a pressure pulse or southward IMF turning. Although the magnetospheric response bore some of the hallmarks of a substorm, the response was much more localized.

The IMF B_V component also exerts an important influence on the magnetosphere, and is known to influence the direction of convection in the magnetotail lobes. Case et al. (2020) examined the statistics of nightside magnetospheric and ionospheric flow surrounding intervals in which the IMF B_V component changed sign. At higher latitudes, in the magnetotail lobe/ionospheric polar cap, magnetic field lines are connected to the IMF; Cluster EDI measurements in the lobe and SuperDARN measurements in the polar cap both confirmed that in the northern hemisphere, positive and negative IMF B_V drives ionospheric flows in the positive and negative Y_{GSM} direction, respectively, with the opposite relation being observed in the southern hemisphere (as expected). Superposed epoch analyses demonstrated that at these higher latitudes, the magnetospheric and ionospheric flows responded promptly to changes in the sign of the IMF B_v component, with the flow direction starting to change within 5 min of the B_V reversal in the lagged IMF, and the average flows reversing around 30–40 min after the IMF B_V reversal. The dayside reconnection rate influenced how the lobes responded, with periods of high dayside driving providing clearer relationships (and reversals) than periods of lower driving. Multiple debated mechanisms predict an element of IMF B_{γ} control on the direction of flow in the plasma sheet too, once the relevant timescales (which differ between mechanisms) are taken into account; however, the authors found no clear reversals in the plasma sheet convection direction associated with IMF B_{ν} reversals, which they suggested may be due to the Dungey cycle complicating their superposed epoch analyses, since under that explanation the control of plasma sheet motion requires the reversed B_{γ} to be transferred onto closed plasma sheet field lines through magnetotail reconnection, which occurs at times that are uncorrelated with the IMF B_v reversal.

7.4. The Open-Closed Field Line Boundary

The open/closed boundary (OCB) is an important quantity for understanding the global state of the magnetosphere, since its variations can be used to calculate the net reconnection rate (i.e., the difference between the dayside and nightside reconnection rates). Wild et al. (2004) used data from several space- and ground-based sources to compare and investigate different means of determining the open-closed field line boundary in the dawn sector, as previous studies had found that the majority of techniques that had been developed to identify the OCB were not generally applicable to all local times. The authors compared the OCB location on the dawn side of the polar cap as determined by Cluster, the FAST and DMSP spacecraft at lower altitudes, global auroral imagery from the IMAGE satellite, and the "spectral width boundary" in SuperDARN HF radar measurements (between low spectral width radar echoes at lower latitudes and high spectral width echoes at higher latitudes). The OCB locations determined from FAST and DMSP observations (at 2 MLT and 7 MLT, respectively) were co-located with those determined from the poleward edge of both the IMAGE WIC and SI13 (Spectrographic Imager 135.6 nm instrument) observations. However, the OCB locations inferred from Cluster 1 and 3 particle observations (at 5 MLT and 4 MLT, respectively) were significantly poleward of that inferred from WIC observations (but comparable to the poleward edge of the IMAGE SI13 emissions). The authors attributed the discrepancy between the Cluster and IMAGE WIC estimates of the OCB as being due to the electron precipitation being relatively soft (<5 keV), and hence leading to emissions in the SI13 band, but much less of a signal in WIC. They noted that the reliability of a given waveband was longitudinally patchy, given the success of WIC at the footprints of the DMSP and FAST spacecraft, and that this was most likely due to the sensitivity of the WIC sensor. They therefore concluded that when determining the OCB location it is best to compare emissions from multiple wavelengths, if possible. The SuperDARN spectral width boundary in this sector generally coincided with the poleward limit of the most intense UV auroral emissions, rather than the poleward edge of auroral luminosity, and therefore did not constitute a reliable proxy in this sector.

Aikio et al. (2008) applied a new method to determine the OCB in EISCAT data, which they used to examine the location of the nightside boundary during the late expansion/early recovery phase of a substorm. They observed a "zig-zag" motion of the boundary, with two and a half oscillations of a poleward/equatorward cycle, and the

FEAR 37 of 46

21699402, 2022, 8, Downloaded from https://agupubs.onlinelibrary.wiley.com/doi/10.1029/20211A029928 by University Of Southampton, Wiley Online Library on [09/11/2022]. See the

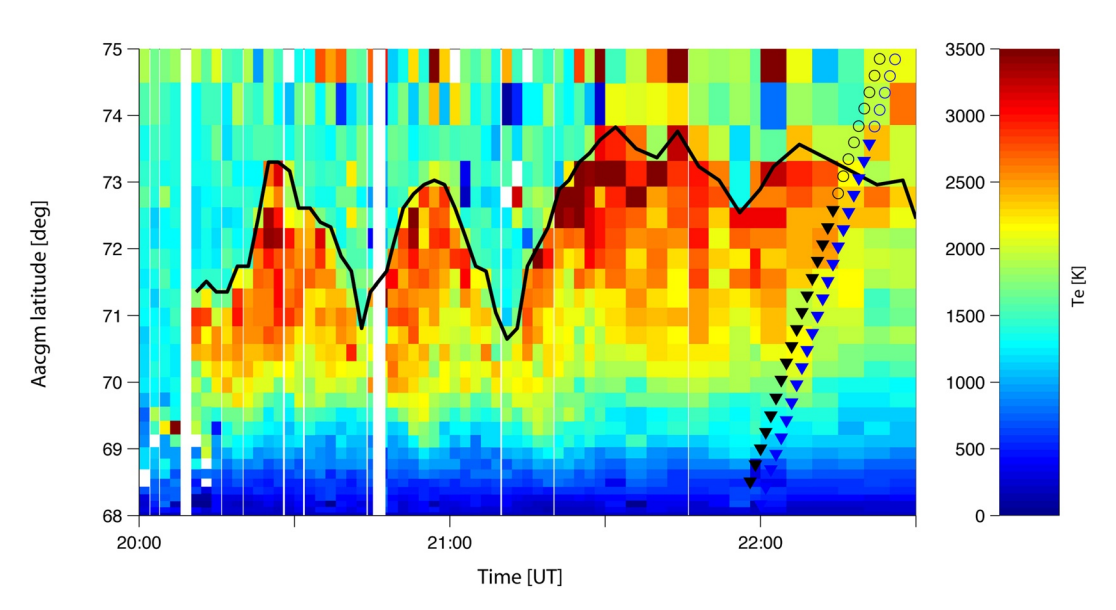


Figure 7. Electron temperature measured by the European Incoherent Scatter facility (EISCAT) VHF radar, indicating (black line) the open-closed field line boundary determined from EISCAT measurements, reproduced from Aikio et al. (2008). The Clusters 1 and 4 footprints are indicated, in black and blue respectively, with triangles in regions where the spacecraft observed ion outflow (indicative of being on closed field lines, and consistent with being equatorward of the black line), and circles where they do not.

boundary moving 2.5° of latitude in each half-cycle (Figure 7). The poleward motions were due to bursts of enhanced reconnection at the NENL, reducing the amount of open flux relative to the background baseline, with the subsequent equatorward motions resulting from the "relaxation" of the system toward equilibrium, in line with the Cowley and Lockwood (1992) paradigm. The poleward expansions of the OCB were associated with enhancements in the westward electrojet immediately equatorward of the boundary, observed in the ionospheric equivalent currents calculated from ground magnetometer measurements. These electrojet enhancements were interpreted as due to precipitation of particles accelerated in the vicinity of the neutral line. At this time, Cluster was situated in the PSBL, and mapped to the vicinity of the EISCAT measurements. Cluster observed an outflow of H⁺ and O⁺ ions within the PSBL, and the PSBL corresponded to a region of enhanced temperature in the ionospheric F region, observed by EISCAT. The outflowing ions were interpreted as originating from the F region, as a result of increased ambipolar diffusion. Cluster also observed broadband extra low frequency waves in the electric field, which it was suggested could accelerate the outflowing ions further. Comparison of particle observations from the four Cluster spacecraft showed evidence of a poleward expansion of the PSBL by 2° within 5 min. The newly formed region of PSBL contained more intense electric field fluctuations, and more intense ion outflows, than the PSBL observed earlier, and the beginning of the poleward expansion of the PSBL was associated with an intensification of the field-aligned current at the boundary. The authors suggested that the downward field-aligned currents observed by Cluster (which PEACE observations indicated were carried by a broad energy range of electrons, from the lowest energies measured [36 eV] to 2 keV) were the counterpart of the earthward flowing field aligned current produced near the neutral line by the Hall effect. Although there were no contemporaneous observations of the NENL, the energy of the electrons was comparable to the energy of electrons streaming into the reconnection site in previous studies. The combined observations, whilst not conclusive, were suggestive that the field-aligned current system created at the reconnection site could continue into the ionosphere.

Recently Matar et al. (2020) have exploited Cluster, SuperDARN, and global-scale auroral data (from the IMAGE satellite) to compare in situ and remote calculations of the magnetotail reconnection rate for two previously studied magnetotail reconnection events. Cluster observations of the inflow region can allow the local reconnection electric field (i.e., rate per unit length of *X*-line) to be determined. Similarly ionospheric radar and auroral measurements can calculate the reconnection electric field, and can also be used to infer the length of the reconnection

FEAR 38 of 46

21699402, 2022, 8, Downloa

line. The authors found excellent agreement between the two methods for both events. Furthermore, they were able to calculate the power associated with precipitating particles (from IMAGE) and the rate at which energy was dissipated to electrons by the reconnection process (from Cluster data); the two were found to be of the same order of magnitude at several times within each event, suggesting that the thermal energy released by reconnection is primarily transferred to the ionosphere, contributing to the auroral activity.

8. Summary

In conclusion, combined space- and ground-based studies have greatly enhanced the scientific return of the Cluster mission, in topics spanning the whole gamut of solar wind-magnetosphere-ionosphere coupling. This has in part been due to the initial embedding of ground-based coordination within the planning of the mission, which led in particular to a large number of conjugate studies in the early years of the mission (Amm et al., 2005); the more recent incorporation of some ground-based data sets into the Cluster Science Archive, facilitating the use of ground-based data in support of Cluster studies, has also played a role. Ultimately, the contribution made by ground-based observatories to the legacy of the Cluster mission reflects the recognition of many authors of the benefits that complementary observations can provide. The fruits of this coordinated approach are evident in subsequent and future missions. Integration of ground-based observatories was a key part of the THEMIS mission and essential for achievement of its scientific objectives (Angelopoulos, 2008). Several studies based on data from the Magnetospheric Multiscale (MMS) and Van Allen Probe missions have employed conjugate ground-based observations (Bezděková et al., 2020; Engebretson et al., 2018; Hwang et al., 2020; Xue et al., 2021). The fact that exploitation of ground-based observations will provide significant additional value to the upcoming SMILE mission has been recognized by the formation of a SMILE Ground-based Working Group following the model set by Cluster (Branduardi-Raymont et al., 2018, p. 74). Furthermore, integration of or collaboration with ground-based facilities forms part of several of the white papers submitted to the recent ESA Voyage 2050 call (Favata et al., 2021), for example, Branduardi-Raymont et al. (2021). In addition to the facilities exploited by the studies outlined in this review paper, these future missions will be able to exploit conjunctions with the forthcoming EISCAT_3D radar, which will enable the community to address new, significant science questions (McCrea et al., 2015). Therefore, the legacy of joint Cluster-ground-based studies is not only the contribution they have made to our understanding of our local geospace environment, beyond what would be possible with in situ observations alone, but the influence they have had on subsequent and future magnetospheric missions.

Nomenclature

DMSP

ACE Advanced Composition Explorer

AE Auroral Electrojet index AL Auroral lower index

AMIE Assimilative Mapping of Ionospheric Electrodynamics

ASI All-sky imager
AU Auroral upper index

BATS-R-US Block-Adaptive-Tree-Solar wind-Roe-Upwind-Scheme

BBF Bursty bulk flow

CANOPUS Canadian Auroral Network for the OPEN Program Unified Study

CDPS Cold dense plasma sheet
CHAMP Challenging Minisatellite Payload

CIS Cluster Ion Spectrometry

CME Coronal mass ejection
CMS Cavity mode model of Samson et al. (1991)

Dst Disturbance Storm-Time index

ECLAT European Cluster Assimilation Technology programme

Defense Meteorological Satellite Program

EDI Electron Drift Instrument

EFW Electric Field and Wave instrument
EISCAT(_3D) European Incoherent Scatter radar (3D)
EMIC Electromagnetic ion cyclotron (wave)

FEAR 39 of 46

21699402, 2022, 8, Downloaded from https://agupubs

.com/doi/10.1029/2021JA029928 by University Of Southampton, Wiley Online Library on [09/11/2022]. See the Terms



ESA European Space Agency
ESR EISCAT Svalbard Radar
EUV Extreme Ultraviolet

FAST Fast Auroral Snapshot (satellite)

FGM Fluxgate magnetometer FTE Flux transfer event

GOES Geostationary Operational Environmental Satellite

HF High frequency HFA Hot flow anomaly

IMAGE Imager for Magnetosphere-to-Aurora Global Exploration (satellite) or International Monitor for

Auroral Geomagnetic Effects (magnetometer chain)

IMF Interplanetary magnetic fieldKHI Kelvin-Helmholtz instability

LANL Los Alamos National Laboratory (satellites)

LLBL Low latitude boundary layer

MAARBLE Monitoring, Analyzing and Assessing Radiation Belt Loss and Energization project

MIRACLE Magnetometers—Ionospheric Radars—All-sky Cameras Large Experiment

MHD Magnetohydrodynamic
MLAT Magnetic latitude
MLT Magnetic local time
MMS Magnetospheric Multiscale
MSP Meridian scanning photometer

NASA National Aeronautics and Space Administration

NENL Near-Earth neutral line

NOAA National Oceanic and Atmospheric Administration

OCB Open-closed (field line) boundary

PC Polar cap (index)

Pc Continuous pulsation (wave)

PEACE Plasma Electron And Current Experiment

Pi Irregular pulsation (wave) PIF Pulsed ionospheric flow

PM(R)AF Poleward moving (radar) auroral form

Ps Substorm pulsation (wave)
PSBL Plasma sheet boundary layer

RAPID Research with Adaptive Particle Imaging Detectors

SAMNET Sub-Auroral Magnetometer Network SAPS Sub-auroral polarization stream

SI-12/13 Spectrographic Imager (121.8 and 135.6 nm wavelength)
SMILE Solar wind Magnetosphere Ionosphere Link Explorer

SoHo Solar and Heliospheric Observatory SPEAR Space Plasma Exploration by Active Radar

STAFF Spatio-Temporal Analysis of Field Fluctuation experiment

STARE Scandinavian Twin Auroral Radar Experiment

SuperDARN Super Dual Auroral Radar Network

SWEPAM Solar Wind Electron Proton Alpha Monitor

SYM-H Symmetric portion of the Horizontal component of the magnetic field

TC-1/2 Tan-Ce 1/2 (Double Star satellites)
TCR Traveling compression region
TCV Traveling convection vortex

THEMIS Time History of Events and Macroscale Interactions during Substorms mission

TRINNI Tail reconnection during IMF Northward, Non-substorm Intervals

ULF Ultralow frequency

UV Ultraviolet UVI Ultraviolet imager

FEAR 40 of 46



Journal of Geophysical Research: Space Physics

10.1029/2021JA029928

VHF Very high frequency

WHISPER Waves of High frequency and Sounder for Probing of Electron density by Relaxation experiment

WIC Wideband Imaging Camera

Data Availability Statement

This is a review paper which contains no new data.

Acknowledgments

During the preparation of this review, the author was supported by the UK Science and Technology Facilities Council Consolidated Grants ST/R000719/1 and ST/V000942/1. The author thanks both reviewers for their constructive and helpful comments.

References

- Aikio, A. T., Mursula, K., Buchert, S., Forme, F., Amm, O., Marklund, G., et al. (2004). Temporal evolution of two auroral arcs as measured by the Cluster satellite and coordinated ground-based instruments. *Annales Geophysicae*, 22(12), 4089–4101. https://doi.org/10.5194/angeo-22-4089-2004
- Aikio, A. T., Pitkänen, T., Fontaine, D., Dandouras, I., Amm, O., Kozlovsky, A., et al. (2008). EISCAT and Cluster observations in the vicinity of the dynamical polar cap boundary. *Annales Geophysicae*, 26(1), 87–105. https://doi.org/10.5194/angeo-26-87-2008
- Amm, O., Aikio, A., Bosqued, J.-M., Dunlop, M., Fazakerley, A., Janhunen, P., et al. (2003). Mesoscale structure of a morning sector ionospheric shear flow region determined by conjugate Cluster II and MIRACLE ground-based observations. *Annales Geophysicae*, 21(8), 1737–1751. https://doi.org/10.5194/angeo-21-1737-2003
- Amm, O., Donovan, E. F., Frey, H., Lester, M., Nakamura, R., Wild, J. A., et al. (2005). Coordinated studies of the geospace environment using Cluster, satellite and ground-based data: An interim review. *Annales Geophysicae*, 23(6), 2129–2170. https://doi.org/10.5194/angeo-23-2129-2005
- Amm, O., Nakamura, R., Frey, H. U., Ogawa, Y., Kubyshkina, M., Balogh, A., & Rème, H. (2006). Substorm topology in the ionosphere and magnetosphere during a flux rope event in the magnetotail. *Annales Geophysicae*, 24(2), 735–750. https://doi.org/10.5194/angeo-24-735-2006 Amm, O., Nakamura, R., Takada, T., Kauristie, K., Frey, H. U., Owen, C. J., et al. (2011). Observations of an auroral streamer in a double oval configuration. *Annales Geophysicae*, 29(4), 701–716. https://doi.org/10.5194/angeo-29-701-2011
- Angelopoulos, V. (2008). The THEMIS Mission. Space Science Reviews, 141(1-4), 5-34. https://doi.org/10.1007/s11214-008-9336-1
- Badman, S. V., Wright, D. M., Clausen, L. B. N., Fear, R. C., Robinson, T. R., & Yeoman, T. K. (2009). Cluster spacecraft observations of a ULF wave enhanced by Space Plasma Exploration by Active Radar (SPEAR). Annales Geophysicae, 27(9), 3591–3599. https://doi.org/10.5194/angeo-27-3591-2009
- Baker, D. N., Peterson, W. K., Eriksson, S., Li, X., Blake, J. B., Burch, J. L., et al. (2002). Timing of magnetic reconnection initiation during a global magnetospheric substorm onset. Geophysical Research Letters, 29, 2190. https://doi.org/10.1029/2002GL015539
- Balan, N., Alleyne, H., Walker, S., Reme, H., Lucek, E., Cornilleau-Wehrlin, N., et al. (2007). Response of the magnetosheath-cusp region to a coronal mass ejection. *Journal of Geophysical Research*, 112(A12), A12211. https://doi.org/10.1029/2006JA012122
- Balan, N., Alleyne, H., Walker, S., Reme, H., McCrea, I., & Aylward, A. (2008). Magnetosphere-ionosphere coupling during the CME events of 07-12 November 2004. Journal of Atmospheric and Solar-Terrestrial Physics, 70(17), 2101–2111. https://doi.org/10.1016/j.jastp.2008.03.015
- Balasis, G., Daglis, I. A., Mann, I. R., Papadimitriou, C., Zesta, E., Georgiou, M., et al. (2015). Multi-satellite study of the excitation of Pc3 and Pc4-5 ULF waves and their penetration across the plasmapause during the 2003 Halloween superstorm. *Annales Geophysicae*, 33(10), 1237–1252. https://doi.org/10.5194/angeo-33-1237-2015
- Balogh, A., Carr, C. M., Acuña, M. H., Dunlop, M. W., Beek, T. J., Brown, P., et al. (2001). The Cluster magnetic field investigation: Overview of in-flight performance and initial results. Annales Geophysicae, 19(10/12), 1207–1217. https://doi.org/10.5194/angeo-19-1207-2001
- Bavassano Cattaneo, M. B., Marcucci, M. F., Retinò, A., Pallocchia, G., Rème, H., Dandouras, I., et al. (2006). Kinetic signatures during a quasi-continuous lobe reconnection event: Cluster Ion Spectrometer (CIS) observations. *Journal of Geophysical Research*, 111(A9), A09212. https://doi.org/10.1029/2006JA011623
- Bezděková, B., Němec, F., Manninen, J., Hospodarsky, G. B., Santolík, O., Kurth, W. S., & Hartley, D. P. (2020). Conjugate observations of quasiperiodic emissions by the Van Allen Probes spacecraft and ground-based station Kannuslehto. *Journal of Geophysical Research*, 125(6), e2020JA027793. https://doi.org/10.1029/2020JA027793
- Bogdanova, Y. V., Marchaudon, A., Owen, C. J., Dunlop, M. W., Frey, H. U., Wild, J. A., et al. (2005). On the formation of the high-altitude stagnant cusp: Cluster observations. *Geophysical Research Letters*, 32(12), L12101. https://doi.org/10.1029/2005GL022813
- Borälv, E., Opgenoorth, H. J., Kauristie, K., Lester, M., Bosqued, J. M., Dewhurst, J. P., et al. (2005). Correlation between ground-based observations of substorm signatures and magnetotail dynamics. *Annales Geophysicae*, 23(3), 997–1011. https://doi.org/10.5194/angeo-23-997-2005
- Borg, A. L., Østgaard, N., Pedersen, A., Øieroset, M., Phan, T. D., Germany, G., et al. (2007). Simultaneous observations of magnetotail reconnection and bright X-ray aurora on 2 October 2002. *Journal of Geophysical Research*, 112(A6), A06215. https://doi.org/10.1029/2006JA011913
- Bosqued, J. M., Escoubet, C. P., Frey, H. U., Dunlop, M., Berchem, J., Marchaudon, A., et al. (2005). Multipoint observations of transient reconnection signatures in the cusp precipitation: A Cluster-IMAGE detailed case study. *Journal of Geophysical Research*, 110(A3), A03219. https://doi.org/10.1029/2004JA010621
- Branduardi-Raymont, G., Berthomier, M., Bogdanova, Y. V., Carter, J. A., Collier, M., Dimmock, A., et al. (2021). Exploring solar-terrestrial interactions via multiple imaging observers. *Experimental Astronomy*. https://doi.org/10.1007/s10686-021-09784-y
- Branduardi-Raymont, G., Wang, C., Escoubet, C. P., Adamovic, M., Agnolon, D., Berthomier, M., et al. (2018). SMILE definition study report (Tech. Rep.). European Space Agency. https://doi.org/10.5270/esa.smile.definition_study_report-2018-12
- Cai, H. T., McCrea, I. W., Dunlop, M. W., Davies, J. A., Bogdanova, Y. V., Pitout, F., et al. (2009). Cusp observations during a sequence of fast IMF B₇ reversals. *Annales Geophysicae*, 27(7), 2721–2737. https://doi.org/10.5194/angeo-27-2721-2009
- Cao, X., Pu, Z. Y., Zhang, H., Mishin, V. M., Ma, Z. W., Dunlop, M. W., et al. (2008). Multispacecraft and ground-based observations of substorm timing and activations: Two case studies. *Journal of Geophysical Research*, 113(A7), A07S25. https://doi.org/10.1029/2007JA012761
- Carlson, C. W., Pfaff, R. F., & Watzin, J. G. (1998). The Fast Auroral SnapshoT (FAST) mission. Geophysical Research Letters, 25(12), 2013–2016. https://doi.org/10.1029/98GL01592
- Case, N. A., Grocott, A., Fear, R. C., Haaland, S., & Lane, J. H. (2020). Convection in the magnetosphere-ionosphere system: A multimission survey of its response to IMF B_Y reversals. *Journal of Geophysical Research*, 125(10), e2019JA027541. https://doi.org/10.1029/2019JA027541

FEAR 41 of 46



Journal of Geophysical Research: Space Physics

- 10.1029/2021JA029928
- Cerisier, J.-C., Marchaudon, A., Bosqued, J.-M., McWilliams, K., Frey, H. U., Bouhram, M., et al. (2005). Ionospheric signatures of plasma injections in the cusp triggered by solar wind pressure pulses. *Journal of Geophysical Research*, 110(A8), A08204. https://doi. org/10.1029/2004JA010962
- Chen, Y.-J., Heelis, R. A., & Cumnock, J. A. (2016). Plasma and convection reversal boundary motions in the high-latitude ionosphere. *Journal of Geophysical Research*, 121(6), 5752–5763. https://doi.org/10.1002/2016JA022796
- Chisham, G., Lester, M., Milan, S. E., Freeman, M. P., Bristow, W. A., Grocott, A., et al. (2007). A decade of the super Dual Auroral Radar Network (SuperDARN): Scientific achievements, new techniques and future directions. Surveys in Geophysics, 28(1), 33–109. https://doi.org/10.1007/s10712-007-9017-8
- Chulliat, A., Matzka, J., Masson, A., & Milan, S. E. (2017). Key ground-based and space-based assets to disentangle magnetic field sources in the Earth's environment. Space Science Reviews, 206(1–4), 123–156. https://doi.org/10.1007/s11214-016-0291-y
- Clausen, L. B. N., & Yeoman, T. K. (2009). Comprehensive survey of Pc4 and Pc5 band spectral content in Cluster magnetic field data. Annales Geophysicae, 27(8), 3237–3248. https://doi.org/10.5194/angeo-27-3237-2009
- Clausen, L. B. N., Yeoman, T. K., Behlke, R., & Lucek, E. A. (2008). Multi-instrument observations of a large scale Pc4 pulsation. *Annales Geophysicae*, 26(1), 185–199. https://doi.org/10.5194/angeo-26-185-2008
- Clausen, L. B. N., Yeoman, T. K., Fear, R. C., Behlke, R., Lucek, E. A., & Engebretson, M. J. (2009). First simultaneous measurements of waves generated at the bow shock in the solar wind, the magnetosphere and on the ground. *Annales Geophysicae*, 27(1), 357–371. https://doi.org/10.5194/angeo-27-357-2009
- Cooling, B. M. A., Owen, C. J., & Schwartz, S. J. (2001). Role of the magnetosheath flow in determining the motion of open flux tubes. *Journal of Geophysical Research*, 106(A9), 18763–18775. https://doi.org/10.1029/2000JA000455
- Cornilleau-Wehrlin, N., Chanteur, G., Perraut, S., Rezeau, L., Robert, P., Roux, A., et al. (2003). First results obtained by the Cluster STAFF experiment. *Annales Geophysicae*, 21(2), 437–456. https://doi.org/10.5194/angeo-21-437-2003
- Cowley, S. W. H. (1982). The causes of convection in the Earth's magnetosphere: A review of developments during the IMS. Reviews of Geophysics and Space Physics, 20(3), 531–565. https://doi.org/10.1029/RG020i003p00531
- Cowley, S. W. H., & Lockwood, M. (1992). Excitation and decay of solar wind-driven flows in the magnetosphere-ionosphere system. Annales Geophysicae, 10, 103–115.
- Daum, P., Wild, J. A., Penz, T., Woodfield, E. E., Rème, H., Fazakerley, A. N., et al. (2008). Global MHD simulation of flux transfer events at the high-latitude magnetopause observed by the Cluster spacecraft and the SuperDARN radar system. *Journal of Geophysical Research*, 113(A7), A07S22. https://doi.org/10.1029/2007JA012749
- Décréau, P. M. E., Fergeau, P., Krasnoselskikh, V., Le Guirriec, E., Lévêque, M., Martin, P., et al. (2001). Early results from the Whisper instrument on Cluster: An overview. *Annales Geophysicae*, 19(10/12), 1241–1258. https://doi.org/10.5194/angeo-19-1241-2001
- Dougal, E. R., Nykyri, K., & Moore, T. W. (2013). Mapping of the quasi-periodic oscillations at the flank magnetopause into the ionosphere. Annales Geophysicae, 31(11), 1993–2011. https://doi.org/10.5194/angeo-31-1993-2013
- Draper, N. C., Lester, M., Cowley, S. W. H., Bosqued, J.-M., Grocott, A., Wild, J. A., et al. (2006). Cluster observations of a magnetic field cavity in the plasma sheet. *Advances in Space Research*, 38(8), 1738–1743, https://doi.org/10.1016/j.asr.2005.09.024
- Draper, N. C., Lester, M., Wild, J. A., Milan, S. E., Provan, G., Grocott, A., et al. (2004). A joint Cluster and ground-based instruments study of two magnetospheric substorm events on 1 September 2002. Annales Geophysicae, 22(12), 4217–4228. https://doi.org/10.5194/ angeo-22-4217-2004
- Dunlop, M. W., Dong, X., Wang, T., Eastwood, J. P., Robert, P., Haaland, S., et al. (2021). Curlometer technique and applications. *Journal of Geophysical Research*, 126(11), e2021JA029538. https://doi.org/10.1029/2021JA029538
- Dunlop, M. W., Zhang, Q.-H., Bogdanova, Y. V., Trattner, K. J., Pu, Z., Hasegawa, H., et al. (2011). Magnetopause reconnection across wide local time. Annales Geophysicae, 29(9), 1683–1697. https://doi.org/10.5194/angeo-29-1683-2011
- Eastwood, J. P., Schwartz, S. J., Horbury, T. S., Carr, C. M., Glassmeier, K.-H., Richter, I., et al. (2011). Transient Pc3 wave activity generated by a hot flow anomaly: Cluster, Rosetta, and ground-based observations. *Journal of Geophysical Research*, 116(A8), A08224. https://doi.org/10.1029/2011JA016467
- Engebretson, M. J., Posch, J. L., Capman, N. S. S., Campuzano, N. G., Bělik, P., Allen, R. C., et al. (2018). MMS, Van Allen Probes, GOES 13, and ground-based magnetometer observations of EMIC wave events before, during, and after a modest interplanetary shock. *Journal of Geophysical Research*, 123(10), 8331–8357. https://doi.org/10.1029/2018JA025984
- Engebretson, M. J., Yeoman, T. K., Oksavik, K., Søraas, F., Sigernes, F., Moen, J. I., et al. (2013). Multi-instrument observations from Svalbard of a traveling convection vortex, electromagnetic ion cyclotron wave burst, and proton precipitation associated with a bow shock instability. Journal of Geophysical Research, 118(6), 2975–2997. https://doi.org/10.1002/jgra.50291
- Escoubet, C. P., Masson, A., Laakso, H., & Goldstein, M. L. (2015). Recent highlights from Cluster, the first 3-D magnetospheric mission. Annales Geophysicae, 33(10), 1221–1235. https://doi.org/10.5194/angeo-33-1221-2015
- Escoubet, C. P., Masson, A., Laakso, H., Goldstein, M. L., Dimbylow, T., Bogdanova, Y. V., et al. (2021). Cluster after 20 years of operations: Science highlights and technical challenges. *Journal of Geophysical Research*, 126(8), e2021JA029474. https://doi.org/10.1029/2021JA029474
- Farrugia, C. J., Lund, E. J., Sandholt, P. E., Wild, J. A., Cowley, S. W. H., Balogh, A., et al. (2004). Pulsed flows at the high-altitude cusp poleward boundary, and associated ionospheric convection and particle signatures, during a Cluster FAST SuperDARN Søndrestrøm conjunction under a southwest IMF. *Annales Geophysicae*, 22(8), 2891–2905. https://doi.org/10.5194/angeo-22-2891-2004
- Favata, F., Hasinger, G., Tacconi, L. J., Arridge, C. S., & O'Flaherty, K. S. (2021). Introducing the Voyage 2050 White Papers, contributions from the science community to ESA's long-term plan for the Scientific Programme. Experimental Astronomy, 51(3), 551–558. https://doi.org/10.1007/s10686-021-09746-4
- Fazakerley, A. N., Lahiff, A. D., Wilson, R. J., Rozum, I., Anekallu, C., West, M., & Bacai, H. (2010). PEACE data in the Cluster Active Archive. In H. Laakso, M. Taylor, & P. Escoubet (Eds.), The Cluster Active Archive - Studying the Earth's space plasma environment (pp. 129–144). Springer Netherlands. https://doi.org/10.1007/978-90-481-3499-1_8
- Fear, R. C. (2021). The northward IMF magnetosphere. In R. Maggiolo, N. André, H. Hasegawa, & D. T. Welling (Eds.), Space physics and aeronomy collection volume 2, Magnetospheres in the solar system (Vol. 259, pp. 293–309). American Geophysical Union. https://doi. org/10.1002/9781119815624.ch19
- Fear, R. C., Milan, S. E., Fazakerley, A. N., Fornaçon, K.-H., Carr, C. M., & Dandouras, I. (2009). Simultaneous observations of flux transfer events by THEMIS, Cluster, Double Star, and SuperDARN: Acceleration of FTEs. *Journal of Geophysical Research*, 114(A10), A10213. https://doi.org/10.1029/2009JA014310
- Fear, R. C., Milan, S. E., Lucek, E. A., Cowley, S. W. H., & Fazakerley, A. N. (2010). Mixed azimuthal scales of flux transfer events. In H. Laakso, M. Taylor, & C. P. Escoubet (Eds.), The Cluster Active Archive Studying the Earth's space plasma environment (pp. 389–398). Springer Netherlands. https://doi.org/10.1007/978-90-481-3499-1_27

FEAR 42 of 46

- Fear, R. C., Milan, S. E., Maggiolo, R., Fazakerley, A. N., Dandouras, I., & Mende, S. B. (2014). Direct observation of closed magnetic flux trapped in the high-latitude magnetosphere. *Science*, 346(6216), 1506–1510. https://doi.org/10.1126/science.1257377
- Fear, R. C., Trenchi, L., Coxon, J. C., & Milan, S. E. (2017). How much flux does a flux transfer event transfer? *Journal of Geophysical Research*, 122, 12310–12327. https://doi.org/10.1002/2017JA024730
- Figueiredo, S., Marklund, G. T., Karlsson, T., Johansson, T., Ebihara, Y., Ejiri, M., et al. (2005). Temporal and spatial evolution of discrete auroral arcs as seen by Cluster. *Annales Geophysicae*, 23(7), 2531–2557. https://doi.org/10.5194/angeo-23-2531-2005
- Folkestad, K., Hagfors, T., & Westerlund, S. (1983). EISCAT: An updated description of technical characteristics and operational capabilities. Radio Science, 18(6), 867–879. https://doi.org/10.1029/RS018i006p00867
- Forsyth, C., Fazakerley, A. N., Rae, I. J., Watt, C. E. J., Murphy, K., Wild, J. A., et al. (2014). In situ spatiotemporal measurements of the detailed azimuthal substructure of the substorm current wedge. *Journal of Geophysical Research*, 119(2), 927–946. https://doi.org/10.1002/2013JA019302
- Forsyth, C., Lester, M., Cowley, S. W. H., Dandouras, I., Fazakerley, A. N., Fear, R. C., et al. (2008). Observed tail current systems associated with bursty bulk flows and auroral streamers during a period of multiple substorms. *Annales Geophysicae*, 26(1), 167–184. https://doi.org/10.5194/angeo-26-167-2008
- Friis-Christensen, E., Lühr, H., Knudsen, D., & Haagmans, R. (2008). Swarm An Earth observation mission investigating geospace. *Advances in Space Research*, 41(1), 210–216. https://doi.org/10.1016/j.asr.2006.10.008
- Fryer, L. J., Fear, R. C., Coxon, J. C., & Gingell, I. L. (2021). Observations of closed magnetic flux embedded in the lobes during periods of northward IMF. *Journal of Geophysical Research*, 126(6), e2021JA029281. https://doi.org/10.1029/2021JA029281
- Gjerloev, J. W. (2012). The SuperMAG data processing technique. *Journal of Geophysical Research*, 117(A9), A09213. https://doi.org/10.1029/2012JA017683
- Greenwald, R. A., Baker, K. B., Dudeney, J. R., Pinnock, M., Jones, T. B., Thomas, E. C., et al. (1995). DARN/SuperDARN: A global view of high-latitude convection. *Space Science Reviews*, 71(1–4), 761–796. https://doi.org/10.1007/BF00751350
- Greenwald, R. A., Weiss, W., Nielsen, E., & Thomson, N. R. (1978). STARE: A new radar auroral backscatter experiment in northern Scandinavia. Radio Science, 13(6), 1021–1039. https://doi.org/10.1029/RS013i006p01021
- Grocott, A., Yeoman, T. K., Milan, S. E., Amm, O., Frey, H. U., Juusola, L., et al. (2007). Multi-scale observations of magnetotail flux transport during IMF-northward non-substorm intervals. *Annales Geophysicae*, 25(7), 1709–1720. https://doi.org/10.5194/angeo-25-1709-2007
- Grocott, A., Yeoman, T. K., Nakamura, R., Cowley, S. W. H., Frey, H. U., Rème, H., & Klecker, B. (2004). Multi-instrument observations of the ionospheric counterpart of a bursty bulk flow in the near-Earth plasma sheet. *Annales Geophysicae*, 22(4), 1061–1075. https://doi.org/10.5194/ angeo-22-1061-2004
- Gustafsson, G., André, M., Carozzi, T., Eriksson, A. I., Fälthammar, C.-G., Grard, R., et al. (2001). First results of electric field and density observations by Cluster EFW based on initial months of operation. Annales Geophysicae, 19(10/12), 1219–1240. https://doi.org/10.5194/ angeo-19-1219-2001
- Haaland, S., & Gjerloev, J. (2013). On the relation between asymmetries in the ring current and magnetopause current. *Journal of Geophysical Research*, 118(12), 7593–7604. https://doi.org/10.1002/2013JA019345
- Hwang, K.-J., Goldstein, M. L., Moore, T. E., Walsh, B. M., Baishev, D. G., Moiseyev, A. V., et al. (2014). A tailward moving current sheet normal magnetic field front followed by an earthward moving dipolarization front. *Journal of Geophysical Research*, 119(7), 5316–5327. https://doi.org/10.1002/2013JA019657
- Hwang, K.-J., Nishimura, Y., Coster, A. J., Gillies, R. G., Fear, R. C., Fuselier, S. A., et al. (2020). Sequential observations of flux transfer events, poleward-moving auroral forms, and polar cap patches. *Journal of Geophysical Research*, 125(6), e2019JA027674. https://doi.org/10.1029/2019JA027674
- Juusola, L., Amm, O., Frey, H. U., Kauristie, K., Nakamura, R., Owen, C. J., et al. (2008). Ionospheric signatures during a magnetospheric flux rope event. Annales Geophysicae, 26(12), 3967–3977. https://doi.org/10.5194/angeo-26-3967-2008
- Juusola, L., Andréeová, K., Amm, O., Kauristie, K., Milan, S. E., Palmroth, M., & Partamies, N. (2010). Effects of a solar wind dynamic pressure increase in the magnetosphere and in the ionosphere. Annales Geophysicae, 28(10), 1945–1959. https://doi.org/10.5194/angeo-28-1945-2010
- Juusola, L., Kubyshkina, M., Nakamura, R., Pitkänen, T., Amm, O., Kauristie, K., et al. (2013). Ionospheric signatures of a plasma sheet rebound flow during a substorm onset. *Journal of Geophysical Research*, 118(1), 350–363. https://doi.org/10.1029/2012JA018132
- Juusola, L., Nakamura, R., Amm, O., & Kauristie, K. (2009). Conjugate ionospheric equivalent currents during bursty bulk flows. *Journal of Geophysical Research*, 114(A4), A04313. https://doi.org/10.1029/2008JA013908
- Kauristie, K., Pulkkinen, T. I., Amm, O., Viljanen, A., Syrjäsuo, M., Janhunen, P., et al. (2001). Ground-based and satellite observations of high-latitude auroral activity in the dusk sector of the auroral oval. Annales Geophysicae, 19(10/12), 1683–1696. https://doi.org/10.5194/ angeo-19-1683-2001
- Kawano, H., Ohtani, S., Uozumi, T., Tokunaga, T., Yoshikawa, A., Yumoto, K., et al. (2011). Pi2 waves simultaneously observed by Cluster and CPMN ground-based magnetometers near the plasmapause. *Annales Geophysicae*, 29(9), 1663–1672. https://doi.org/10.5194/angeo-29-1663-2011
- Kelly, J. D. (1983). Sondrestrom radar initial results. Geophysical Research Letters, 10(11), 1112–1115. https://doi.org/10.1029/ GL010i011p01112
- Kelly, J. D., Heinselman, C. J., Vickrey, J. F., & Vondrak, R. R. (1995). The Sondrestrom radar and accompanying ground-based instrumentation. Space Science Reviews, 71(1-4), 797-813. https://doi.org/10.1007/BF00751351
- Kerridge, D. (2001). INTERMAGNET: Worldwide near-real-time geomagnetic observatory data. In *Proceedings of the workshop on space weather*. Retrieved from https://www.intermagnet.org/publications/IM_ESTEC.pdf
- Liu, Z. X., Escoubet, C. P., Pu, Z., Laakso, H., Shi, J. K., Shen, C., & Hapgood, M. (2005). The Double Star mission. Annales Geophysicae, 23(8), 2707–2712. https://doi.org/10.5194/angeo-23-2707-2005
- Lockwood, M., Denig, W. F., Farmer, A. D., Davda, V. N., Cowley, S. W. H., & Lühr, H. (1993). Ionospheric signatures of pulsed reconnection at the Earth's magnetopause. *Nature*, 361(6411), 424–428. https://doi.org/10.1038/361424a0
- Lockwood, M., Fazakerley, A., Opgenoorth, H., Moen, J., van Eyken, A. P., Dunlop, M., et al. (2001). Coordinated Cluster and ground-based instrument observations of transient changes in the magnetopause boundary layer during an interval of predominantly northward IMF: Relation to reconnection pulses and FTE signature. *Annales Geophysicae*, 19(10/12), 1613–1640. https://doi.org/10.5194/angeo-19-1613-2001
- Lockwood, M., Opgenoorth, H., van Eyken, A. P., Fazakerley, A., Bo, J.-M., Denig, W., et al. (2001). Coordinated Cluster, ground-based instrumentation and low-altitude satellite observations of transient poleward-moving events in the ionosphere and in the tail lobe. *Annales Geophysicae*, 19(10/12), 1589–1612. https://doi.org/10.5194/angeo-19-1589-2001
- Lockwood, M., & Opgenoorth, H. J. (1995). Opportunities for magnetospheric research using EISCAT/ESR and Cluster. *Journal of Geomagnetism and Geoelectricity*, 47(8), 699–719. https://doi.org/10.5636/jgg.47.699

FEAR 43 of 46

- Lui, A. T. Y., Zheng, Y., Zhang, Y., Angelopoulos, V., Parks, G. K., Mozer, F. S., et al. (2007). Prelude to THEMIS tail conjunction study. Annales Geophysicae, 25(4), 1001–1009. https://doi.org/10.5194/angeo-25-1001-2007
- Maggiolo, R., Echim, M., Simon Wedlund, C., Zhang, Y., Fontaine, D., Lointier, G., & Trotignon, J.-G. (2012). Polar cap arcs from the magnetosphere to the ionosphere: Kinetic modelling and observations by Cluster and TIMED. *Annales Geophysicae*, 30(2), 283–302. https://doi.org/10.5194/angeo-30-283-2012
- Mailyan, B., Shi, Q. Q., Kullen, A., Maggiolo, R., Zhang, Y., Fear, R. C., et al. (2015). Transpolar arc observation after solar wind entry into the high-latitude magnetosphere. *Journal of Geophysical Research*, 120(5), 3525–3534. https://doi.org/10.1002/2014JA020912
- Mann, I. R., Milling, D. K., Rae, I. J., Ozeke, L. G., Kale, A., Kale, Z. C., et al. (2008). The upgraded CARISMA magnetometer array in the THEMIS era. Space Science Reviews, 141(1–4), 413–451. https://doi.org/10.1007/s11214-008-9457-6
- Mann, I. R., Voronkov, I., Dunlop, M., Donovan, E., Yeoman, T. K., Milling, D. K., et al. (2002). Coordinated ground-based and Cluster observations of large amplitude global magnetospheric oscillations during a fast solar wind speed interval. *Annales Geophysicae*, 20(4), 405–426. https://doi.org/10.5194/angeo-20-405-2002
- Marchaudon, A., Cerisier, J.-C., Bosqued, J.-M., Dunlop, M. W., Wild, J. A., Décréau, P. M. E., et al. (2004). Transient plasma injections in the dayside magnetosphere: One-to-one correlated observations by Cluster and SuperDARN. *Annales Geophysicae*, 22(1), 141–158. https://doi.org/10.5194/angeo-22-141-2004
- Marchaudon, A., Cerisier, J.-C. C., Dunlop, M. W., Pitout, F., Bosqued, J.-M. M., & Fazakerley, A. N. (2009). Shape, size, velocity and field-aligned currents of dayside plasma injections: A multi-altitude study. *Annales Geophysicae*, 27(3), 1251–1266. https://doi.org/10.5194/angeo-27-1251-2009
- Marcucci, M. F., Coco, I., Ambrosino, D., Amata, E., Milan, S. E., Bavassano Cattaneo, M. B., & Retinò, A. (2008). Extended SuperDARN and IMAGE observations for northward IMF: Evidence for dual lobe reconnection. *Journal of Geophysical Research*, 113(A2), A02204. https://doi.org/10.1029/2007JA012466
- Marklund, G., & Lindqvist, P.-A. (2021). Cluster multi-probing of the aurora during two decades. *Journal of Geophysical Research*, 126(6), e2021JA029497. https://doi.org/10.1029/2021JA029497
- Matar, J., Hubert, B., Yao, Z., Guo, R., Cowley, S. W. H., Milan, S. E., & Gurgiolo, C. (2020). Concurrent observations of magnetic reconnection from Cluster, IMAGE and SuperDARN: A comparison of reconnection rates and energy conversion. *Journal of Geophysical Research*, 125(4), e2019JA027264. https://doi.org/10.1029/2019JA027264
- Maynard, N. C., Ober, D. M., Burke, W. J., Scudder, J. D., Lester, M., Dunlop, M., et al. (2003). Polar, Cluster and SuperDARN evidence for high-latitude merging during southward IMF: Temporal/spatial evolution. *Annales Geophysicae*, 21(12), 2233–2258. https://doi.org/10.5194/ angeo-21-2233-2003
- McCrea, I., Aikio, A., Alfonsi, L., Belova, E., Buchert, S., Clilverd, M., et al. (2015). The science case for the EISCAT_3D radar. *Progress in Earth and Planetary Science*, 2(1), 21, https://doi.org/10.1186/s40645-015-0051-8
- Mende, S. B., Heetderks, H., Frey, H. U., Lampton, M., Geller, S. P., Habraken, S., et al. (2000). Far ultraviolet imaging from the IMAGE space-craft: 1. System design. Space Science Reviews, 91(1/2), 243–270. https://doi.org/10.1023/A:1005271728567
- Milan, S. E., Wild, J. A., Hubert, B., Carr, C. M., Lucek, E. A., Bosqued, J. M., et al. (2006). Flux closure during a substorm observed by Cluster, Double Star, IMAGE FUV, SuperDARN, and Greenland magnetometers. *Annales Geophysicae*, 24(2), 751–767. https://doi.org/10.5194/angeo-24-751-2006
- Moen, J., Holtet, J. A., Pedersen, A., Lybekk, B., Svenes, K., Oksavik, K., et al. (2001). Cluster boundary layer measurements and optical observations at magnetically conjugate sites. *Annales Geophysicae*, 19(10/12), 1655–1668. https://doi.org/10.5194/angeo-19-1655-2001
- Motoba, T., Hosokawa, K., Ogawa, Y., Sato, N., Kadokura, A., Milan, S. E., & Lester, M. (2012). Simultaneous ground-satellite observations of meso-scale auroral arc undulations. *Journal of Geophysical Research*, 117(A6), A06213. https://doi.org/10.1029/2011JA017291
- Motoba, T., Takahashi, K., Gjerloev, J., Ohtani, S., & Milling, D. K. (2013). The role of compressional Pc5 pulsations in modulating precipitation of energetic electrons. *Journal of Geophysical Research*, 118(12), 7728–7739. https://doi.org/10.1002/2013JA018912
- Nakamura, R., Amm, O., Laakso, H., Draper, N. C., Lester, M., Grocott, A., et al. (2005). Localized fast flow disturbance observed in the plasma sheet and in the ionosphere. *Annales Geophysicae*, 23(2), 553–566. https://doi.org/10.5194/angeo-23-553-2005
- Nowada, M., Lin, C.-H., Pu, Z.-Y., Fu, S.-Y., Angelopoulos, V., Carlson, C. W., & Auster, H.-U. (2012). Substorm-like magnetospheric response to a discontinuity in the B_x component of interplanetary magnetic field. *Journal of Geophysical Research*, 117(A4), A04218. https://doi.org/10.1029/2011JA016894
- Opgenoorth, H. J. (1993). Coordination of ground-based observations with Cluster. In *Cluster: Mission, payload and supporting activities* (pp. 301–305). ESA.
- Opgenoorth, H. J., Bromage, B., Fontaine, D., La Hoz, C., Huuskonen, A., Kohl, H., et al. (1989). Coordinated observations with EISCAT and the Viking satellite: The decay of a westward travelling surge. *Annales Geophysicae*, 7, 479–500.
- Opgenoorth, H. J., & Lockwood, M. (1997). Opportunities for magnetospheric research with coordinated Cluster and ground-based observations. Space Science Reviews, 79, 599–637. https://doi.org/10.1007/978-94-011-5666-0_20
- Opgenoorth, H. J., Lockwood, M., Alcaydé, D., Donovan, E., Engebretson, M. J., van Eyken, A. P., et al. (2001). Coordinated ground-based, low altitude satellite and Cluster observations on global and local scales during a transient post-noon sector excursion of the magnetospheric cusp. Annales Geophysicae, 19(10/12), 1367–1398. https://doi.org/10.5194/angeo-19-1367-2001
- Østgaard, N., Snekvik, K., Borg, A. L., Åsnes, A., Pedersen, A., Øieroset, M., et al. (2009). Can magnetotail reconnection produce the auroral intensities observed in the conjugate ionosphere? *Journal of Geophysical Research*, 114(A6), A06204. https://doi.org/10.1029/2009JA014185
- Palin, L., Opgenoorth, H. J., Ågren, K., Zivkovic, T., Sergeev, V. A., Kubyshkina, M. V., et al. (2016). Modulation of the substorm current wedge by bursty bulk flows: 8 September 2002 Revisited. *Journal of Geophysical Research*, 121(5), 4466–4482. https://doi.org/10.1002/2015JA022262
- Parkinson, M. L., Wild, J. A., Waters, C. L., Lester, M., Lucek, E. A., & Décréau, P. M. E. (2007). An auroral westward flow channel (AWFC) and its relationship to field-aligned current, ring current, and plasmapause location determined using multiple spacecraft observations. *Annales Geophysicae*, 25(1), 59–76. https://doi.org/10.5194/angeo-25-59-2007
- Paschmann, G., Quinn, J. M., Torbert, R. B., Vaith, H., McIlwain, C. E., Haerendel, G., et al. (2001). The Electron Drift Instrument on Cluster: Overview of first results. *Annales Geophysicae*, 19(10/12), 1273–1288. https://doi.org/10.5194/angeo-19-1273-2001
- Paxton, L. J., Morrison, D., Zhang, Y., Kil, H., Wolven, B., Ogorzalek, B. S., et al. (2002). Validation of remote sensing products produced by the Special Sensor Ultraviolet Scanning Imager (SSUSI): A far UV-imaging spectrograph on DMSP F-16. In A. M. Larar & M. G. Mlynczak (Eds.), Optical spectroscopic techniques, remote sensing, and instrumentation for atmospheric and space research IV (pp. 338–348). https://doi.org/10.1117/12.454268
- Pinnock, M., Rodger, A. S., Dudeney, J. R., Baker, K. B., Newell, P. T., Greenwald, R. A., & Greenspan, M. E. (1993). Observations of an enhanced convection channel in the cusp ionosphere. *Journal of Geophysical Research*, 98(A3), 3767–3776. https://doi.org/10.1029/92JA01382

FEAR 44 of 46

- Pitkänen, T., Aikio, A. T., Amm, O., Kauristie, K., Nilsson, H., & Kaila, K. U. (2011). EISCAT-Cluster observations of quiet-time near-Earth magnetotail fast flows and their signatures in the ionosphere. *Annales Geophysicae*, 29(2), 299–319. https://doi.org/10.5194/angeo-29-299-2011 Pitkänen, T., Aikio, A. T., & Juusola, L. (2013). Observations of polar cap flow channel and plasma sheet flow bursts during substorm expansion.
- Pitkänen, T., Aikio, A. T., & Juusola, L. (2013). Observations of polar cap flow channel and plasma sheet flow bursts during substorm expansion. Journal of Geophysical Research, 118(2), 774–784. https://doi.org/10.1002/jgra.50119
- Pitkänen, T., Hamrin, M., Norqvist, P., Karlsson, T., Nilsson, H., Kullen, A., et al. (2015). Azimuthal velocity shear within an Earthward fast flow Further evidence for magnetotail untwisting? *Annales Geophysicae*, 33(3), 245–255. https://doi.org/10.5194/angeo-33-245-2015
- Pitout, F., & Bogdanova, Y. V. (2021). The polar cusp seen by Cluster. Journal of Geophysical Research, 126(9), e2021JA029582. https://doi.org/10.1029/2021JA029582
- Pitout, F., Bosqued, J.-M., Alcaydé, D., Denig, W. F., & Rème, H. (2001). Observations of the cusp region under northward IMF. Annales Geophysicae, 19(10/12), 1641–1653, https://doi.org/10.5194/angeo-19-1641-2001
- Geophysicae, 19(10/12), 1641–1653. https://doi.org/10.5194/angeo-19-1641-2001
 Pitout, F., Escoubet, C. P., & Lucek, E. A. (2004). Ionospheric plasma density structures associated with magnetopause motion: A case study using
- the Cluster spacecraft and the EISCAT Svalbard Radar. Annales Geophysicae, 22(7), 2369–2379. https://doi.org/10.5194/angeo-22-2369-2004
 Potemra, T. A., Erlandson, R. E., Zanetti, L. J., Arnoldy, R. L., Woch, J., & Friis-Christensen, E. (1992). The dynamic cusp. Journal of Geophysical Research, 97(A3), 2835–2844. https://doi.org/10.1029/91JA02654
- Rae, I. J., Donovan, E. F., Mann, I. R., Fenrich, F. R., Watt, C. E. J., Milling, D. K., et al. (2005). Evolution and characteristics of global Pc5 ULF waves during a high solar wind speed interval. *Journal of Geophysical Research*, 110(A12), A12211. https://doi.org/10.1029/2005JA011007
- Redmon, R. J., Denig, W. F., Kilcommons, L. M., & Knipp, D. J. (2017). New DMSP database of precipitating auroral electrons and ions. *Journal of Geophysical Research*, 122(8), 9056–9067. https://doi.org/10.1002/2016JA023339
- Reigber, C., Lühr, H., & Schwintzer, P. (2002). CHAMP mission status. Advances in Space Research, 30(2), 129–134. https://doi.org/10.1016/ S0273-1177(02)00276-4
- Reinisch, B. W., Galkin, I. A., Khmyrov, G., Kozlov, A., & Kitrosser, D. (2005). Automated collection and dissemination of ionospheric data from the digisonde network. *Advances in Radio Science*, 2, 241–247. https://doi.org/10.5194/ars-2-241-2004
- Rème, H., Aoustin, C., Bosqued, J. M., Dandouras, I., Lavraud, B., Sauvaud, J. A., et al. (2001). First multispacecraft ion measurements in and near the Earth's magnetosphere with the identical Cluster ion spectrometry (CIS) experiment. *Annales Geophysicae*, 19(10/12), 1303–1354. https://doi.org/10.5194/angeo-19-1303-2001
- Retinò, A., Vaivads, A., André, M., Sahraoui, F., Khotyaintsev, Y., Pickett, J. S., et al. (2006). Structure of the separatrix region close to a magnetic reconnection X-line: Cluster observations. Geophysical Research Letters. 33(6), L06101, https://doi.org/10.1029/2005GL024650
- Robinson, T. R., Yeoman, T. K., Dhillon, R. S., Lester, M., Thomas, E. C., Thornhill, J. D., et al. (2006). First observations of SPEAR-induced artificial backscatter from CUTLASS and the EISCAT Svalbard radars. *Annales Geophysicae*, 24(1), 291–309. https://doi.org/10.5194/angeo-24-291-2006
- Rosenqvist, L., Buchert, S., Opgenoorth, H., Vaivads, A., & Lu, G. (2006). Magnetospheric energy budget during huge geomagnetic activity using Cluster and ground-based data. *Journal of Geophysical Research*, 111(A10), A10211. https://doi.org/10.1029/2006JA011608
- Rosenqvist, L., Opgenoorth, H., Buchert, S., McCrea, I., Amm, O., & Lathuillere, C. (2005). Extreme solar-terrestrial events of October 2003: High-latitude and Cluster observations of the large geomagnetic disturbances on 30 October. *Journal of Geophysical Research*, 110(A9), A09S23. https://doi.org/10.1029/2004JA010927
- Rostoker, G., Samson, J. C., Creutzberg, F., Hughes, T. J., McDiarmid, D. R., McNamara, A. G., et al. (1995). CANOPUS a ground-based instrument array for remote sensing the high latitude ionosphere during the ISTP/GGS program. *Space Science Reviews*, 71(1–4), 743–760. https://doi.org/10.1007/BF00751349
- Runov, A., Baumjohann, W., Nakamura, R., Sergeev, V. A., Amm, O., Frey, H., et al. (2008). Observations of an active thin current sheet. *Journal of Geophysical Research*, 113(A7), A07S27. https://doi.org/10.1029/2007JA012685
- Samson, J. C., Greenwald, R. A., Ruohoniemi, J. M., Hughes, T. J., & Wallis, D. D. (1991). Magnetometer and radar observations of magnetohydrodynamic cavity modes in the Earth's magnetosphere. *Canadian Journal of Physics*, 69(8–9), 929–937. https://doi.org/10.1139/p91-147
- Sergeev, V. A., Kubyshkina, M. V., Baumjohann, W., Nakamura, R., Amm, O., Pulkkinen, T., et al. (2005). Transition from substorm growth to substorm expansion phase as observed with a radial configuration of ISTP and Cluster spacecraft. *Annales Geophysicae*, 23(6), 2183–2198. https://doi.org/10.5194/angeo-23-2183-2005
- Sibeck, D. G., & Angelopoulos, V. (2008). THEMIS science objectives and mission phases. Space Science Reviews, 141(1-4), 35-59. https://doi.org/10.1007/s11214-008-9393-5
- Sung, S.-K., Kim, K.-H., Lee, D.-H., Takahashi, K., Cattell, C. A., André, M., et al. (2006). Simultaneous ground-based and satellite observations of Pc5 geomagnetic pulsations: A case study using multipoint measurements. *Earth Planets and Space*, 58(7), 873–883. https://doi.org/10.1186/BF03351992
- Tan, L. C., Shao, X., Sharma, A. S., & Fung, S. F. (2011). Relativistic electron acceleration by compressional-mode ULF waves: Evidence from correlated Cluster, Los Alamos National Laboratory spacecraft, and ground-based magnetometer measurements. *Journal of Geophysical Research*, 116(A7), A07226. https://doi.org/10.1029/2010JA016226
- Taylor, M. G. G. T., Lavraud, B., Escoubet, C. P., Milan, S. E., Nykyri, K., Dunlop, M. W., et al. (2008). The plasma sheet and boundary layers under northward IMF: A multi-point and multi-instrument perspective. Advances in Space Research, 41(10), 1619–1629. https://doi. org/10.1016/j.asr.2007.10.013
- Torr, M. R., Torr, D. G., Zukic, M., Johnson, R. B., Ajello, J., Banks, P., et al. (1995). A far ultraviolet imager for the International Solar-Terrestrial Physics mission. Space Science Reviews, 71(1–4), 329–383. https://doi.org/10.1007/BF00751335
- Trattner, K. J., Fuselier, S. A., Petrinec, S. M., Yeoman, T. K., Mouikis, C., Kucharek, H., & Rème, H. (2005). Reconnection sites of spatial cusp structures. *Journal of Geophysical Research*, 110(A4), A04207. https://doi.org/10.1029/2004JA010722
- Trattner, K. J., Fuselier, S. A., Yeoman, T. K., Korth, A., Fraenz, M., Mouikis, C., et al. (2003). Cusp structures: Combining multi-spacecraft observations with ground-based observations. *Annales Geophysicae*, 21(10), 2031–2041. https://doi.org/10.5194/angeo-21-2031-2003
- Viljanen, A., & Hakkinen, L. (1997). IMAGE magnetometer network. In M. Lockwood, M. N. Wild, & H. J. Opgenoorth (Eds.), Satellite-ground-based coordination sourcebook (pp. 111–118). ESA-SP-119.
- Volwerk, M., Berchem, J., Bogdanova, Y. V., Constantinescu, O. D., Dunlop, M. W., Eastwood, J. P., et al. (2011). Interplanetary magnetic field rotations followed from L1 to the ground: The response of the Earth's magnetosphere as seen by multi-spacecraft and ground-based observations. Annales Geophysicae, 29(9), 1549–1569. https://doi.org/10.5194/angeo-29-1549-2011
- Volwerk, M., Glassmeier, K.-H., Runov, A., Nakamura, R., Baumjohann, W., Klecker, B., et al. (2004). Flow burst-induced large-scale plasma sheet oscillation. *Journal of Geophysical Research*, 109(A11), A11208. https://doi.org/10.1029/2004JA010533
- Volwerk, M., Lui, A. T. Y., Lester, M., Walsh, A. P., Alexeev, I., Cao, X., et al. (2008). Magnetotail dipolarization and associated current systems observed by Cluster and Double Star. *Journal of Geophysical Research*, 113(A8), A08S90. https://doi.org/10.1029/2007JA012729

FEAR 45 of 46

- Wang, C., Zong, Q., & Wang, Y. (2010). Propagation of interplanetary shock excited ultralow frequency (ULF) waves in magnetosphere-ionosphere-at-mosphere Multi-spacecraft "Cluster" and ground-based magnetometer observations. Science China Technological Sciences, 53(9), 2528–2534. https://doi.org/10.1007/s11431-010-4064-7
- Wang, H., Ma, S. Y., Lühr, H., Liu, Z. X., Pu, Z. Y., Escoubet, C. P., et al. (2006). Global manifestations of a substorm onset observed by a multi-satellite and ground station network. *Annales Geophysicae*, 24(12), 3491–3496. https://doi.org/10.5194/angeo-24-3491-2006
- Wannberg, G., Wolf, I., Vanhainen, L. G., Koskenniemi, K., Röttger, J., Postila, M., et al. (1997). The EISCAT Svalbard radar: A case study in modern incoherent scatter radar system design. *Radio Science*, 32(6), 2283–2307. https://doi.org/10.1029/97RS01803
- Wei, D., Dunlop, M. W., Yang, J., Dong, X., Yu, Y., & Wang, T. (2021). Intense dB/dt variations driven by near-earth bursty bulk flows (BBFs): A case study. Geophysical Research Letters, 48(4), e2020GL091781. https://doi.org/10.1029/2020GL091781
- Wild, J. A., Cowley, S. W. H., Davies, J. A., Khan, H., Lester, M., Milan, S. E., et al. (2001). First simultaneous observations of flux transfer events at the high-latitude magnetopause by the Cluster spacecraft and pulsed radar signatures in the conjugate ionosphere by the CUTLASS and EISCAT radars. *Annales Geophysicae*, 19(10/12), 1491–1508. https://doi.org/10.5194/angeo-19-1491-2001
- Wild, J. A., Milan, S. E., Cowley, S. W. H., Dunlop, M. W., Owen, C. J., Bosqued, J. M., et al. (2003). Coordinated interhemispheric SuperDARN radar observations of the ionospheric response to flux transfer events observed by the Cluster spacecraft at the high-latitude magnetopause. Annales Geophysicae, 21(8), 1807–1826. https://doi.org/10.5194/angeo-21-1807-2003
- Wild, J. A., Milan, S. E., Davies, J. A., Cowley, S. W. H., Carr, C. M., & Balogh, A. (2005). Double Star, Cluster, and ground-based observations of magnetic reconnection during an interval of duskward oriented IMF: Preliminary results. *Annales Geophysicae*, 23(8), 2903–2907. https://doi.org/10.5194/angeo-23-2903-2005
- Wild, J. A., Milan, S. E., Davies, J. A., Dunlop, M. W., Wright, D. M., Carr, C. M., et al. (2007). On the location of dayside magnetic reconnection during an interval of duskward oriented IMF. *Annales Geophysicae*, 25(1), 219–238. https://doi.org/10.5194/angeo-25-219-2007
- Wild, J. A., Milan, S. E., Owen, C. J., Bosqued, J. M., Lester, M., Wright, D. M., et al. (2004). The location of the open-closed magnetic field line boundary in the dawn sector auroral ionosphere. *Annales Geophysicae*, 22(10), 3625–3639. https://doi.org/10.5194/angeo-22-3625-2004
- Wild, J. A., Woodfield, E. E., Donovan, E., Fear, R. C., Grocott, A., Lester, M., et al. (2011). Midnight sector observations of auroral omega bands. Journal of Geophysical Research, 116(A5), A00130. https://doi.org/10.1029/2010JA015874
- Wilken, B., Daly, P. W., Mall, U., Aarsnes, K., Baker, D. N., Belian, R. D., et al. (2001). First results from the RAPID imaging energetic particle spectrometer on board Cluster. *Annales Geophysicae*, 19(10/12), 1355–1366. https://doi.org/10.5194/angeo-19-1355-2001
- Woodman, R. F., & Hagfors, T. (1969). Methods for the measurement of vertical ionospheric motions near the magnetic equator by incoherent scattering. *Journal of Geophysical Research*, 74(5), 1205–1212. https://doi.org/10.1029/JA074i005p01205
- Xue, Z., Yuan, Z., & Yu, X. (2021). Prompt emergence and disappearance of EMIC waves driven by the sequentially enhanced solar wind
- dynamic pressure. Geophysical Research Letters, 48(2), e2020GL091479. https://doi.org/10.1029/2020GL091479
 Yeoman, T. K., Milling, D., & Orr, D. (1990). Pi2 pulsation polarization patterns on the U.K. sub-auroral magnetometer network (SAMNET).
- Planetary and Space Science, 38(5), 589–602. https://doi.org/10.1016/0032-0633(90)90065-X

 Yordanova, E., Sundkvist, D., Buchert, S. C., André, M., Ogawa, Y., Morooka, M., et al. (2007). Energy input from the exterior cusp into the ionosphere: Correlated ground-based and satellite observations. Geophysical Research Letters 34(4), 1.04102. https://doi.
- into the ionosphere: Correlated ground-based and satellite observations. Geophysical Research Letters, 34(4), L04102. https://doi.org/10.1029/2006GL028617
- Zhang, Q.-H., Dunlop, M. W., Liu, R.-Y., Yang, H.-G., Hu, H.-Q., Zhang, B.-C., et al. (2011). Coordinated Cluster/Double Star and ground-based observations of dayside reconnection signatures on 11 February 2004. Annales Geophysicae, 29(10), 1827–1847. https://doi.org/10.5194/angeo-29-1827-2011
- Zhang, Q.-H., Dunlop, M. W., Lockwood, M., Liu, R. Y., Hu, H. Q., Yang, H. G., et al. (2010). Simultaneous observations of reconnection pulses at Cluster and their effects on the cusp aurora observed at the Chinese Yellow River Station. *Journal of Geophysical Research*, 115(A10), A10237. https://doi.org/10.1029/2010JA015526
- Zhang, Q.-H., Liu, R. Y., Dunlop, M. W., Huang, J. Y., Hu, H. Q., Lester, M., et al. (2008). Simultaneous tracking of reconnected flux tubes: Cluster and conjugate SuperDARN observations on 1 April 2004. Annales Geophysicae, 26(6), 1545–1557. https://doi.org/10.5194/angeo-26-1545-2008
- Zhang, Y. C., Shen, C., Liu, Z. X., Pu, Z. Y., Dandouras, I., Marchaudon, A., et al. (2011). Magnetopause response to variations in the solar wind: Conjunction observations between Cluster, TC-1, and SuperDARN. *Journal of Geophysical Research*, 116(A8), A08209. https://doi.org/10.1029/2011JA016462
- Zheng, Y., Lui, A. T. Y., Mann, I. R., Takahashi, K., Watermann, J., Chen, S.-H., et al. (2006). Coordinated observation of field line resonance in the mid-tail. *Annales Geophysicae*, 24(2), 707–723. https://doi.org/10.5194/angeo-24-707-2006
- Zong, Q.-G., Fu, S. Y., Baker, D. N., Goldstein, M. L., Song, P., Slavin, J. A., et al. (2007). Earthward flowing plasmoid: Structure and its related ionospheric signature. *Journal of Geophysical Research*, 112(A7), A07203. https://doi.org/10.1029/2006JA012112
- Zong, Q.-G., Reinisch, B. W., Song, P., Galkin, I., & Liu, X. J. (2008). Ionospheric response to the interplanetary shock. In P. Song, J. Foster, M. Mendillo, & D. Bilitza (Eds.), Radio sounding and plasma physics (pp. 52–57), https://doi.org/10.1063/1.2885033

FEAR 46 of 46